cop 1

GEOLOGY OF THE CLINTON CREEK ASBESTOS DEPOSIT, YUKON TERRITORY

by

MYAT HTOON

B.Sc., Rangoon Arts and Sciences University, 1967

A THESIS SUBMITTED IN PARTIAL FULFILLMENT OF

THE REQUIREMENT FOR THE DEGREE OF

MASTER OF SCIENCE

in

THE FACULTY OF GRADUATE STUDIES

THE DEPARTMENT OF GEOLOGICAL SCIENCES

We accept this thesis as conforming

to the required standard

THE UNIVERSITY OF BRITISH COLUMBIA

March, 1979

In presenting this thesis in partial fulfilment of the requirements for an advanced degree at the University of British Columbia, I agree that the Library shall make it freely available for reference and study. I further agree that permission for extensive copying of this thesis for scholarly purposes may be granted by the Head of my Department or by his representatives. It is understood that copying or publication of this thesis for financial gain shall not be allowed without my written permission.

Department of Geological Sciences

The University of British Columbia
2075 Wesbrook Place
Vancouver, Canada
V6T 1W5

Date March, 23rd, 1979.

ABSTRACT

Clinton Creek asbestos deposit is situated at 77 kilometres northwest of Dawson City on Clinton Creek in Yukon Territory.

Yukon Metamorphic Complex of Ordovician to Devonian age (470 Ma, Rb-Sr date) covers most of the Clinton Creek area. The most prominent metamorphism of the area occurred in Permian time (245 to 278 Ma, K-Ar dates). Based on intensity and style of deformation of ultramafic bodies and country rocks it is suggested that the ultramafic rocks were emplaced probably during the Permian period. Tintina fault is a weak zone along which the alpine ultramafic bodies of Clinton Creek and probably some of the others along and close to the Tintina Trench were tectonically emplaced. These were later folded and metamorphosed with the country rocks. During latest Cretaceous-earliest Tertiary time (64.9 Ma, K-Ar date) the area was intruded by acid intrusive rocks. The youngest undeformed and fresh basalt is probably of Selkirk volcanics equivalent.

Three prominent phases of deformation were delineated. Probably the oldest and most complex phase occurred during the Permian, along with the initial movement of the Tintina fault. Small, tight, isoclinal folds are characteristics of this phase. The structural trend (300° to 315°) is roughly parallel to the direction of the Tintina Trench. Due to later deformations changes in direction of fold axes of this phase (190° to 350°) is common. The second phase of deformation gave rise to large recumbent folds with trends varying from 270° to 290° with southerly vergence. Third phase of deformation gave rise to antiform structure of regional scale.

The Porcupine and Snow Shoe ultramafic bodies are mined for chrysotile asbestos. Afew other ultramafic bodies contain appreciable amount of chrysotile-fibre but not of adequate quantity to be mined. Most of the ultramafic bodies are sheared or massive, and are devoid of known chrysotile-fibre. In general, if serpentinization is less than 75 percent there is no chance of commercial mineralization. Fairly intense fractures are essential to provide adequate openings for chrysotile-fibre formation in ore grade concentrations. Chrysotile-fibre bearing serpentinized ultramafic masses within argillite unit or at the contact of argillite and other units seem to carry ore grade or substantial amount of chrysotile-fibre.

Evidence of Clinton Creek asbestos deposit mainly supports formation of chrysotile-fibre as fracture filling. Although evidence of fracture filling rather than replacement seems convincing and exists on a wide scale, a few evidence indicates replacement characteristics on minor scale. The main phase of mineralization is believed to occur at the end of Cretaceous when acid intrusive rocks intruded the vicinity of the Clinton Creek area. These intrusions could have provided warm aqueous solution to react with the existing serpentine along fractures. This resulted deposition of chrysotile-fibre in an essentially closed system.

Analysis of isotopic dates of the Yukon Crystalline Plateau shows a distinct grouping of igneous activity at mid Cretaceous and latest Cretaceous time. Some isotopic dates of igneous and metamorphic rocks ranging from 135 to 230 Ma show a distinct younging trend away from the Tintina Trench. The trend suggests that the date at the Tintina Trench is about 200 Ma, and 250 kilometres perpendicular distance from the trench is 150 Ma. The apparent horizontal rate of isotherm migration is about 0.5 cm/yr. However, more data is required to confirm the speculation that the Tintina Trench represents an extinct geosuture and vanished ocean.

CONTENTS

LIST OF TABLES

LIST OF FIGURES

LIST OF PLATES

ACKANOWLEDGEMENT

This thesis was supervised by Drs. K.C. McTaggart, A.J. Sinclair and C.I. Godwin, whose advice and guidance are greatly appreciated.

The writer wishes to thank Dr. R.L. Armstrong for his discussion and advice in isotopic dating; K.C. Scott and J. Harakel for their help in Rb-Sr and K-Ar dating processes; and G. Georgakopoulos for his assitance in microprobe analysis. The technical assitance of B. Cranston in preparation of thin sections and microprobe sections is greatly appreciated. Co-operation of Cassiar Asbestos Corp. Ltd. is also greatly appreciated.

The work was supported by the Dept. of Indian and Northern Affairs, White Horse, Yukon Territory. The writer was supported financially by the United Nations Development Programme, United Nations, New York.

Most of all the writer likes to thank again to Dr. K.C. McTaggart for his painstaking teaching and his guidance in English and writing.

CHAPTER I

INTRODUCTION

1-1 PRELIMINARY STATEMENT

The subject of this thesis is the geological investigation of Clinton Creek Asbestos deposit and its surrounding area in Yukon Territory, Canada (Figure 1-1). The deposit, held by Cassiar Asbestos Cooperation Ltd., is the only known economic asbestos deposit in Yukon Territory. It was important to study the deposit and the controls of asbestos formation before 1978 when the mine was closed and the open pit became inaccessible. It is hoped that this study might be useful in the exploration and understanding of other ultramafic bodies with asbestos mineralization.

1-2 SCOPE OF THESIS

Purpose of the study is twofold. The first objective

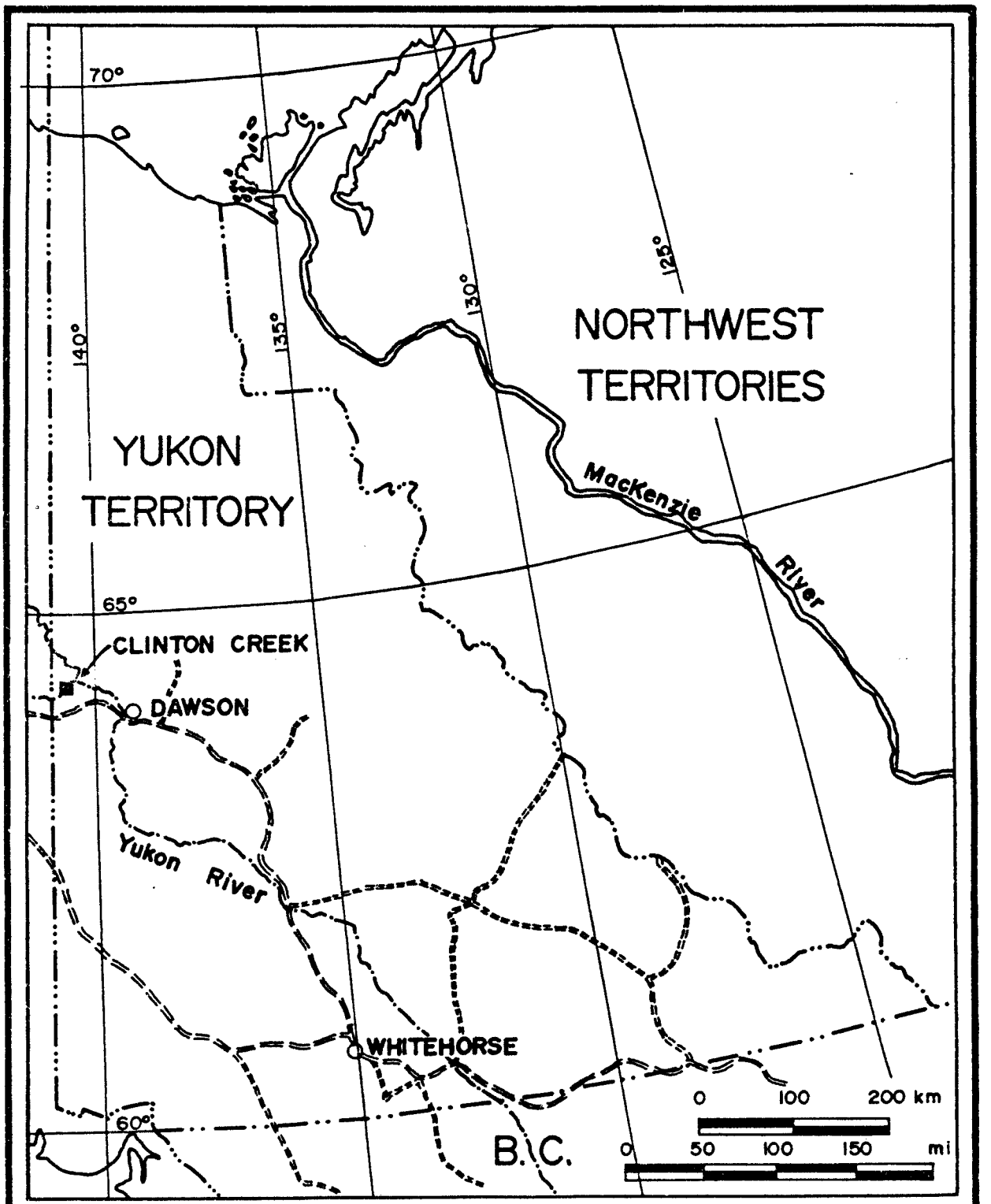

FIG 1-1: LOCATION OF THE CLINTON CREEK ASBESTOS DEPOSIT

is to develop genetic concepts that could guide future exploration for chrysotile asbestos, especially in the Tintina region of the Yukon. The second objective is to describe the geology of the mine, the genesis of the deposit and to consider the origin and emplacement of ultramafic rocks of the area. Mapping was difficult because of limited outcrops which amount to less than five percent of the area. Because drill core had been logged by at least eight persons, records were inconsistent and the writer relogged all the core that could be documented.

Field work was carried out from June to August in 1975 and 1976. During these periods the property, which covers about one square mile, was mapped at a scale of one inch to forty feet, and a seventy-square-mile area around the deposit was mapped at a scale of one inch to 1,000 feet.

1-3 LOCATION AND ACCESS

The Clinton Creek asbestos deposit (lat. 64°23'N, long. 140°23'W. Figure 1-1) is situated about 77 kilometres northwest of Dawson City, Yukon Territory on Clinton Creek, eight kilometres upstream from its confluence with Forty Mile river. Sixty Mile road which connects Dawson City and Fairbanks passes 32 kilometres to the southeast of the mine.

A gravel air-strip on the property is adequate for commercial aeroplanes of moderate size. The deposit occurs on a north-east and trending ridge (elevation 545 metres) some 155 metres above the valley of Clinton Creek.

1-4 CLIMATE AND VEGETATION

The area lies within the zone of discontinuous permafrost and is subject to severe climatic conditions during winter months. The thickness and nature of permafrost appear to vary depending on the type of soil or rock water content and the direction that the ground surface faces. Precipitation is approximately 33 centimetres per year, most of which occurs as rain in June, July and August. Temperatures range between -56° celsius in winter and +32° celsius in summer. Freeze-up usually occurs around late September; spring break-up is expected in late April or early May. The average annual snowfall is about one metre. The highest ridges within the mapped area (elevation 1,000 metres) are below tree line. Black spruce, birch and poplar are abundant. Alpine fir, willow and balsam poplar are less common. In general, heavy forest growth is restricted to the main valley floors, but sparse growth extends up the hillsides. South-facing slopes are more heavily forested than north facing slopes

which are covered by thick moss and sparse timber.

1-5 PHYSIOGRAPHY

Clinton Creek deposit lies in the Klondike Plateau which extends northwestward into Alaska where it is called Yukon-Tanana Uplift (Wahrhaftig, 1965). The Klondike Plateau is bounded on the northeast by the Tintina Trench and the southwest by the Nisling River, and is a subdivision of the Yukon Chrystalline Plateau (Douglas, et al., 1970) most of which escaped glaciation during the Pleistocene (Prest, et al., 1968). The Klondike Plateau is marked by long, irregular main and spur ridges characteristic of a highly developed dendritic stream pattern. Crests of most ridges are between 1,000 and 1,350 metres elevation and probably represent an old uplifted erosion surface. Clinton Creek has a gentle gradient compared to its tributary streams which occupy narrow v-shaped valleys with steep gradients. Dome-shaped hills are quite prominent and vegetation is thich within the mapped area. Outcrops are scarce and most of these are found along and near ridge crests.

1-6 HISTORY OF THE CLINTON CREEK DEPOSIT

The original discovery was made in 1957 and is credited to Art Anderson, an Indian trapper; he was listed an "No.1" on the payroll of Clinton Creek mine. The property consists of 94 claims and two placer leases. One adit was driven in 1957-58. This work was followed by magnetometer surveys and drilling; the first phase of exploration was completed in 1963. Geological study was undertaken mainly by N.W. Plumb and D.R. Budinsky. From 1963 to 1966, underground and surface diamond drilling as well as geological and geophysical mapping were carried out. Construction of an access road was undertaken in 1965 and 1966. The mine began to produce in 1967.

Both the mine and the primary crushing plant were situated at a lower level than the mill and plant site. A belt conveyor carries ore from the primary crusher to the tramway feeder. The ore is elevated 152 metres by a 1,600 metre long tramline to the plant site and was delivered at 300 tons per hour. The mine had produced ore for eleven years with an average waste-to-ore ratio of about 5.5 to 1. Operations ceased in 1978 when the ore was exhausted.

CHAPTER II

GEOLOGY OF THE CLINTON CREEK AREA

2-1 INTRODUCTION

The regional geology of map sheet 1284A which includes the Clinton Creek area has been described by Green and Roddick (1961) and Green (1972). Figure 2-1 was prepared from their map. The oldest rocks in the area (Table 2-1) belong to the Yukon Metamorphic Complex (Tempelman-Kluit, 1974). Ultramafic rocks were probably emplaced in Permian time. Grandiorite plutons were intruded in latest Cretaceous to earliest Tertiary. The youngest unit, not included in Figure 2-1 is basalt, probably of Pleistocene or Holocene age. Distribution of all units and locations of specimens are shown in (Figure 2-2).

2-2 METAMORPHIC ROCKS OF THE YUKON CRYSTALLINE PLATEAU

2-2-A REGIONAL SETTING

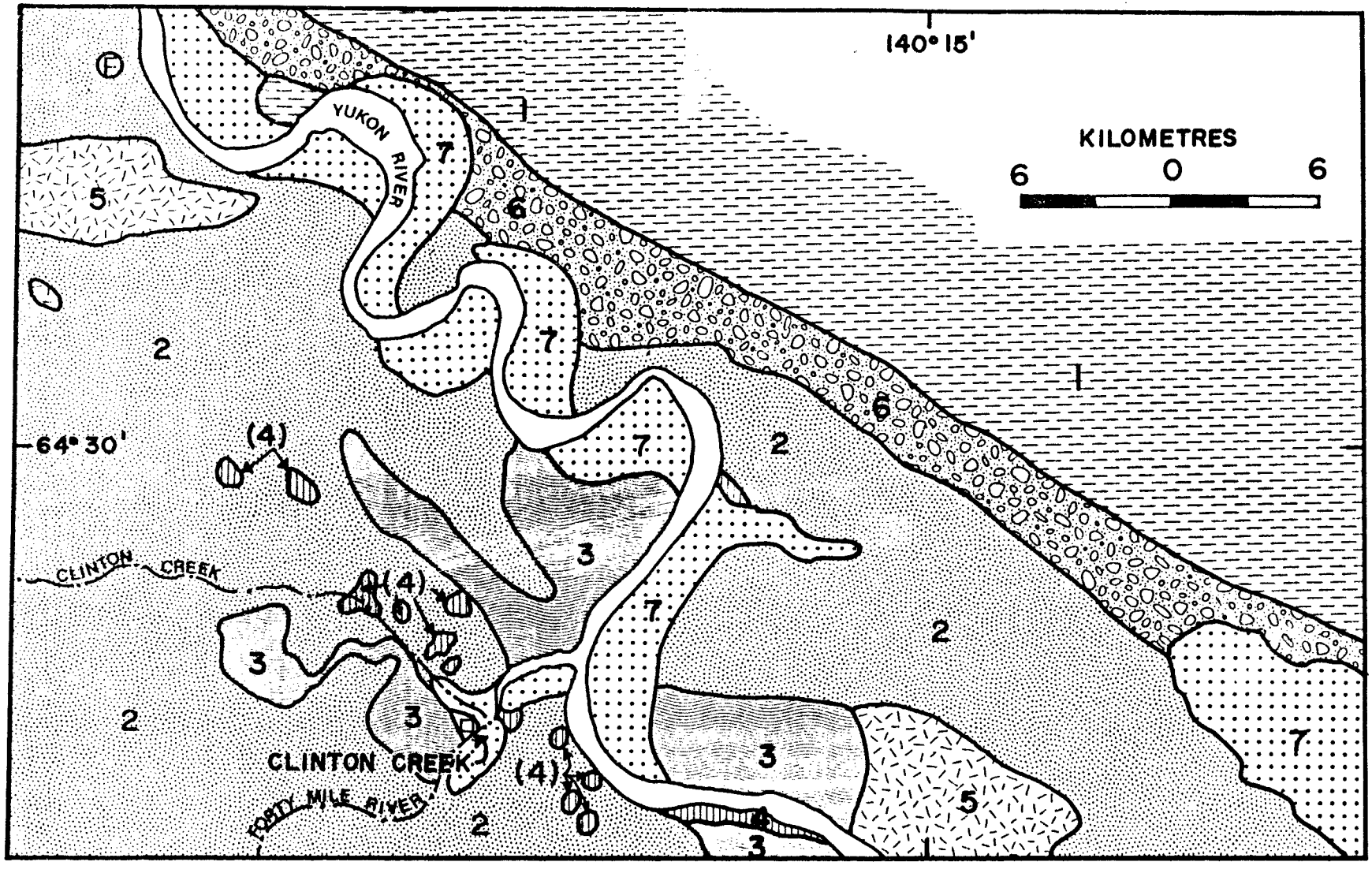

FIGURE 2-1: REGIONAL GEOLOGY. 1= Grit and slate; 2= Quartz-mica schist and quartzite; 3= Greenstone and quartz-muscovite-chlorite schist; 4= Serpentinized ultramafic rocks; 5= Biotite granodiorite and quartz monzonite; 6= Sandstone, shale, conglomerate and lignite; 7= Alluvial deposits; F= Fossil locality. (Modified after Green, 1972.)

TABLE 2-1

UNITS IN THE CLINTON CREEK AREA, Y.T.

ERA	PEROID	UNIT	LITHOLOGY	ISOTOPIC AGES[1] (Ma)
CENOZOIC	Late Tertiary	Selkirk Group(?)	Basalt	
	Early Tertiary	Nisling Alaskite Group(?)	Biotite Granodiorite	64.9±2.3
PALEOZOIC	Permian	Main phase of metamorphism of the Clinton Creek area. Derived from K-Ar dates of muscovite and hornblende, and Rb-Sr date of whole rock.		245±8 255.8±22.3 278±10
	Pensylvanian and/or Permian		Ultramafic Rocks	
	Devonian(?) or earlier Ordovician and earlier(?)	Yukon Metamorphic Complex	Carbonaceous argillite, limy argillite, limestone, sandstone Greenstone, quartz-muscovite-chlorite schist, quartz-muscovite schist, quartz-muscovite-biotite schist, micaceous quartzite and crystalline limestone	470

1: Isotopic ages are discussed in Chapter II, section seven.

Metasedimentary and metavolcanic rocks of the Yukon Crystalline Plateau are refferred to as Yukon Metamorphic Complex (Templeman-Kluit, 1974). These rocks underlie most of the area between Tintina and Shakwak-Denali faults in Yukon Territory (Figure 2-3) and are equivalent with the Birch Creek Schist of Alaska, originally mapped by Mertie in 1937. The Terrane has been called by different names in different areas. The first person who mapped the area was D.D. Cairnes (1914) who assigned the Yukon Group to Pre-Cambrian. Names such as "Pelly Gneiss", "Klondike Schist", "Nasina Quartzite" were also given to various parts of this terrane (McConnell, 1905). The Klondike schist, Nasina quartzite and Pelly gneiss cover the northern and west-central parts of the Terrane near the Yukon-Alaska border, and contain large lenses of crystalline limestone, serpentinite and amphibolite (Green and Roddick, 1972). Metasediments, just west of the Clinton Creek area across the border in Alaska were considered to be of continental assemblages rather than an island arc or oceanic crustal assemblages (Foster and Keith, 1974). Rocks of the Clinton Creek area resemble those of the Eagle area in Alaska and form part of the same belt.

Ages of rocks in the Yukon Crystalline Plateau range from Pre-Cambrian to Cenozoic. The Pelly gneiss, near the west-central part of the Plateau south of the Clinton Creek yields a Rb-Sr age of about 750 Ma (R.L. Armstrong, personal

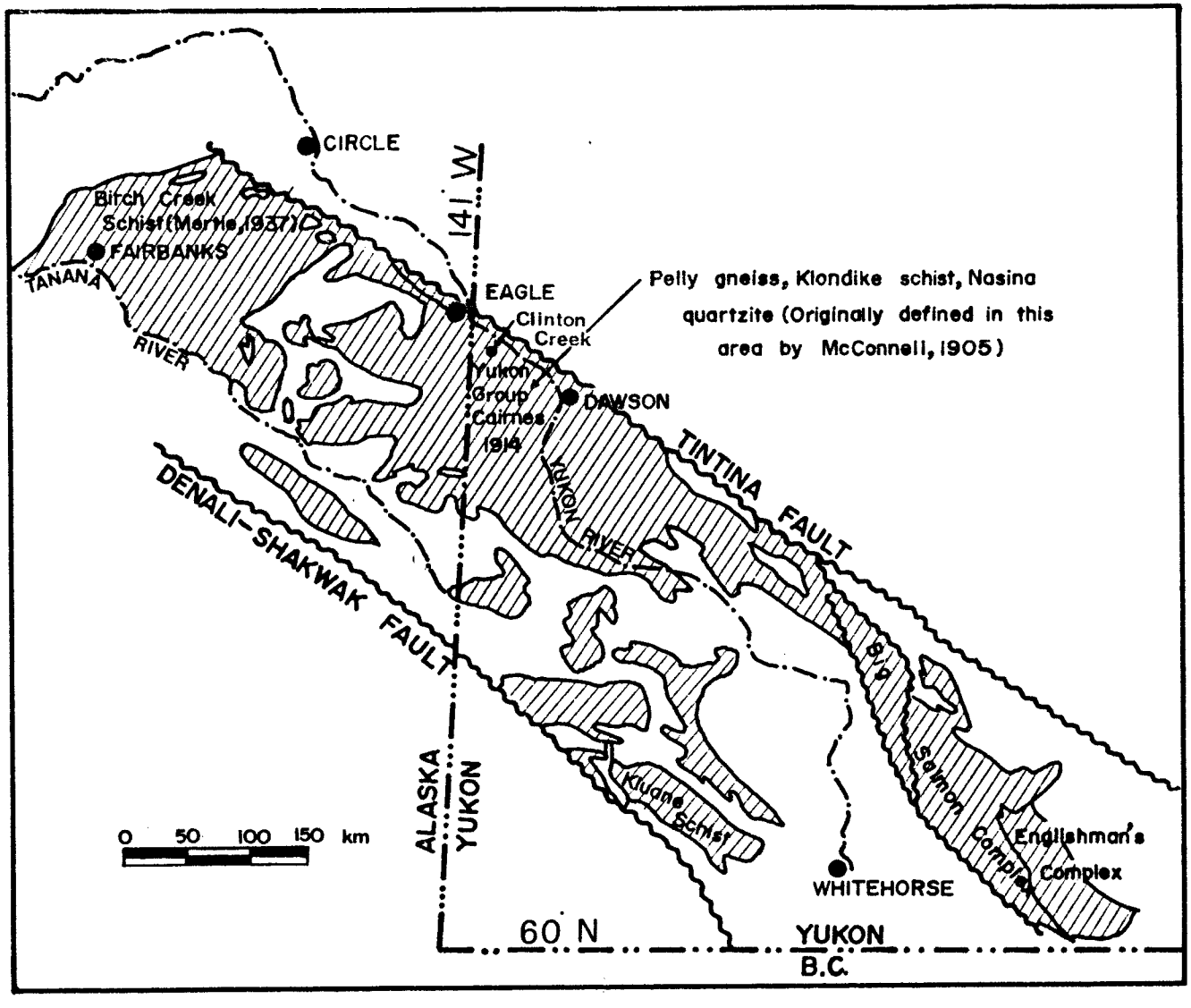

FIGURE 2-3: DISTRIBUTION OF THE YUKON METAMORPHIC COMPLEX AND EQUIVALENTS IN THE YUKON TERRITORY AND ALASKA. (After Tempelman-Kluit, 1975.)

communication, 1978). Rocks which are lithologically equivalent to the Nasina quartzite and Klondike schist, in the Clinton Creek area have yielded a Rb-Sr model age of 470 Ma[1]. However, in an area just west of the Yukon River near the Alaska border (64°39.5'N, 140°57.5'W) echinoderm columnals in limestone associated with metasedimentary rocks indicate a Paleozoic age (Mertie, 1937; Douglas, et al., 1970; Green, 1972), probably Devonian. The youngest igneous rocks recorded in this Terrane are Tertiary[1].

2-2-B Clinton Creek Area

More than 80 percent of the area is underlain by metamorphic rocks with lithologic characteristics similar to those of the Klondike schist and Nasina quartzite (Figure 2-3). The writer distinguished the following lithologic units (Htoon, 1977) which are listed in probable chronologic order from d to a:

a. Carbonaceous and limy argillite (youngest),

b. Greenstone[2] and quartz-muscovite-chlorite schist,

c. Quartz-muscovite schist and quartzite, and

d. Quartz-muscovite-biotite schist (oldest).

---

1 : See Chapter two section seven.
2 : Greenstone is described in Appendix A

a. Carbonaceous and limy argillites

This unit underlies the main Clinton Creek valley. It consist mostly of interbedded carbonaceous argillite, limy argillite, black to dark gray limestone and limy sandstone. Carbonaceous argillite is jet black, very fragile, cleaves easily along parting planes, and constitutes most of this unit (Plate 2-1). Bedding is difficult to recognize. Limy argillite is relatively harder than carbonaceous agrillite, is dull to brownish and normally is found as a transitional rock between carbonaceous argillite and limestone or sandstone. Limestone, black and highly fractured (Plate 2-2), is well laminated but seldom thickly bedded. Partings and fractures are coated for the most part with carbonaceous matter or muscovite. Sandstone, ordinarily buff to brownish and very limy, is uncommon but locally forms conspicuous beds in argillite.

Carbonaceous argillite in thin section is seen to consist of quartz, carbonaceous matter, sercite, clay,magnetite, chlorite, pyrite and traces of epidote, albite and biotite. Quartz and carbonaceous matter usually total more than 50 percent and 20 percent respectively. Clay minerals constitute as much as 15 percent and sericite up to 10 percent of the rock. There are two generations of quartz, original and stringers of metamorphic quartz which cut across the bedding. Two cleavages cross at angles of about 120° and sericite elonga-

PLATE 2-1: Carbonaceous argillite (black layers on top) in contact with quartz-muscovite schist (light coloured layers at bottom).

PLATE 2-2: Dark, bedded limestone within the carbonaceous argillite unit. Thin layers of carbonaceous argillite also occur between each limestone bed.

tion parallels these cleavages. Most chlorite has formed by the replacement of biotite. Much of the argillite is weakly mylonitized.

In thin section limy argillite consists of 35 percent quartz, 35 percent calcite, 20 percent clay minerals, 5 to 10 percent carbonaceous matter with minor sericite, pyrite and chlorite. Textures are much like those of the carbonaceous argillite.

Dark gray limestone, weakly foliated and metamorphosed, is of two types. Sandy limestone has up to 35 percent quartz and carbonaceous limestone has as much as 15 percent carbonaceous matter. Sericite, magnetite and traces of clinozoisite are also present. Limestone with abundant carbonaceous matter and sericite is finely laminated whereas quartz-rich limestones are massive thick bedded. Quartz grains are elongated in the foliation and show highly undulose extinction. Limy sandstone, not abundant, grades into sandy limestone.

b. Greenstone and quartz-muscovite-chlorite schist

This unit is composed of greenstone, quartz-muscovite-chlorite schist and minor amount of quartz-feldspar-muscovite schist. The rocks of this unit are fine to medium-grained and colour ranges from dark green to silvery-green. Degree of foliation varies from poor to well. Shearing is not pervasive.

Greenstone is generally dark green, massive or obscurely foliated but locally well foliated. In thin-section it consists of a foliated mass of quartz, chlorite, epidote, sericite, calcite, amphibole, plagioclase and opaque minerals. Quartz nowhere exceeds 25 percent, chlorite, epidote, carbonates and sericite increase with higher degree of shearing. In less sheared rock, plagioclase (albite to oligoclase) occurs with a lesser amount of epidote group minerals, sericite and carbonates. Shearing in greenstone has largely destroyed the texture of the original rock. In rocks which were not intensely sheared lath-like pseudomorphs of feldspars are still recognizable, even though they have been altered to albite and saussurite. Generally the original crystal forms of ferromagnesium minerals are not recognizable, but in a very few specimens amphibole pseudomorphs after pyroxene are preserved. Actinolite, the common amphibole, is common in massive altered greenstone but is less prominent in sheared greenstone where chlorite takes its place. Carbonate tends to be arranged in streaks parallel to the foliation. Relict textures and minerals suggest that the greenstone was originally a basic igneous rock.

Quartz-muscovite-chlorite schist is pale to medium green, moderately to well foliated and lacks shiny micaceous partings. It consists of 40 to 60 percent quartz, 15 percent muscovite, 10 percent chlorite, 8 percent epidote and the rest is calcite. Quartz and muscovite are more abundant than in greenstone.

Schistosity is mainly parallel to layers of muscovite and quartz. Although it resembles greenstone, except for its pronounced schistosity, the high quartz content suggests a sedimentary origin.

In the field it is difficult to distinguish between greenstone and quartz-muscovite-chlorite schist, especially if former is highly sheared. But after thin section study, it was found that the southern part of the study area is underlain largely by greenstone and the northern part predominently by quartz-muscovite-chlorite schist. It is impossible, however, to draw a geologic contact between the two rocks on the basis of available information. In some places, greenstone and argillite are interbedded.

c. Quartz-muscovite schist and quartzite

This unit is composed mainly of quartz-muscovite schist and micaceous quartzite. These alternate one with the other and contacts between them are generally gradational. A few lenses of white to whitish-gray crystalline limestone also occur (Plate 2-3). At the base of the unit quartzite is dominant. It is gray to dark gray, medium to coarse grained with minor muscovite and is well foliated. Variation of size of quartz grains between foliation planes is not uncommon. At higher levels quartz-muscovite schist is prominent. Locally, quartz-muscovite schist becomes very coarse-grained and

PLATE 2-3: Lens of marble (gray zone in the middle) in quartz-muscovite schist and quartzite unit.

mica flakes grow as large as four milimetres in diameter.

In thin section quartzite consists of more than 80 percent quartz, about ten percent muscovite, about five percent carbonaceous matter and about one to five percent calcite. Most of the quartz grains are elongated and interlayered with carbonaceous matter. Bands of muscovite and carbonaceous matter parallel the foliation of the rock.

In thin section, quartz-muscovite schist consists of 50 to 60 percent quartz, 35 percent muscovite, 1 to 4 percent calcite, 1 percent magnetite and rarely traces of albite, iron-oxide, chlorite and carbonaceous matter (Plate 2-4). Quartz in post metamorphic fractures cuts the foliation. Muscovite layers alternate with quartz layers; muscovite is also scattered within quartz layers with its elongation parallel to schistosity. Locally, schists are unusually rich in calcite, albite, graphite and/or chlorite. Carbonate in places occurs as large crystals and poikiloblastically encloses quartz grains, but generally it fills fractures. Generally schistosity planes are sinuous.

d. Quartz-muscovite-biotite schist

Quartz-muscovite-biotite schist unit rarely crops out and its distribution was determined mostly by the distribution of float. Specimens are deeply weathered and rusty. It is medium to fine-grained and has well-developed schistosi-

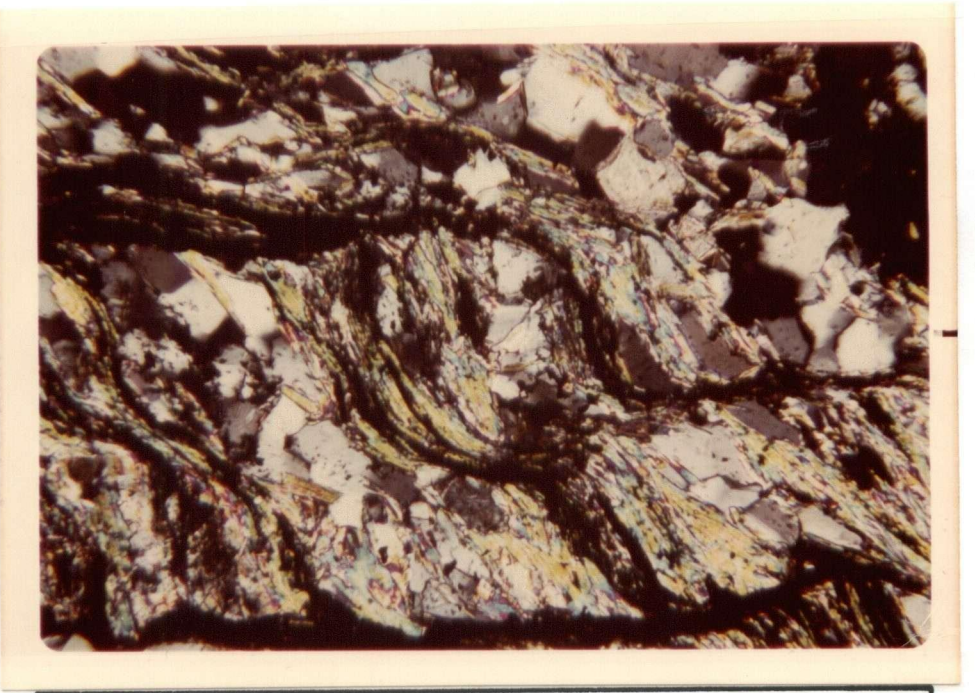

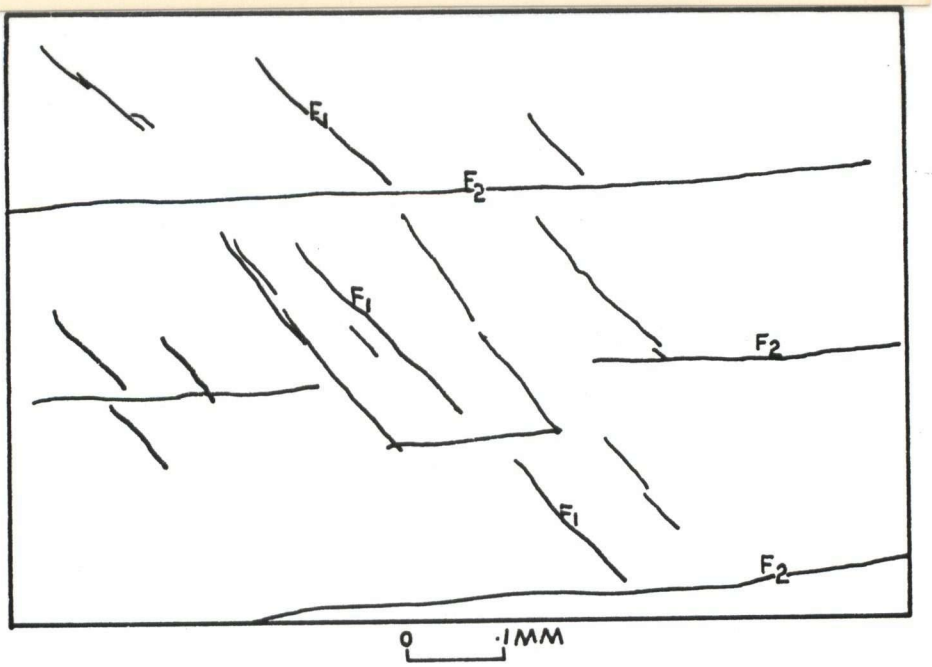

PLATE 2-4: Two sets of foliation planes are common in quartz-muscovite schist. Foliation F_1 is parallel to the elongation of muscovite and foliation F_2 cuts F_1 at 60°. Note the development of preferred orientationof muscovite parallels F_2 shear zones which is initially oriented parallel to F_1. (Crossed nicols.)

ty. In thin section it consists of more than 55 percent quartz, about 30 percent muscovite, about 5 percent biotite and about one to ten percent calcareous and limonitic alteration minerals. Minor amounts of garnet are also contained in a few rocks of this unit.

2-3 ULTRAMAFIC ROCKS

2-3-A Regional Setting

Ultramafic rocks form a distinctive unit in the Yukon Metamorphic Complex. The discontinuous belt of sheared ultramafic rocks and their serpentinized equivalents (Figure 2-4) are interlayered with metamorphic rocks of the Yukon Crystalline Plateau. Ultramafic bodies are found as sill,dyke and stock-like bodies, that range in size from a few hundred feet to several miles across. In general, the larger stock-like masses occur near the Tintina Trench, whereas the smaller ones which are highly serpentinized, are found further from the trench. The number of ultramafic exposures is much greater to the northwest in the Alaskan part of the belt. The ultramafic belt seems to be controlled, at least in alignment, by the Tintina Trench (Roddick, 1967) which is a major northwest trending structure, separating unmetamorphosed Pre-

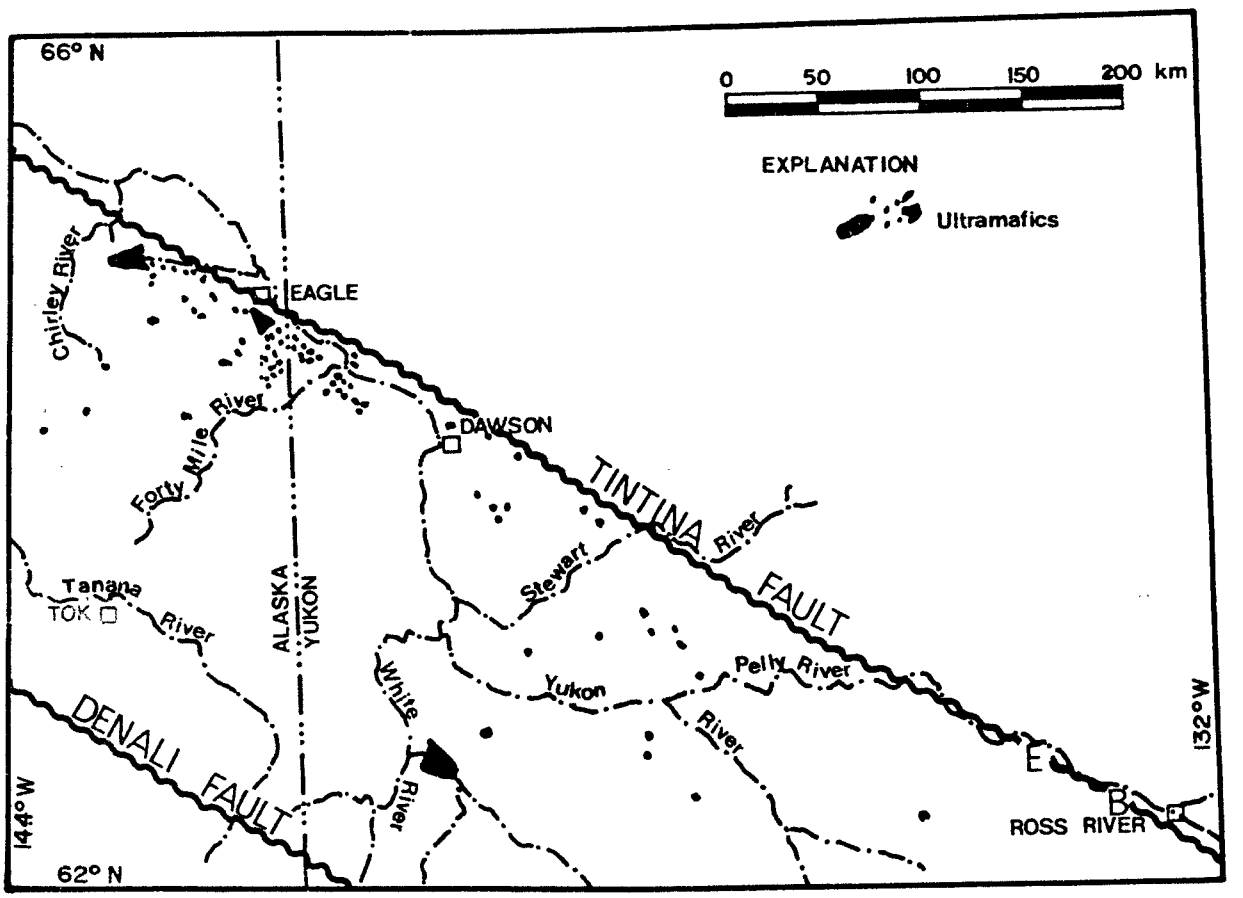

FIGURE 2-4: GENERALIDED DISTRIBUTION OF SERPENTINIZED ULTRAMAFIC ROCKS IN YUKON TERRITORY AND ALASKA. E = eclogite locality; B = glaucophane occurrance. (Modified after Foster, 1974; Godwin, 1975; Tempelman-Kluit, 1976.)

Cambrian, Paleozoic and Mesozoic sedimentary rocks on the northeast from metamorphic rocks on the southwest. On the basis of field observation and aeromagnetic data (Veach, 1972) most of the ultramafic bodies are believed to be separate masses or lenses that are not connected beneath the surface. The time of emplacement of the ultramafic rocks is uncertain but has been assigned a Permian age by Tempelman-Kluit (1975).

2-3-B Clinton Creek Area

The distribution of ultramafic bodies within the mapped area is shown in Figure 2-2. There is a general lack of heavy vegetation wherever these rocks are exposed and the characteristic dark green to orange weathering blocky talus they produce can be recognized easily from a distance or from the air. Rock types include serpentinite, harzburgite, iherzolite, dunite, and pyroxenite. Most of the bodies are completely serpentinized, so it is very hard to find original olivine or pyroxene. Identification of ultramafic rocks as harzburgite, iherzolite, dunite and pyroxenite was based on relict textures and surviving original minerals. No original layering was found and mutual relationships of these rocks are practically unknown.

Serpentinite ranges in colour from dark greenish black to olive green and all stages from massive to highly sheared conditions were observed. Sugary texture is not uncommon.

Highly polished, fish scale serpentinite in thin section are antigorite, chrysotile, brucite, chlorite, talc, idocrase, magnetite, chrome spinel and chromite. Several different kinds of serpentinite are distinguished: fibre bearing serpentinite, fine grained dark green serpentinite, mesh serpentinite and sugary textured serpentinite.

2-4 ACID INTRUSIVE ROCKS

There are at least four distinct plutonic events that affected the Yukon Crystalline Plateau. The oldest period of intrusion may be represented by the Klotassin quartz diortie, dated by Tempelman-Kluit (1975) as late Triassic, but considered by Godwin (1975) to be mid-Cretaceous; Pink quartz monzonite was emplaced about mid-Jurassic; mid-Cretaceous intrusions are typified by the Coffee Creek quartz monzonite; and the youngest period involved the Nisling Range alaskite (Tempelman-Kluit, 1975).

The granodiorite of the Clinton Creek area is not exposed within the area of Figure 2-2. Two large stocks, one 10 kilometres northwest and the other 14 kilometres east, and a small stock 26 kilometres southeast of the Clinton Creek area are shown on Figure 2-1. Several small bodies are even closer to the study area. Lithologically the rocks are simi-

lar to those of the Klotassin granodiorite and quartz monzonite suite. The rock, medium grained biotite granodiorite, consists of quartz, plagioclase (oligoclase to andesine commonly with normal zoning), potash feldspar, biotite, hornblende and magnetite. Potash feldspar (22 percent) in some rocks is free from alteration but more commonly is faintly cloudy in thin section due to development of fine-grained clay minerals. Quartz (14 percent) and orthoclase are anhedral and interstitial to the plagioclase (40 percent). Plagioclase is partly altered to saussurite and serite. Hornblende (5 percent) rarely occurs in fairly well-formed prisms, but more commonly it is in plates with ragged edges and has altered in part to chlorite. Biotite (17 percent) formed as flakes, with ragged edges and as irregular and discontinuous fringes on hornblende and normally alters to chlorite.

2-5 BASALT

Two basaltic sequences are found in the Yukon Crystalline Plateau. The older is the Carmacks Group of Bostock (1936), widespread in the central part of the Yukon Crystalline Plateau. The younger is the Selkirk Volcanics. These, exposed at stream banks along the Yukon River, are Holocene ore Pleistocene in age (Bostock, 1966). The

Selkirk lavas are the product of local fissure eruptions and are roughly equivalent to Pliocene Plateau Lavas of Central British Columbia (Campbell and Tipper, 1971).

Selkirk Volcanics are exposed in the south-central part of the study area (Figure 2-2). These are fresh, undeformed columnar jointed flows (Plate 2-5), lying unconformably on the metamorphic rocks. The basalt is dense, dark gray with phenocrysts of olivine. In thin section the rock is seen to consist of labradorite, pyroxene, olivine, minor magnetite and glass. Pale brown augite occurs both as a groundmass mineral and as phenocrysts. It usually occupies a position interstitial to the plagioclase as small grains. Eudhdral olivine phenocrysts have more or less corroded borders. Much of the glass is altered to yellowish-brown palagonite.

2-6 STRUCTURE

2-6-A Introduction

Evidence of at least three phases of deformation has been observed. The earliest highly sheared isoclinal folds have been deformed during a second folding, into small, tight, recumbent folds which in turn have been refolded by

PLATE 2-5: Columnar jointed basalt of the Selkirk volcanic rocks. Columns plunge NNW at 70°. Contact with the country rock is not exposed.

an open third phase fold of regional extent. All of these structures have undergone later faulting. Measurements of linear and planar structures and determination of relative age relationships was done in the field. Analysis of such data was aided by examination of microscopic structures and stereographic projections. The most prominent feature of most units of the area is foliation parallel to compositional layering. This penetrative structure was developed during the first phase of folding as a result of tight compression and shearing which forced original bedding and axial plane foliation into near parallelism. Platy and prismatic minerals developed along foliation planes in response to metamorphism which accompanied folding. This intense deformation and metamorphism has obscured the original stratigraphic succession. Very few determinations of stratigraphic tops and bottoms have been made because sedimentary structures have been destroyed by severe deformation. Facies changes and unconformities, if present, are impossible to observe for the same reason.

Certain structural elements observed in the Clinton Creek area are listed in Table 2-2.

2-6-B Folds

Two groups of mesoscopic folds and related structural features have been observed in the field. Major fold (Figure

TABLE 2-2

STRUCTURAL ELEMENTS OF THE CLINTON CREEK AREA

Symbol	Structural Element
F_0	Bedding or compositional layering
F_1	Axial planes and axial plane cleavage of earliest isoclinal folds
L_1	Intersection of F_0 and F_1 and fold axes of earliest isoclinal folds
F_2	Axial planes and axial plane cleavage of recumbent second folds
L_2	Intersections of F_2 with F_1 and F_0, fold axes and crenulations associated with recumbent second folds
F_3	Axial plane of third phase fold
L_3	Intersections of F_3 with F_0, F_1 and F_2 and axis of the third fold

2-2) represent a third group. The first folds (L_1) have been refolded along L_2 axes and have, in turn, been folded by large scale L_3 fold along its axis.

Only a few first phase folds (L_1) are exposed in the Clinton Creek area. This group has parallel to sub-parallel limbs and axial planes. An example of this first deformation is shown in Plate 2-6. Gleitbrett structures (Plate 2-7) are quite common, especially in schistose rocks. Massive units like quartzite and massive greenstone were also tightly folded but, in these, foliation (F_1) is not well developed. Compositional layering is not everywhere sheared and dislocated; relict fold closures are preserved in relatively competent rocks like sandstone and limestone (Plate 2-8). Most of such structures were destroyed in less competent schistose rocks. Lineations associated with L_1 folds are seen as small fold axes, intersection of bedding (F_0) and foliation (F_1) and aligned minerals. These are best seen in phyllitic schist and argillitic sandstone units. Due to the scarcity and unequal distribution of outcrops it is impossible to divide the area into different domains of approxiamte homogeniety with respect to fold system. L_1 fold axes, which have been modified by the second and third phase folds, are shown in Figure 2-5. Most of the axial planes of L_1 fold set approach the horizontal but the dip can be as high as 20°. Typical L_1 folds and associated F_0, F_1 foliations, sketched in the field, are shown in Figure 2-6.

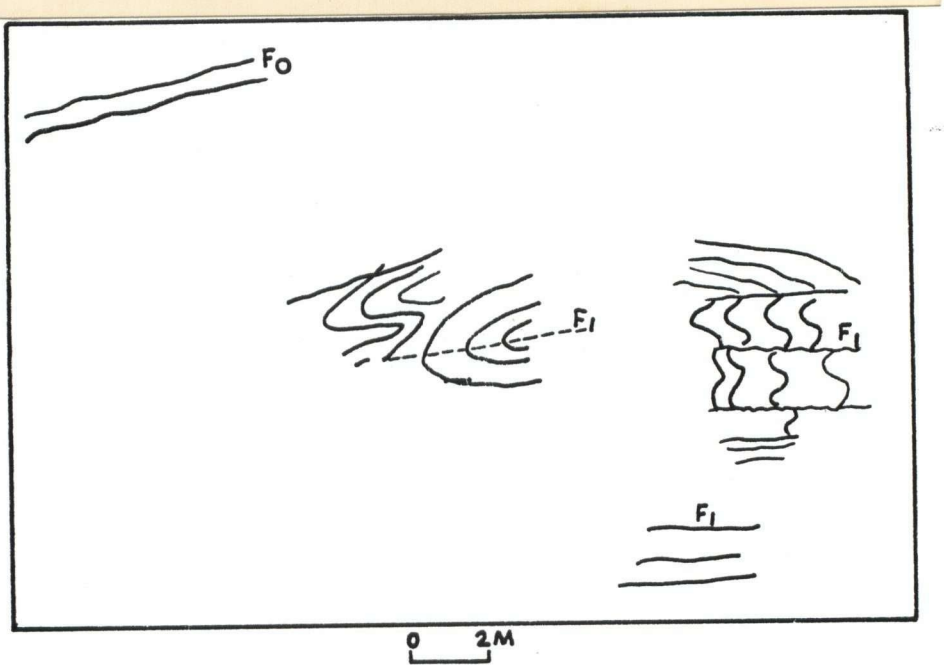

PLATE 2-6: Tight isoclinal folds in carbonaceous argillite, where F_1 parallels F_0. Although continuity of some layers is well preserved, in many places layers are cut into short segments.

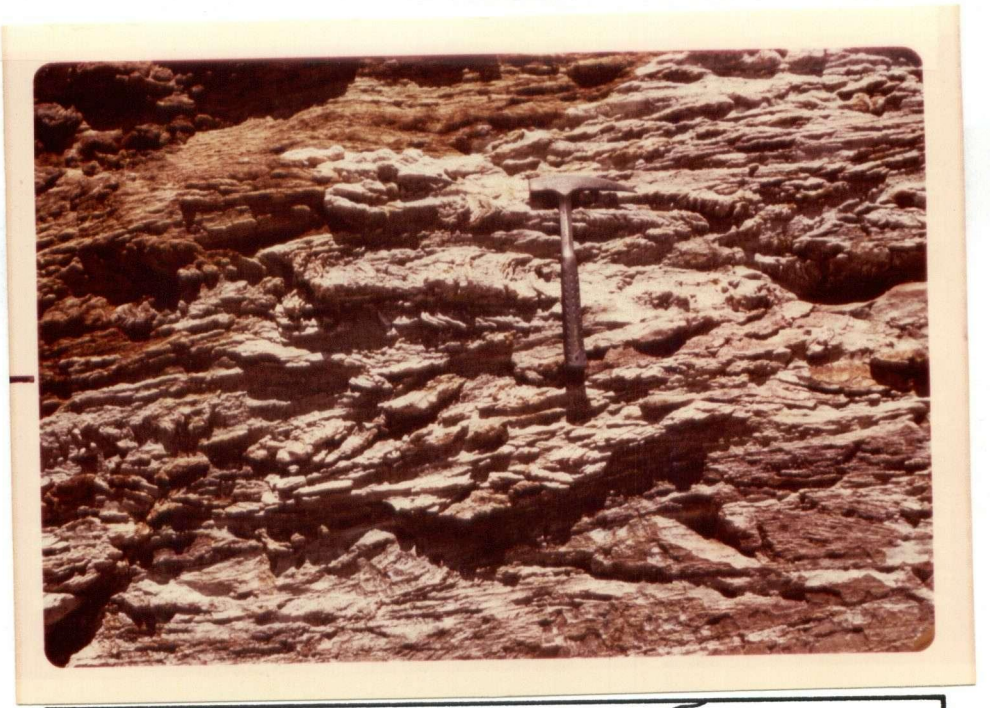

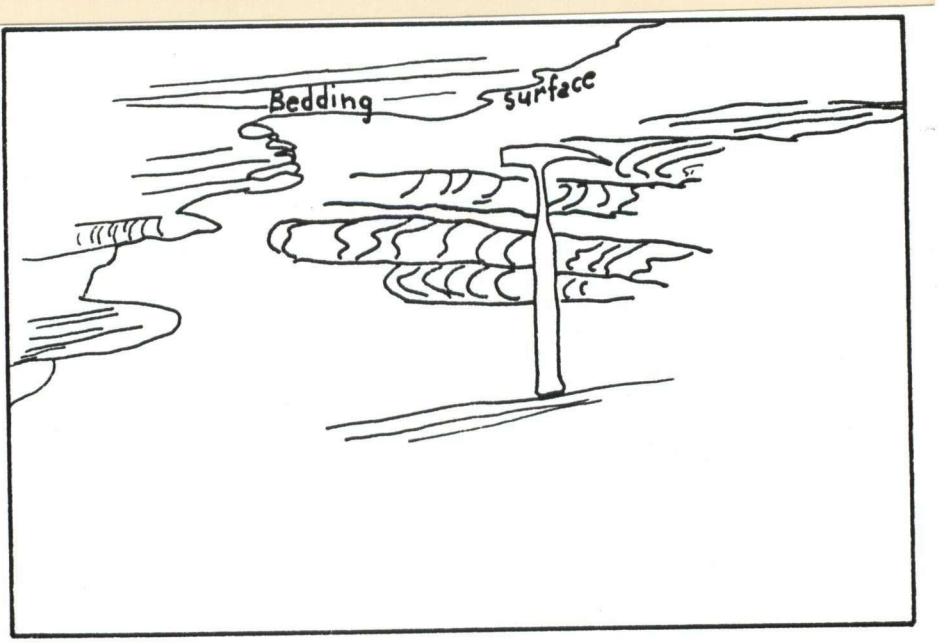

PLATE 2-7: Gleitbrett structure in schistose rocks. This style of deformation associates mainly with first phase of folding. Note bedding surface between iron-stained beds and siliceous beds.

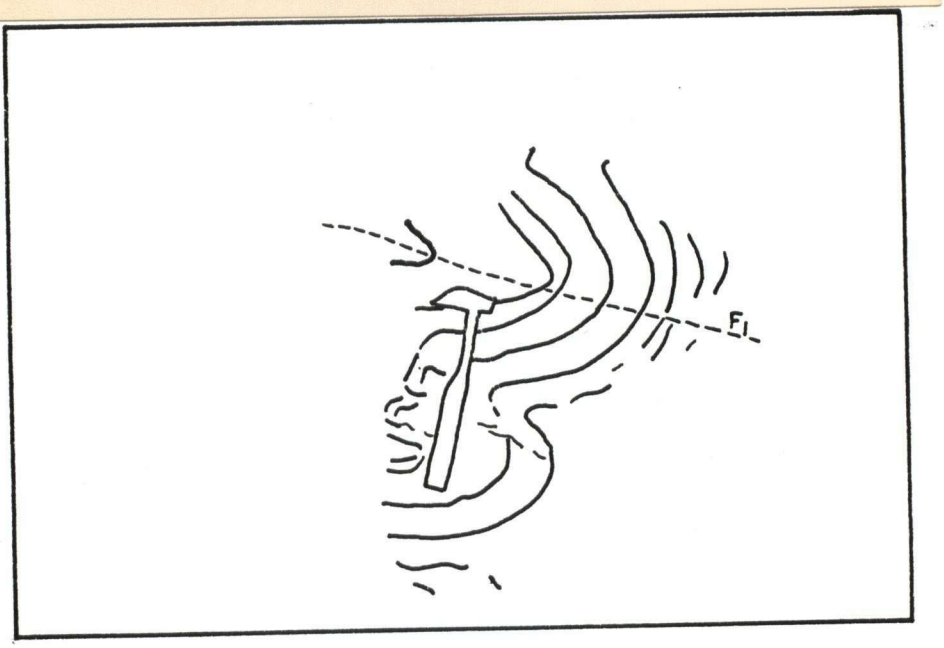

PLATE 2-8: Relict of L_1 fold closures in the enclosing argillitic sandstone. Fold wavelength of this type is rarely greater than two metres.

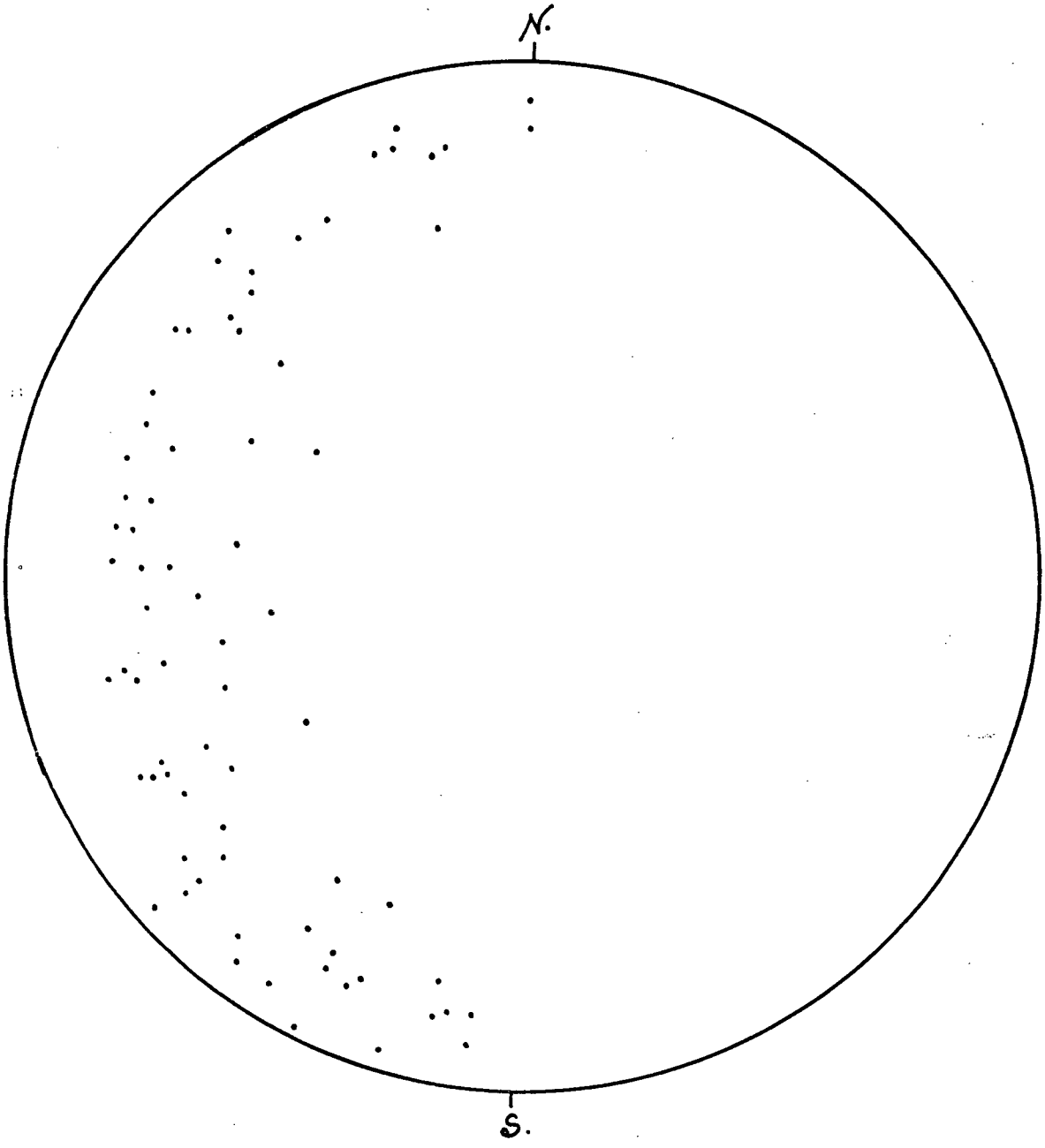

FIGURE 2-5: DISTRIBUTION OF 73 L_1 LINEATIONS.

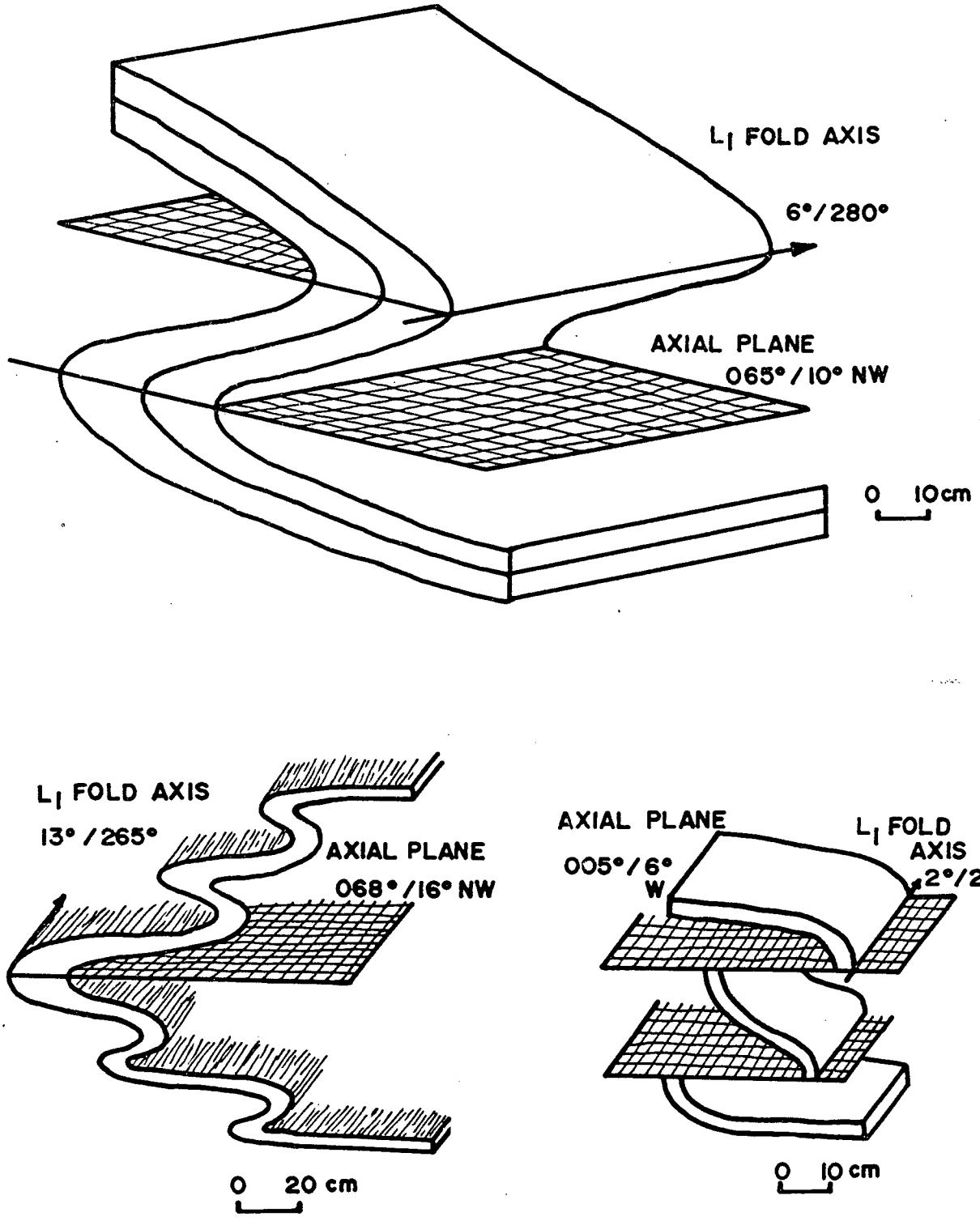

FIGURE 2-6: FIELD SKETCH OF FIRST PHASE FOLDS.

In the second group of folds, F_0, F_1 and L_1 are deformed about axial surfaced F_2. Cheveron folds (Plate 2-9) and crenulations (Plate 2-10) are common in this group of folds. In well bedded units overturned L_2 folds are observed. Associated foliation (F_2) lies at a large angle to F_1 or F_0 (Plate 2-11) in some cases. F_2 is generally parallel to the axial planes of the overturned L_2 folds. Lineations L_2 are commonly fine crenulations (Plate 2-10), axes of small folds or intersection of F_0 or F_1 with F_2 (Plate 2-11). Examples of L_1 folds refolded by L_2 folds are not seen. Field sketches of L_2 folds and related structures, with their orientations, are illustrated in Figure 2-7. Axial planes (F_2) can be divided into two domains (Figure 2-2), north and south in which F_2 shows different orientations. Most axial planes and foliations (F_2) are nearly horizontal or dip either about 20° northeasterly or 30° southwesterly (Figure 2-8). Lineations and fold axes of L_2 plunge at about 15° westerly (Figure 2-9). In addition to the mesoscopic folds described above, mapping shows the presence of L_2 recumbent folds with lengths of 600 to 900 metres (Figure 2-2).

A regional gentle open antiform of the third group, with related joints and fractures, deforms the previously mentioned structures. The data of Figure 2-8 suggest that the axis of L_3 is about horizontal and trends northwesterly. This fold is shown on Figure 2-2.

PLATE 2-9: L_2 chevron folds shown by yellow sandstone beds in carbonaceous argillite. Foliation planes F_2 in argillite are parallel to axial plane of the chevron fold.

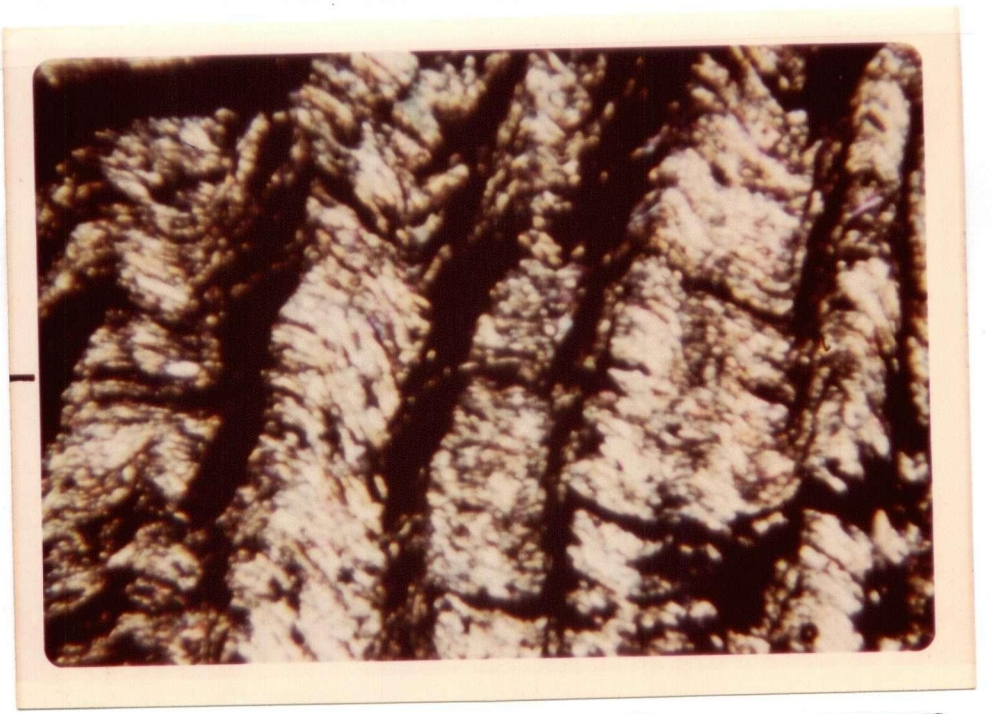

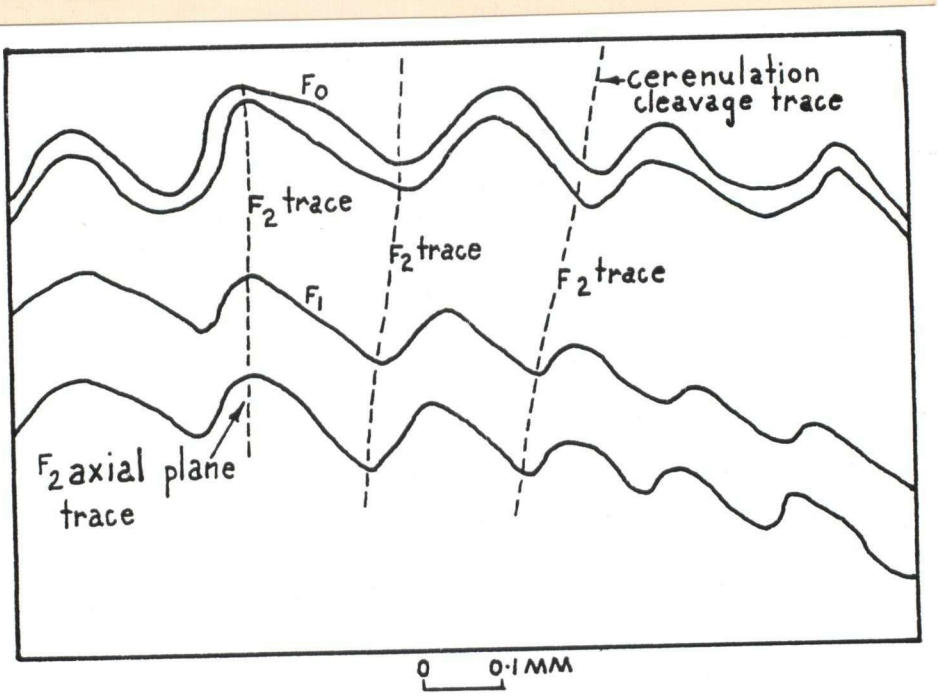

PLATE 2-10: Crenulations related to L_2 fold. Crenulation cleavage parallels to axial plane of small fold in quartz-muscovite schist. In the outcrop, F_2 is gently dipping.(Crossed nicols.)

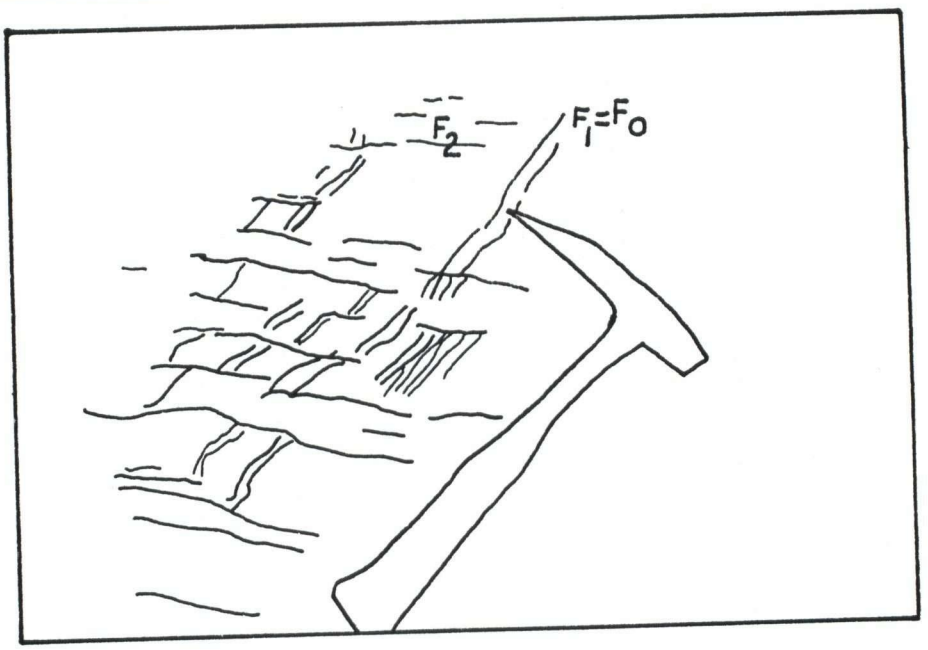

PLATE 2-11: Foliation F_1 and F_2 in quartz-muscovite schist. L_2 is marked by the intersection of F_1 and F_2.

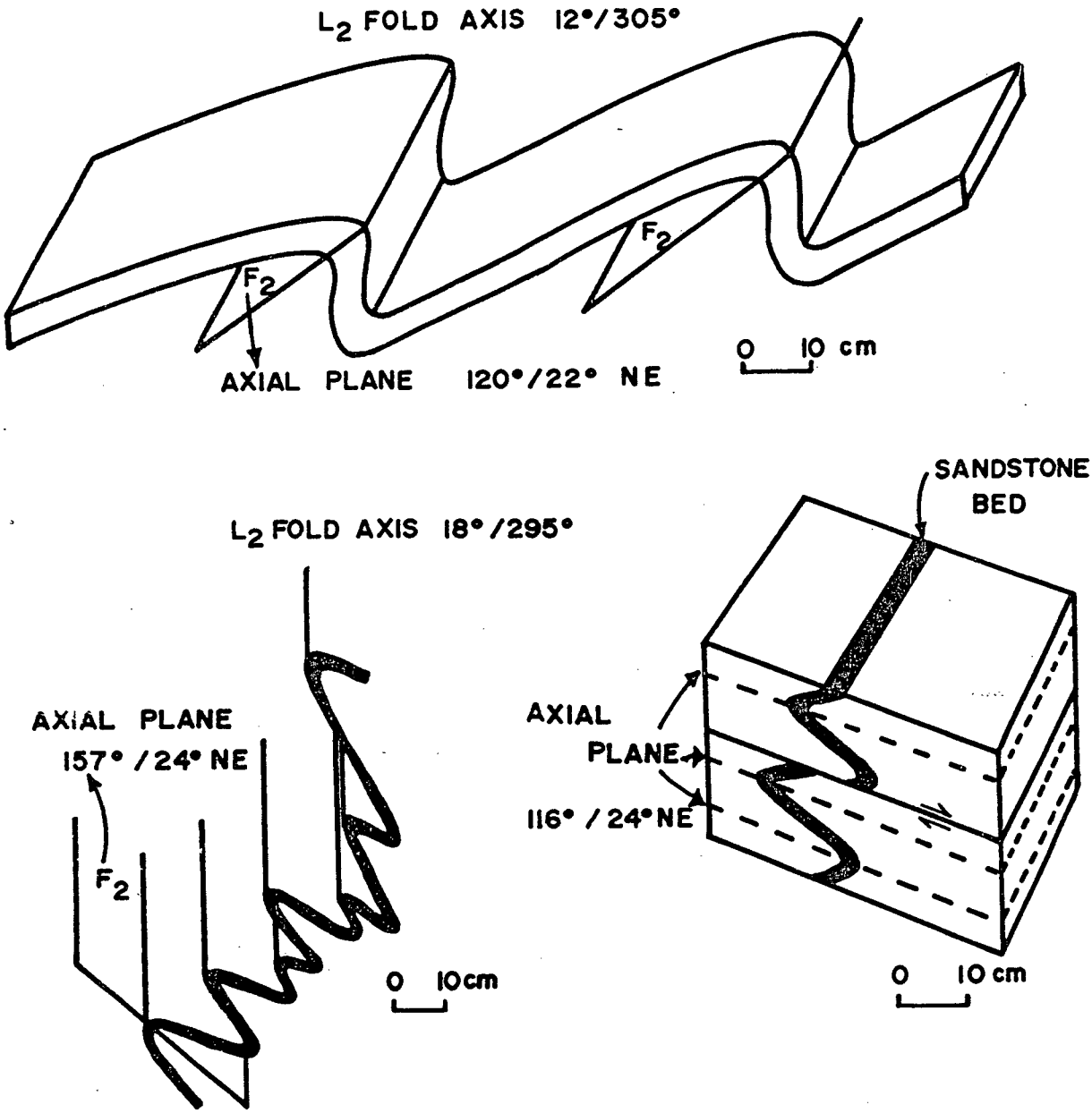

FIGURE 2-7: FIELD SKETCH OF SECOND PHASE FOLDS.

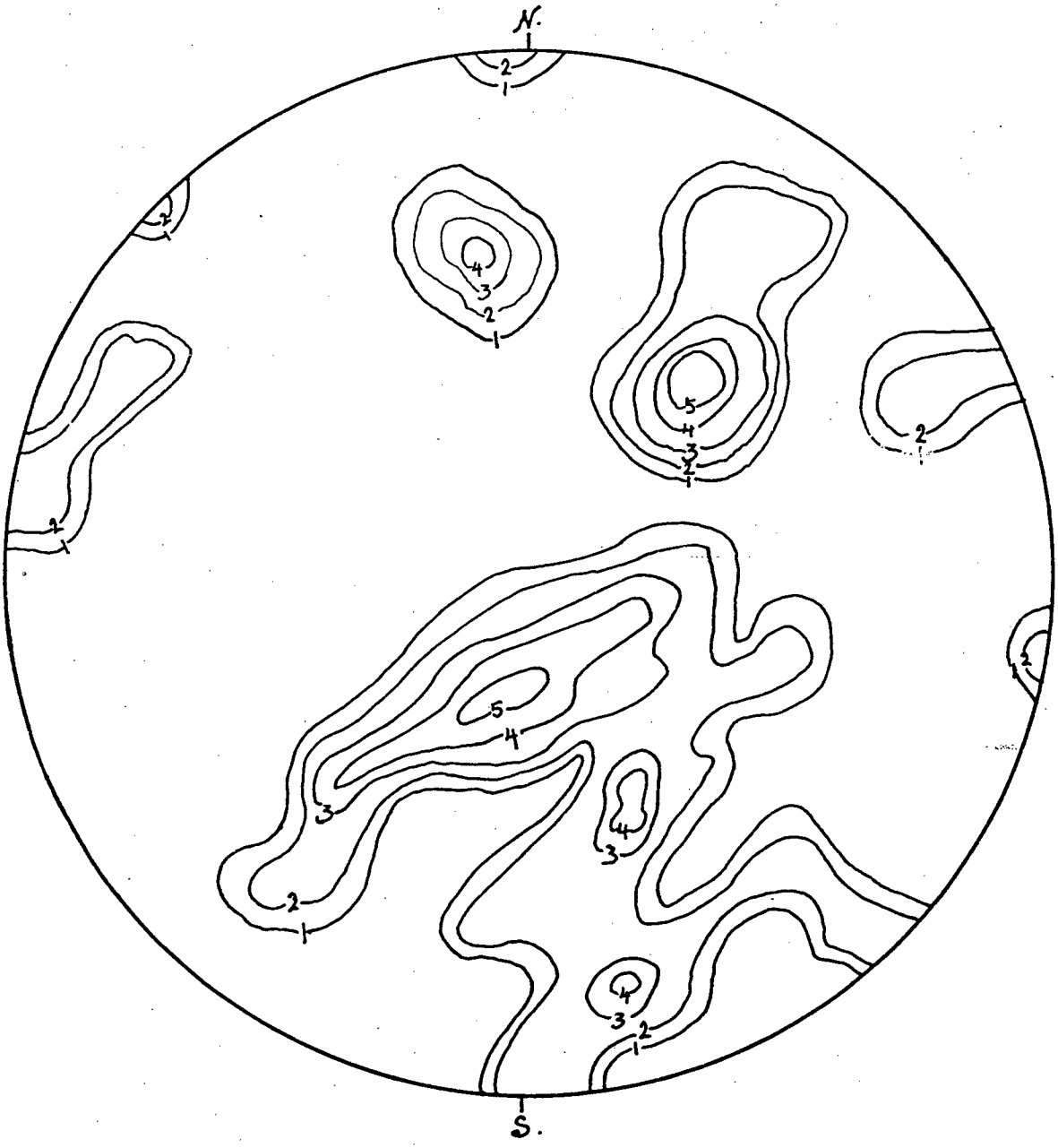

FIGURE 2-8: POLES TO 75 (F_2) FOLIATIONS AND AXIAL PLANES.

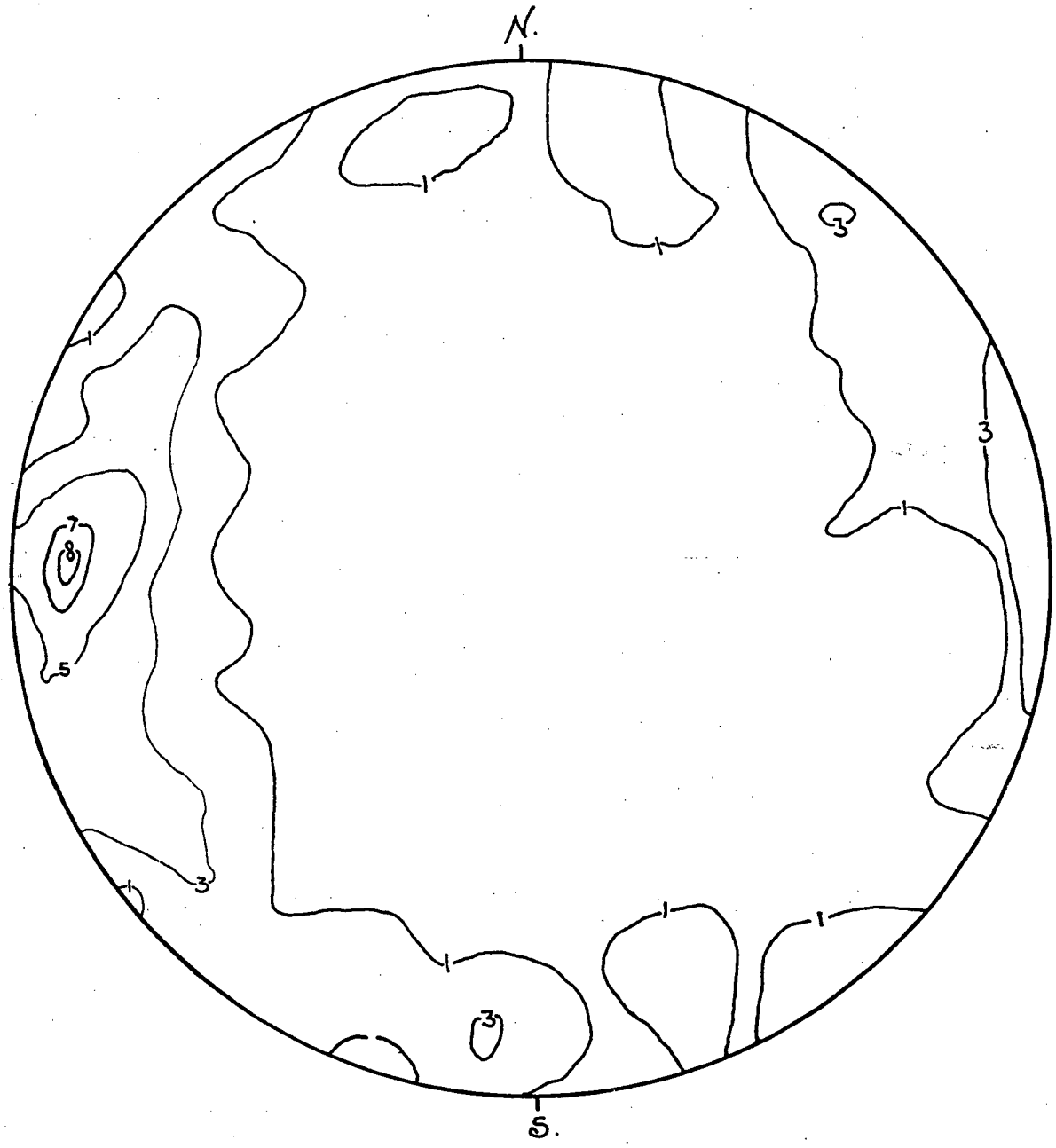

FIGURE 2-9: POLES TO 123 L_2 LINEATIONS.

2-6-C Faults

Rocks of this area have been faulted extensively both during and after the three phases of deformation described above. Many faults show small dislocations of only a few centimetres but major ones with displacement of probably 20 to 30 metres have been identified. Large faults are seen only as lineaments across which lithologic contacts are displaced. Mesoscopic faults have been observed in many localities (Plate 2-12, 2-13) in the study area, particularly in mine walls and road cuts. The frequency of faulting in these exposed areas suggests that such faulting is common throughout the Clinton Creek area.

Lineaments detected in the field and on aerial photographs have been interpreted as probable faults. Such an interpretation is confirmed by the presence, on the ground, of minor faults and breccia zones, and displaced lithologic units and structures. In rare cases, these lineaments have been shown to be fault lines by diamond drilling and mining (Plate 2-13). Such evidence indicates that many faults trend 130° to 160°.

Comparison of Figure 2-8 and 2-10 shows that many of the faults of the area are parallel to F_2 foliations. A group of northeasterly dipping faults cannot, however, be related to any other structural features. Some displacement of lithologic unit is evident on some of these faults,

PLATE 2-12: Minor fault displacing rodingite body surrounded by serpentinite, in the Porcupine pit. (Hammer produces scale.)

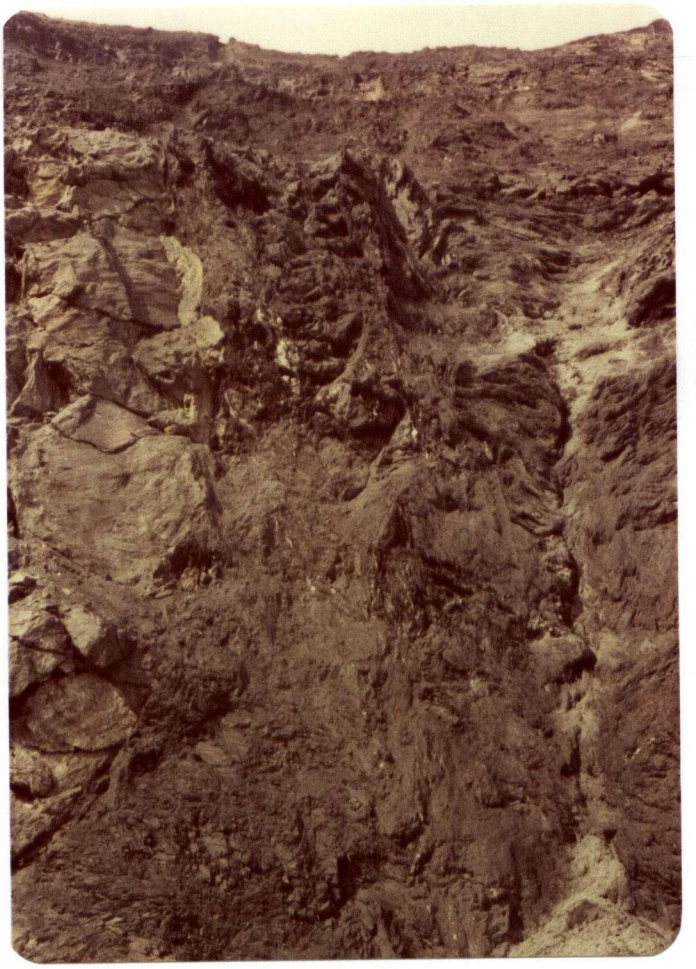

PLATE 2-13: Northerly trending vertical fault with considerable displacementin the Porcupine pit. The fault surface is curved. Relatively clean and light rock on the left is serpentinite and dark and dirty looking rock on the right is argillite. (The height of the wall is about 20 metres.)

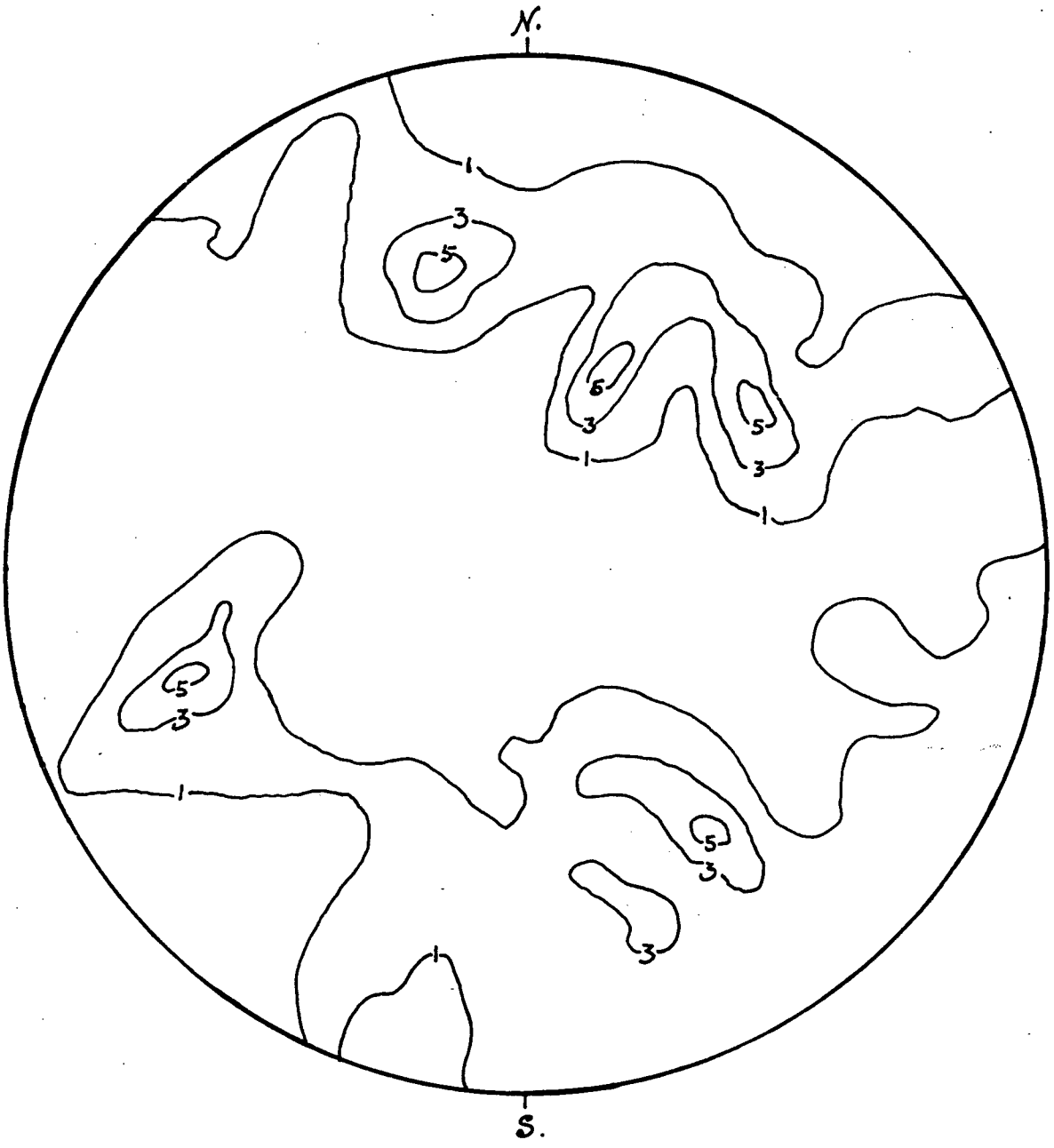

FIGURE 2-10: POLES TO 66 FAULTS.

but generally magnitude of movement is unknown.

2-6-D Joints

Joints have been observed in all outcrops. A stereographic projection of measured joints (Figure 2-11) indicates at least five sets. One (A) strikes 150° and dips almost vertically, another (B) strikes 000° to 20° and dips 80° to 90° both easterly and westerly, a third (C) strikes 080° and dips vertically, a fourth (D) strikes 115° and dips 70° southerly and a fifth (E) strikes 060° and dips vertically. Age relationship of joint sets to different phases of deformation is uncertain. In general, joints trending 115°(D) contain the axis of the third phase fold and probably represents its axial plane. The one trending 150° is parallel to the Tintina Trench.

2-6-E Regional Structure

The rocks are considered to lie in chronological order as stated previously, based mainly on isotopic age determinations (see chapter two, section seven) and fossil evidence. The argillite and limestone of the area are similar to those where a probable Devonian fossils were found,about eight kilometres northwest of the Clinton Creek area. Quartz-muscovite-biotite schist, quartz-muscovite schist and greenstone of the area yielded an Ordovician radiometric age.

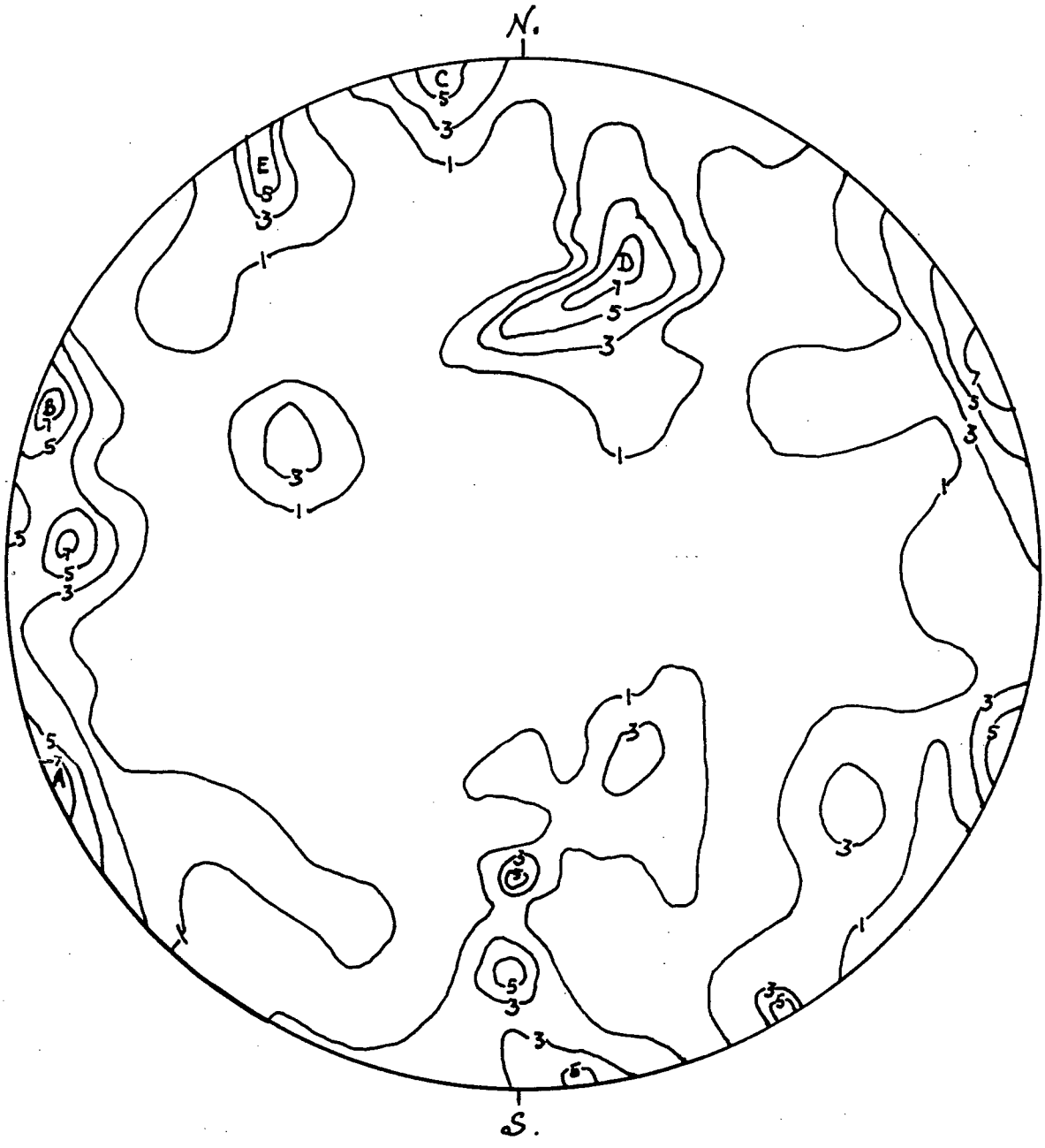

FIGURE 2-11: POLES TO 133 JOINTS. (Joints measured in the mine are not included.)

However, the cross section (Figure 2-2) of the study area reveals, the oldest rock, quartz-muscovite-biotite schist, at the top and the youngest meta-sedimentary rock, argillites and limestone at the bottom. Hence, the area is interpreted as a part of a gigantic overturned fold.

2-7 ISOTOPIC AGE DETERMINATIONS

2-7-A Introduction

Clinton Creek is in the northwestern portion of the Yukon Crystalline Plateau (Douglas et al., 1970) in the Yukon Territory (Figure 1-1). The Yukon Metamorphic Complex (Tempelman-Kluit, 1974) consists of metasedimentary and metavolcanic rocks that are continuous with the Birch Creek schists of Alaska (Foster, 1973). The metamorphic rocks near Clinton Creek (Figure 2-1) are similar to the rocks of west-central Yukon where Cairnes (1914) first described Yukon Group. Within this group different lithologic divisions are recognized. McConnell (1905) defined the Pelly gneiss which is in the northern part of the Stewart River map sheet, the Klondike schist in the Klondike gold-field which is immediately south of Dawson City and the Nasina quartzite which occurs prominently in the northernmost part of the Stewart

River map area. All these type localities are just south and southeast of the Clinton Creek area. Green (1972) noted the continuation of the Nasina quartzite and Klondike schist into the Clinton Creek area. These metamorphic rocks generally have been thought to be of Precambrian age. However, limestones associated with metasedimentary rocks just west of the Yukon River at the Alaska Boundary (Figure 2-1: at 64°39.5'N, 140°57.5'W) contain crinoid ossicles and echinoderm columnals that indicate a Paleozoic age (Mertie, 1937; Douglas, et al., 1970; Green, 1972). Tempelman-Kluit (1976) has speculated that many of the metamorphic units might be equivalent to parts of the Englishman's Complex and Big Salmon Complex (Figure 2-3) of the Pelly Platform which are of Upper Paleozoic age (Mulligan, 1963).

No geochronometric data exist for Cairnes (1914) type area. Therefore, eight samples (Table 2-3 and 2-4) of the metamorphic rock, equivalent lithologically to Nasina quartzite and Klondike schist, were collected in the Clinton Creek area during 1975 and 1976 (Figure 2-12). One sample (Table 2-3) was also obtained from a granodiorite stock near the western edge of Figure 2-12. These samples were analysed to provide estimates of the age of deposition, major metamorphism and post-metamorphic intrusion.

TABLE 2-3

POTASSIUM-ARGON ANALYTICAL DATA[a]

Sample No.[b]	Location[b] Lat.(N);	Long.(W)	Rock unit : Rock name[b]	Mineral dated	%K ± S[c]	$^{40}Ar^{*}$[d] / ^{40}Ar total	$^{40}Ar^{*}$[d] (10^{-5} cm^3STP/g)	Apparent age(Ma)[e]	Time
SP 21A	64°27'	140°54'	Kb : biotite granodiorite	biotite	5.60 ±.01	0.812	1.475	64.9±2.3	Late Cretaceous[f,g]
MH 62	64°27.5'	140°41.2'	Pzq: amphibolite	hornblende	0.152±.001	0.629	0.182	278 ±10	Early Permian[f]
MH 105	64°29'	140°45.5'	Pzq: quartz-muscovite schist	muscovite	6.06 ±.06	0.910	6.31	245 ±8	Early Permian[f]
MH 122	64°24'	140°40'	Pzg: greenstone	hornblende-actinolite	0.674±.009	0.898	0.542	191 ±7	Early Jurassic[f]

a. All analyses done in Geochronology Laboratory, Department of Geological Sciences, The University of British Columbia, K by K.L. Scott, Ar by J.E. Harakal.
b. See Figure 2-12.
c. 'S' is one standard deviation of quadruplicate analysis.
d. $^{40}Ar^{*}$ means radiogenic argon.
e. Constants used in model age calculations: $K\lambda_e = 0.585\times10^{-10}yr^{-1}$; $K\lambda_\beta = 4.72\times10^{-10}yr^{-1}$; 40K/K = 0.0119 atom percent.
f. Time designation after Armstrong (1978).
g. Time designation after Obradovich and Cobban (1974).

TABLE 2-4

RUBIDIUM-STRONTIUM DATA FOR ANALYSED WHOLE ROCK SAMPLES[a]

Sample No.[b]	Location[b] Lat.(N);	Long.(W)	Rock unit : Rock name	Rb (ppm)	Sr (ppm)	Rb^{87}/Sr^{86}[c]	Sr^{87}/Sr^{86}[d]
MH 61	64°26.8'	140°41.3'	Pzq : quartz-muscovite schist	80.0	41.2	5.63	0.7279
MH 81A	64°25.4'	140°38.7'	Pzg : quartz-muscovite-chlorite schist	69.0	25.3	7.90	0.7330
MH 101	64°29.4'	140°45'	Pzg : greenstone	1.8	278	0.019	0.7080
MH 105	64°29'	140°45.5'	Pzq : quartz-muscovite schist	27.1	24.1	3.25	0.7188
MH 112	64°24.7'	140°37.4'	Pzq : quartz-muscovite schist	129	63.3	5.89	0.7300
MH 112A	64°24.7'	140°37.4'	Pzqm: quartz-muscovite-biotite schist	37.7	22.5	4.85	0.7365
MH 122	64°24'	140°40'	Pzg : greenstone	122	127	2.78	0.7209
Sp 21A	64°27'	140°54'	Kb : biotite granodiorite	131	1020	0.377	0.7065

a. All analyses done in the Geochronology Laboratory, Department of Geological Sciences, The University of British Columbia by K.L. Scott.
b. See Figure 2-12.
c. One standard deviation error in measurment is (±2%).
d. One standard deviation error in measurment is (±.00015).

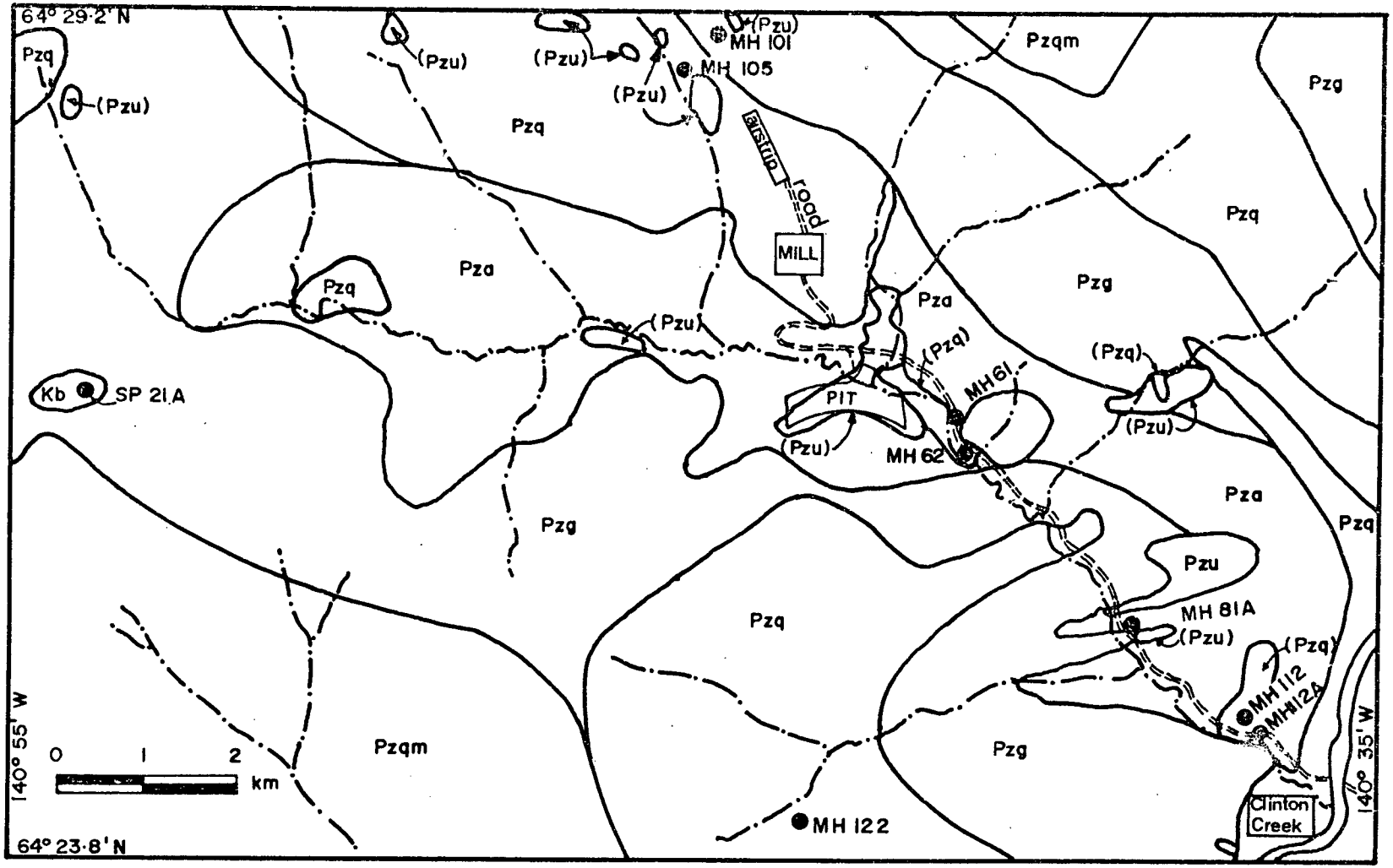

FIGURE 2-12: GEOLOGY OF THE CLINTON CREEK AREA. Kb= biotite granodiorite; Pzu= serpentinite; Pza= argillite, limestone and sandstone; Pzg= greenstone and quartz-muscovite-chlorite schist; Pzq= quartz-muscovite schist; Pzqm= quartz-muscovite-boitite schist; ● = K-Ar and Rb-Sr sample site; ⬭ = geological contact.

2-7-B Isotopic Analysis

Potassium-Argon analyses for minerals from three samples of metamorphic rock and one sample of intrusive rock are given in Table 2-3. Five whole-rock samples of schist, two of greenstone and one of granodiorite were analysed for rubidium-strontium and strontium isotopic composition; results are given in Table 2-4.

a. Potassium-Argon

The oldest potassium-argon date obtained from metamorphic rocks (Figure 2-12) is Early Permian (Table 2-3: MH 62 - 278±10 Ma) for hornblende separated from amphibolite (Pzq). The date probably closely represents the main episode of metamorphism because hornblende is the least likely mineral to suffer argon loss during later reheating or slow cooling (York and Farquhar, 1972). A date for muscovite from quartz-muscovite schist (Pzq), although muscovite is less retentive than hornblende, supports a Permian age (Table 2-3: MH 105 - 245±8 Ma) for metamorphism. The Early Jurassic date for a hornblende-actinolite mixture (Table 2-3: MH 122 - 191±7Ma) from greenstone (Pzg) provides, at best, a minimum age of metamorphism. In thin section this hornblende exists as relatively coarser-grains and actinolite as finer grains mixed with epidote, a product of alteration of the hornblende.

Hence, the date (191±7 Ma) may not be the age of metamorphism, but a result of partial or total argon loss during later retrogressive alteration.

Biotite granodiorite (Kb), sausurutized but with fresh biotite, was sampled from a stock that intruded the metamorphic rocks (Figure 2-12). The biotite yielded a latest Cretaceous-earliest Tertiary date (Table 2-3: Sp 21A - 64.9± 2.3 Ma). This is distinctly younger than crystallization of the metamorphic rocks. This rock is mineralogically similar to Nisling Range granodiorite, but the date is within the range of dates for the Nisling Range alaskite suite (Tempelman-Kluit, 1975).

b. Rubidium-Strontium

Rubidium-strontium analysis, listed in Table 2-4, are plotted and interpreted in Figure 2-13. An isochron (Figure 2-13: line A[1]) can be obtained from two greenstone samples (MH 101 and MH 122) and four schist whole rock samples (MH 61, MH 81A, MH 105, MH 112). The Permian age (255.8±22.3 Ma) indicated is comparable to the metamorphic age defined by potassium-argon analysis (Table 2-3: 245±8 to 278±10 Ma). This is further illustrated in Figure 2-13 by line B which is a reference line drawn using the initial ratio indicated by

---

1: Best fit line (line A) is drawn by using Least Square Regression Treatment, Model I of York (1967).

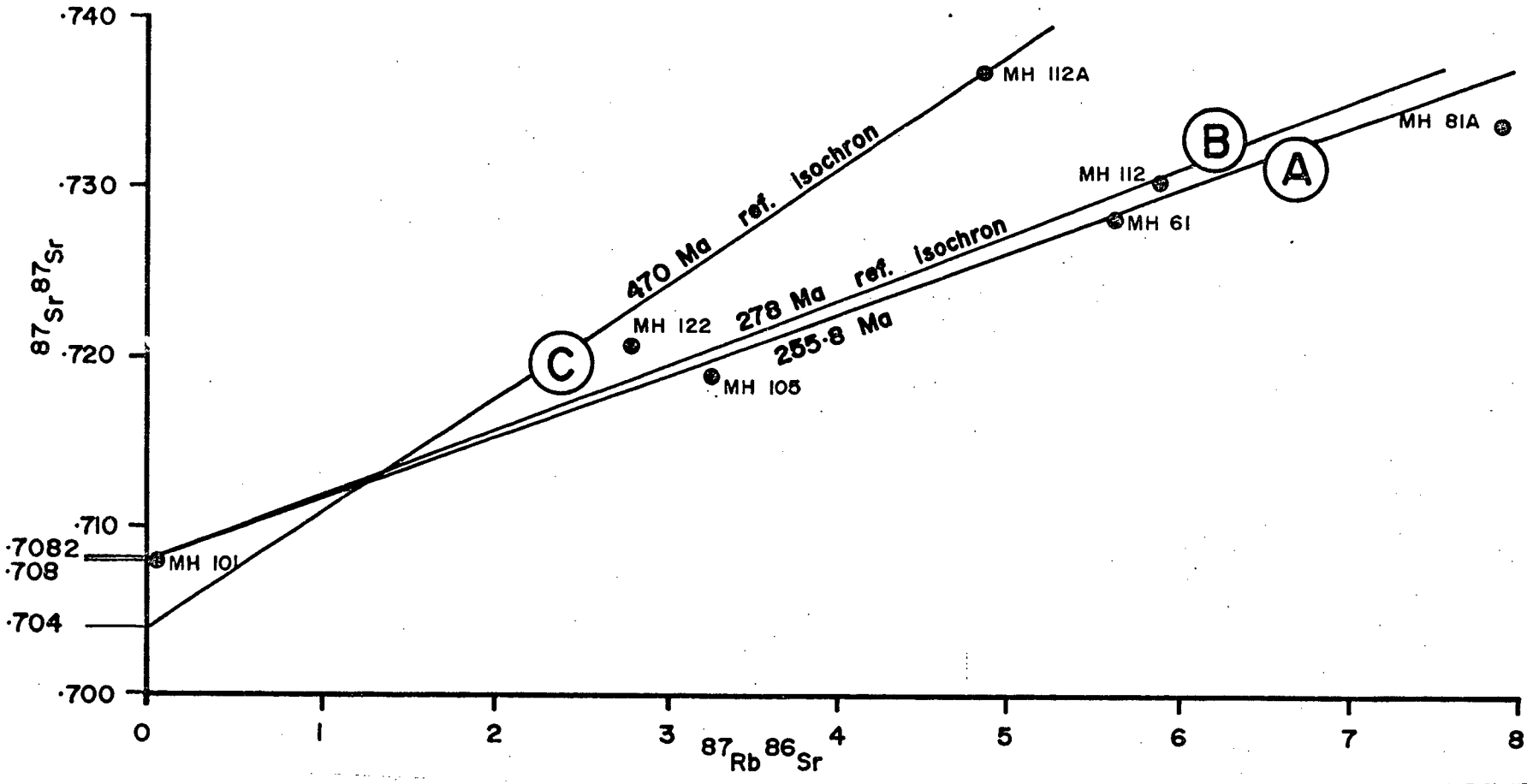

FIGURE 2-13: PLOT OF $^{87}Sr/^{86}Sr$ vs. $^{87}Rb/^{86}Sr$ FOR WHOLE ROCK ANALYSES OF SAMPLES FROM THE CLINTON CREEK AREA, YUKON TERRITORY. Line A represents the best fit line for Clinton Creek data (MH 112A omitted) and reflects metamorphic resetting. Line B is a reference line based on the oldest K-Ar date (278 Ma.) and initial ratio indicated by MH 101. Line C is model, probably minimum, deposition age (Ordovician) for schists of the Clinton Creek area based on MH 112A and an assumed low initial $^{87}Sr/^{86}Sr$.

the rubidium-poor greenstone sample (Table 2-4: MH 101) and a slope given by the oldest metamorphic date determined by potassium-argon (278±10 Ma). Initial ratios defined by lines A and B are 0.7082 and 0.7080, respectively, and are higher than the initial ratio 0.7040 assumed for line C. Initial ratios of 0.7040 to 0.7060 would be expectable for Paleozoic eugeosynclinal sediments. The high initial ratios of lines A and B probably reflect widespread, extensive metamorphic resetting (Hart, 1962).

An Ordovician whole-rock date is possible for one sample is markedly different isotopically from the other six samples analysed (Table 2-4 and Figure 2-13). A model date of 470 Ma (Figure 2-13: line C) is obtained if an initial ratio of 0.7040 is assumed. Support for such an age comes from a whole rock isochron of 465 Ma obtained for metamorphic rocks from the Yukon Metamorphic Complex near the Casino porphry deposit, about 250 kilometres south-west of Clinton Creek (Godwin and Armstrong, 1978, personal communication).

Rubidium-Strontium data for biotite granodiorite (Sp 21A) is listed in Table 2-4. As the rock is different from other dated (Rb-Sr) rocks in origin and time, it is not included in calculating the isochrons in Figure 2-13.

2-7-C Regional Synthesis

Clinton Creek data may be compared to regional iso-

topic data (K-Ar and Rb-Sr) collected by other workers from the northern part of Yukon Crystalline Plateau. The area considered, shown in Figure 2-3, is bounded on the northeast by the Tintina Trench and on the southwest by the Shakwak-Denali fault. Documentation for dates discussed here is in Table 2-5.

The 67 isotopic dates in Table 2-5 are plotted in the histogram of Figure 2-14. In this figure distinct grouping of igneous activity at 45 to 75 Ma (open circle) and 85 to 120 Ma (closed circle) are apparent. In addition, mixed igneous and metamorphic dates scatter in the 135 to 205 Ma range (open and closed squares); three additional dates, possibly extend this distribution to 280 Ma (open diamond). A plot of these dates by symbol onto Figure 2-15 indicates that there may be a general pattern of younging away from the Tintina Trench, a major structure in the Yukon Territory. Although the trench is still enigmatic, Roddick (1967) described it as a transcurrent fault with right lateral movement of 400 kilometres and Tempelman-Kluit (1972) noted that there occurred three separate periods of movement. The earliest recorded movement occurred in Early Triassic time along steep southwest-dipping faults with vertical displacement that might have transcurrent component. The second movement occurred during mid-Cretaceous time and the third during Eocene or Oligocene time (Tempelman-Kluit, 1976).

TABLE 2-5

RELATIONSHIPS OF ISOTOPIC DATES AND ITS PERPENDICULAR DISTANCE FROM THE TINTINA TRENCH OF THE YUKON CRYSTALLINE PLATEAU

Sample No.	Material Dated	Rb-Sr Date(Ma) Metamorphic	Rb-Sr Date(Ma) Igneous	K-Ar Date(Ma) Metamorphic	K-Ar Date(Ma) Igneous	Distance(km)	Reference
1	Biotite				48.9	216	I
2	Biotite				50.8	216.5	I
3	Biotite				51.7	196.5	I
4	Biotite				52.7	217	I
5	Biotite				51.6	215	I
6	Biotite				58	236.5	I
7	Biotite				58	256	I
8	Hornblende				55.4	216	I
9	Biotite				55.7	164.5	I
10	Whole rock				58.4	143	I
11	Biotite				64.9	14	II
12	Biotite				65	215.5	I
13	Hornblende				67.3	190	I
14	Biotite				67.6	200.5	I
15	Analyses ave.				70.3	121	III
16	Biotite				89.1	133.5	I
17	Biotite				85.2	234.5	I
18	Biotite				93.8	149	I
19	Biotite				93.7	104	I
20	Hornblende				92	127	I
21	Biotite				91.5	103	I
22	Biotite				92	103.5	I
23	Biotite				94.4	205	I
24	Biotite				95	123	I

Table 2-5 (continued):

Sample No.	Material Dated	Rb-Sr Date(Ma) Metamorphic	Rb-Sr Date(Ma) Igneous	K-Ar Date(Ma) Metamorphic	K-Ar Date(Ma) Igneous	Distance(km)	Reference
25	Horblende				92	104.5	I
26	Biotite			93		121	III
27	Biotite			97.6		64	I
28	Analyses ave.				99.3	121	III
29	Biotite				99.6	94	I
30	Hornblende				99	123	I
31	Hornblende				100.8	210	I
32	Hornblende				103	122	I
33	Whole rock		105			128	III
34	Biotite				117	127	I
35	Biotite				137	121	I
36	Muscovite			138		12.5	I
37	Biotite			140		229	I
38	Biotite			137		88.5	I
39	Biotite			147		202	I
40	Biotite			164		93.5	I
41	Muscovite			168		92	I
42	Biotite			161		97	I
43	Muscovite			160		97	I
44	Muscovite			175		46	I
45	Biotite			187		101.5	I
46	Horblende			181		101.5	I
47	Biotite			182		106.5	I
48	Muscovite			178		106.5	I
49	Biotite			202		42.5	I
50	Hornblende			191		14	II
51	Hornblende			278		14	II
52	Muscovite			245		14	II

Table 2-5 (continued):

Sample No.	Material Dated	Rb-Sr Date(Ma) Metamorphic	Rb-Sr Date(Ma) Igneous	K-Ar Date(Ma) Metamorphic	K-Ar Date(Ma) Igneous	Distance(km)	Reference
53	Biotite				160	182	I
54	Biotite				160	135.5	I
55	Hornblende				165	141.5	I
56	Biotite				164	165	I
57	Biotite				166	134	I
58	Hornblende				174	135.5	I
59	Hornblende				174	131	I
60	Biotite				174	81.5	I
61	Hornblende				190	165	I
62	Biotite				176	224	I
63	Biotite				177	81.5	IV
64	Biotite				180	81.5	IV
65	Hornblende				199	130	I
66	Whole rock		165			128	III
67	Whole rock	255.8				14	II

I: Tempelman-Kluit and Wanless (1975); II: See chapter two, section seven; III: C.I. Godwin(1975); IV: W. Pearson (1977)

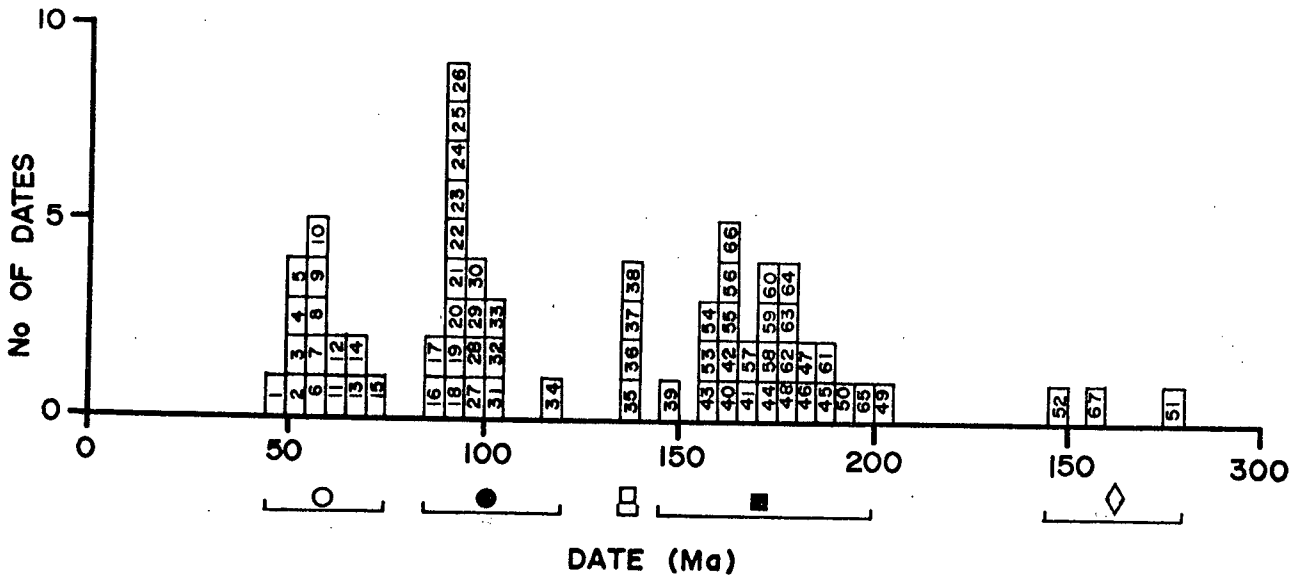

FIGURE 2-14: HISTOGRAM OF K-Ar AND Rb-Sr DATES OF IGNEOUS AND METAMORPHIC ROCKS OF THE YUKON CRYSTALLINE PLATEAU. (Numbers within histogram refer to date listing of Table 2-5.)

Distance-date trends are analysed further in Table 2-5 and Figure 2-15. Igneous rock dates in the 45 to 75 Ma and 85 to 120 Ma groups in the histogram of Figure 2-14 appear to cluster near 200 kilometres (Figure 2-15: Line A) and 100 kilometres (Figure 2-15: line B) respectively. Otherwise dates for line A and B in Figure 2-15 scatter along both lines from near the trench to a distance of 250 kilometres.

Metamorphic and igneous rocks with dates ranging from 135 to 230 Ma, however, show a distinct younging trend away from the Tintina Trench (Figure 2-15; line C: number of data(n) = 27; correlation coefficient(r) = -0.627; slope(m) = -0.199; standard deviation on $Y(S_y)$ = 17.3; standard deviation on $X(S_x)$ = 54.6; migration rate = 0.5 cm/yr). Line C, the best fit line through the data suggests that the date at the Tintina Trench is about 200 Ma, and 250 kilometres perpendicularly from the Trench is near 150 Ma. The apparent horizontal rate of isotherm migration is about 0.5 cm/yr.

Younging of intrusive events have been related to Benioff zoned by numerous writers (Dewey and Bird, 1970; James, 1971). Thermal zone migration at the rate of 0.5 cm/yr is compatible with those shifts attributed to Benioff zone induced magmatism elsewhere (Godwin, 1975). Therefore, the possibility that line C in Figure 2-15 might reflect migrating igneous activity above a Benioff zone is an attractive one. Foster (1974) suggested that the Tintina Trench marked a plate boundary for the juxtaposition of markedly different

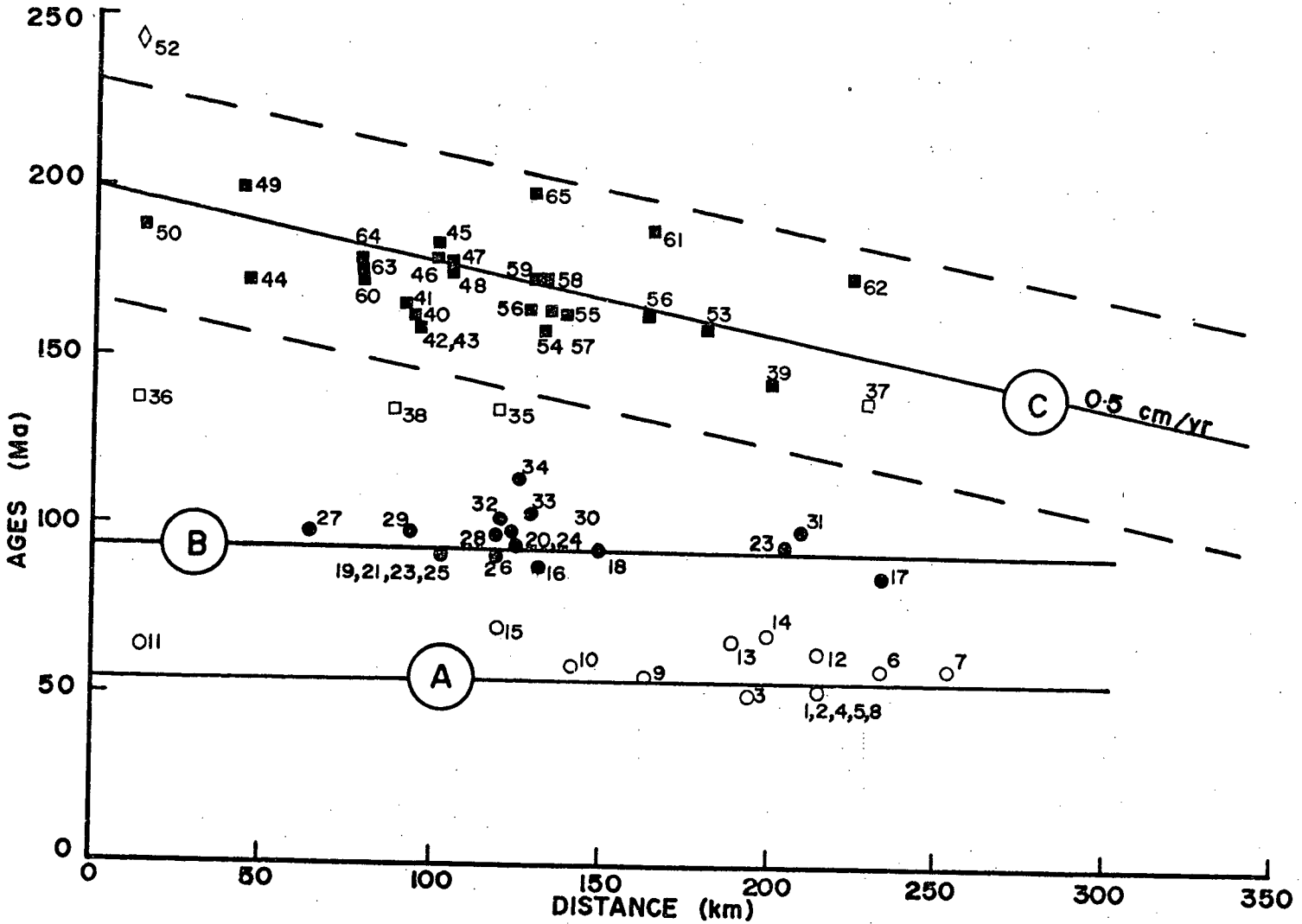

FIGURE 2-15: K-Ar AND Rb-Sr DATES OF IGNEOUS AND METAMORPHIC ROCKS OF THE YUKON CRYSTALLINE PLATEAU VS. PERPENDICULAR DISTANCE FROM THE TINTINA TRENCH. Line A represents widespread igneous activity around 60 Ma. Line B represents widespread igneous activity around 95 Ma. Line C represents a younging of dates away from the Tintina Trench from early Triassic to early Cretaceous time. Number of points (n) used to define line C is 27. Correlation coefficient (r) for line C is -0.627. Sample nos., symbols and references are in Figure 2-14 and Table 2-5 respectively. (Sample 51 and 67 excluded.)

terranes on each side of the great length of the Tintina fault system. However, more data is needed to confirm the speculation that the Tintina Trench represents an extinct suture and vanished ocean.

2-7-D Summary

The pre-metamorphic age of a schist of the Yukon Metamorphic Complex near Clinton Creek is possibly Ordovician (470 Ma by Rb-Sr). This is tenously based on one whole rock sample and an assumed initial ratio. However, the age is supported by unpublished data from the Casino area and by Tempelman-Kluit (1976) who suggested the Nasina quartzite and Klondike schist are Paleozoic in age, namely Ordovician to Mississippian.

Potassium-argon and rubidium-strontium analytical data further indicate a major regional metamorphism before or in Early Permian time; the most significant date is Early Permian (278±10 Ma) from K-Ar analysis of hornblende. Permian metamorphism in the Yukon Crystalline Plateau has not been documented previously. The oldest single K-Ar date on metamorphic rock recorded by Tempelman-Kluit (1975) was 202 Ma (Table 2-5: sample no. 49).

A small granodiorite stock in the map area is latest Cretaceous or earliest Tertiary. This isotopic date is the youngest in the northwestern part of the Yukon Crystalline

Plateau. This might represent equivalence to the Casino Complex, 70.3 Ma (Godwin, 1975). Previously these intrusions were classified as mid-Cretaceous (Green, 1972) and equivalent to the Coffee Creek quartz-monzonite, 90 to 100 Ma (Tempelman-Kluit, 1976).

Within the central and northern part of the Yukon Crystalline Plateau a fairly well defined younging trend in igneous and metamorphic isotopic dates away from the Tintina Trench is present.

CHAPTER III

CLINTON CREEK ULTRAMAFIC BODIES

3-1 INTRODUCTION

Eighteen ultramafic bodies were mapped within the study area (Figure 2-2), of which five bodies are known to contain chrysotile asbestos. These are a part of a discontinuous belt of ultramafic and associated rocks extending along almost the entire length of Tintina Trench. In some places the belt reaches a width of 60 kilometres (Figure 2-4). In Pelly and Stewart River areas large ultramafic bodies form the lower structural unit of a series of stratified allocthonous sheets (Tempelman-Kluit, 1977). These sheets have been thrust over Paleozoic rocks and later folded with country rock. Some of the ultramafic rocks in the Pelly River and Stewart River areas and the Eagle quadrangle in Alaska are overlain by a unit consisting of gabbroic rocks, pillow lavas and cherty argillites, a suite of rocks typical of ophiolite[1] that closely resembles

---

1: See Appendix B for definition of ophiolite.

rock sequences of present day oceanic ridges and sea floor. Ophiolites are regarded as tectonically emplaced fragments of the oceanic crust and upper mantle (Coleman, 1971). Foster and Keith (1974) described the ultramafic rocks in Yukon Territory which appears to be the southeast extension of the zone of ultramafic rocks of the Eagle quadrangle.

3-2 PETROLOGY

3-2-A Ultramafic Rock Types

All of the ultramafic rocks in this area are at least 75 percent serpentinized and most of them about 95 percent serpentinized. The nature of original rock was inferred from relict structures and textures, and from the nature and chemistry of the primary minerals. Host rocks of the asbestos deposit are mainly harzburgite and lherzolite with minor dunite (Figure 3-1).

Specimens of serpentinized harzburgite in thin section contain several of the following: olivine, orthopyroxene (Plate 3-1), bastite pseudomorphs after pyroxene, antigorite with relict olivine network texture, chromite, magnetite, chrome-spinel, talc, magnesite, brucite and chrysotile. According to microprobe analyses (Appendix C) the olivine

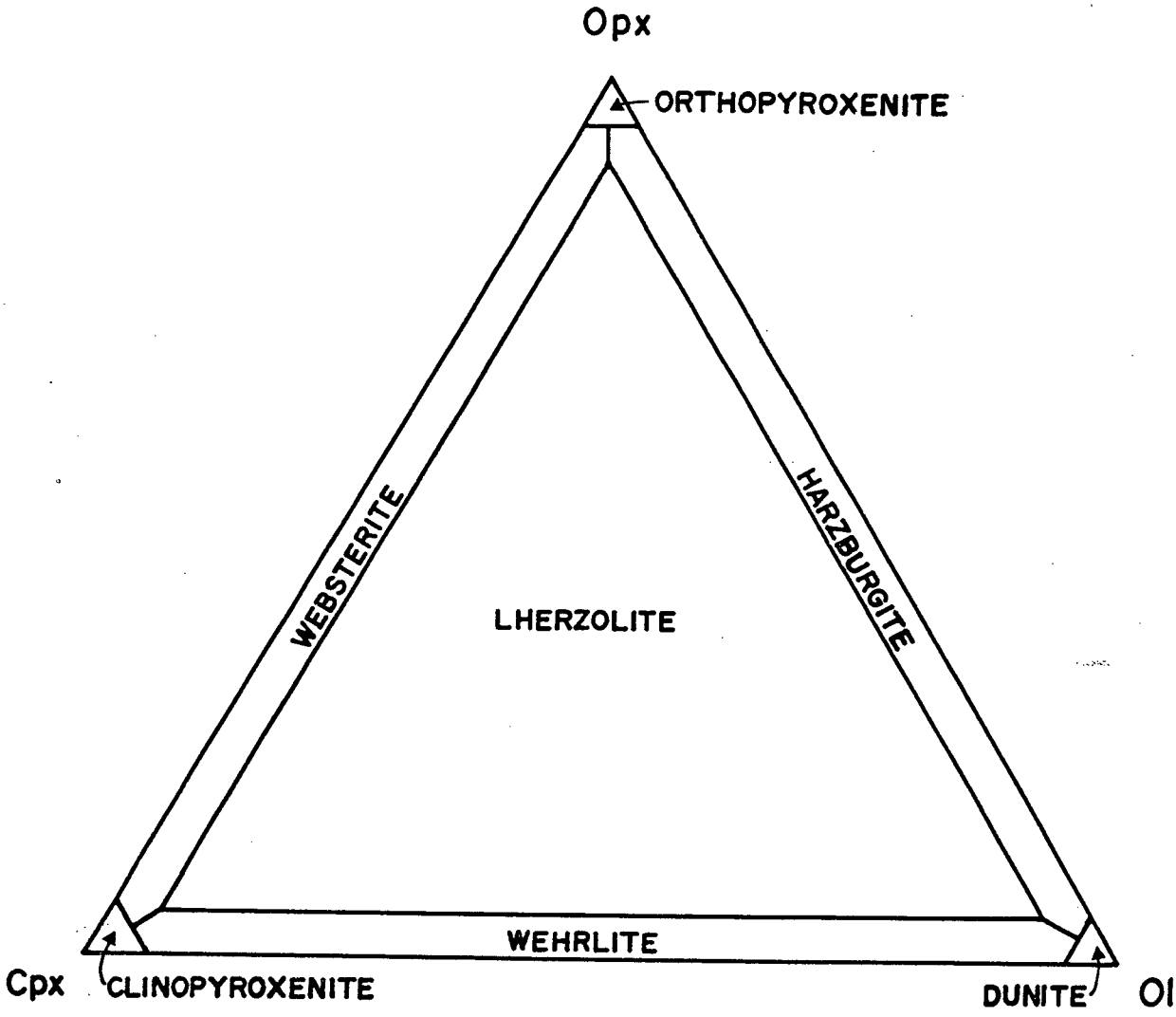

FIGURE 3-1: MODAL CLASSIFICATION OF ULTRAMAFIC ROCKS (after Jackson, 1968).

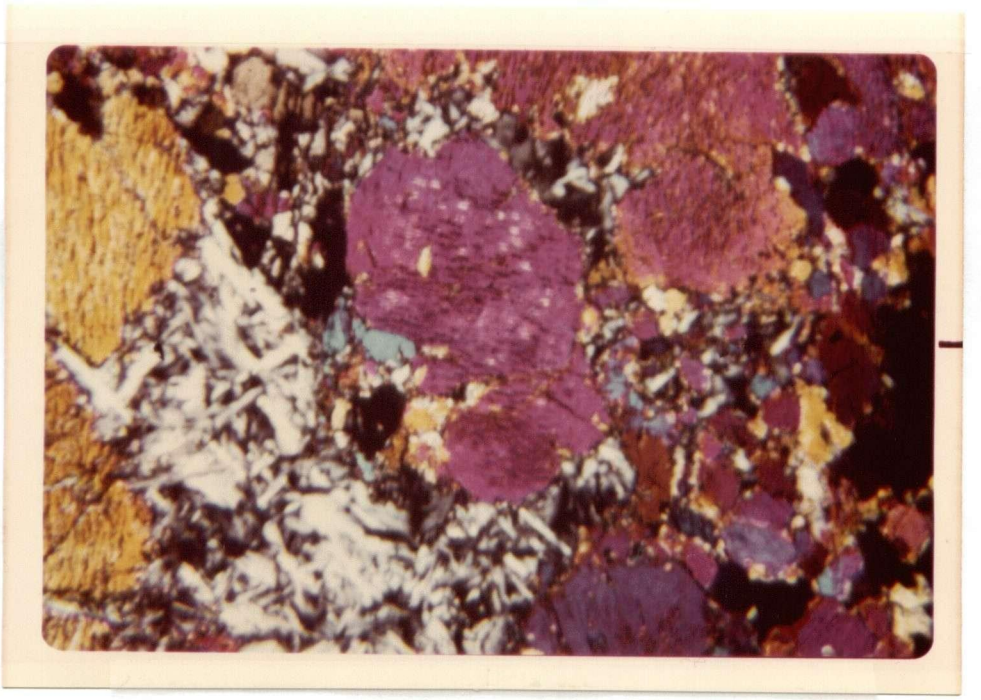

PLATE 3-1: Serpentinized harzburgite with unstrained mosaic olivine surrounding larger pyroxenes. Ribbon textured antigorite replaces fine-grained granular olivine. (Crossed nicols.)

network is forsteritic ($Fo_{88.3-92.4}$). Orthopyroxene is enstatite ($En_{91.7-91.9}$) and generally exhibits abundant exsolution lamellae of clinopyroxene. The most significant feature of the harzburgite is its tectonic fabric in which orthopyroxene forms porphyroclasts 1 to 10 mm long, whereas the olivine grains, 0.1 to 1 mm in modal diameter, form a cataclastic matrix. The orthopyroxenes are bent and show undulatory extinction. Olivine grains are highly granulated and strongly fractured. Mosaics of unstrained much finer-grained olivine are frequently observed enclosing the orthopyroxene porphyroclasts (Plate 3-1).

Serpentinized lherzolite consists of orthopyroxene, clinopyroxene, olivine, antigorite, bastite, chlorite and magnetite (Plate 3-2). Large anhedral grains of pyroxene total about 45 percent. Some orthopyroxene shows strained extinction, others are slightly bent and sheared. A few pyroxenes are partially replaced by bastite. The ratio of clinopyroxene to orthopyroxene is about 4 to 1. Very few olivine grains are preserved, but typical serpentine network after olivine is still preserved. In some specimens chlorite also has replaced olivine.

3-2-B Early State Alteration

a. Serpentinization

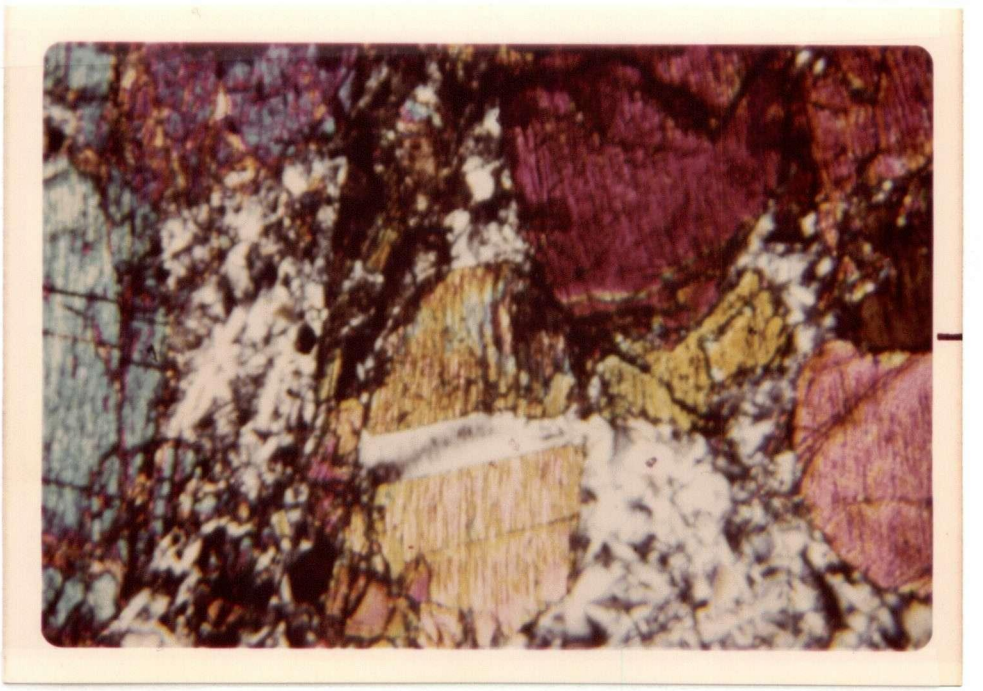

PLATE 3-2: Serpentinized lherzolite. All of the olivine has been serpentinized. Serpentinization of pyroxene in the middle of photograph seems to have taken place at constant volume. (Crossed nicols.)

Serpentinization is a pervasive alteration common to all ultramafic bodies in the study area. The degree of serpentinization varies with rock type. Generally, dunite is more serpentinized than harzburgite or lherzolite, apparently because olivine is more susceptible to alteration than pyroxenes. Serpentine minerals[1] in the Clinton Creek area are antigorite and chrysotile. Lizardite appears to be absent. Most serpentinization in this area occurred in two main episodes. The first was partial to complete replacement of ferromagnesium silicates by antigorite. The second stage, which will be discussed in Chapter IV, was the formation of antigorite, chrysotile, picrolite and brucite, mostly on fractures and fault surfaces.

Two types of olivine are observed, fine grained granulated olivine and unstrained, mosaic olivine. The former generally is replaced by ribbon textured antigorite (Plate 3-1). The latter resists serpentinization longer and is largely replaced by lamellar antigorite. In specimens where serpentinization is complete, the cores of olivine are replaced by serpophite.

Serpentinization can form in two ways: in one, the volume remains constant and in the other there is a change in volume. The constant volume replacement model (Thayer,

---

1: Serpentine minerals were identified by single crystal x-ray work and x-ray powder diffraction techniques. See Appendix D for the definition of different serpentine minerals used here.

1966) involves the removal of large amounts of MgO and SiO_2 in solution, the serpentinization reaction possible being of the type (Tuner and Verhoogen, 1960):

Forsterite + Water $\rightarrow\rightarrow\rightarrow$ Serpentine + Solution

$$5Mg_2SiO_4 + 4H_2O \rightarrow\rightarrow\rightarrow 2Mg_3Si_2O_7.2H_2O + (4MgO + SiO_2)$$

In some thin sections antigorite appears to have replaced pyroxene without any expansion (Plate 3-2). Some ribbon-textured antigorite fills what appears to be expansion fractures in olivine. Hostetler et al. (1966) argue that the development of brucite indicated volume increase. The Clinton Creek ultramafic body contains, on the average, one percent brucite (Plate 3-3, 3-4). A loss of MgO rather than a gain of SiO_2 would minimize an increase in volume. The writer concludes that serpentinization was partly volume for volume but that there was some volume increase.

Scarfe and Wiley (1967) and Johannes (1969) have shown the breakdown temperature of forsterite to serpentine in the reaction,

Forsterite + Water $\rightarrow\rightarrow\rightarrow$ Serpentine + Brucite

$$2Mg_2SiO_4 + 3H_2O \rightarrow\rightarrow\rightarrow Mg_3Si_2O_7.2H_2O + Mg(OH)_2$$

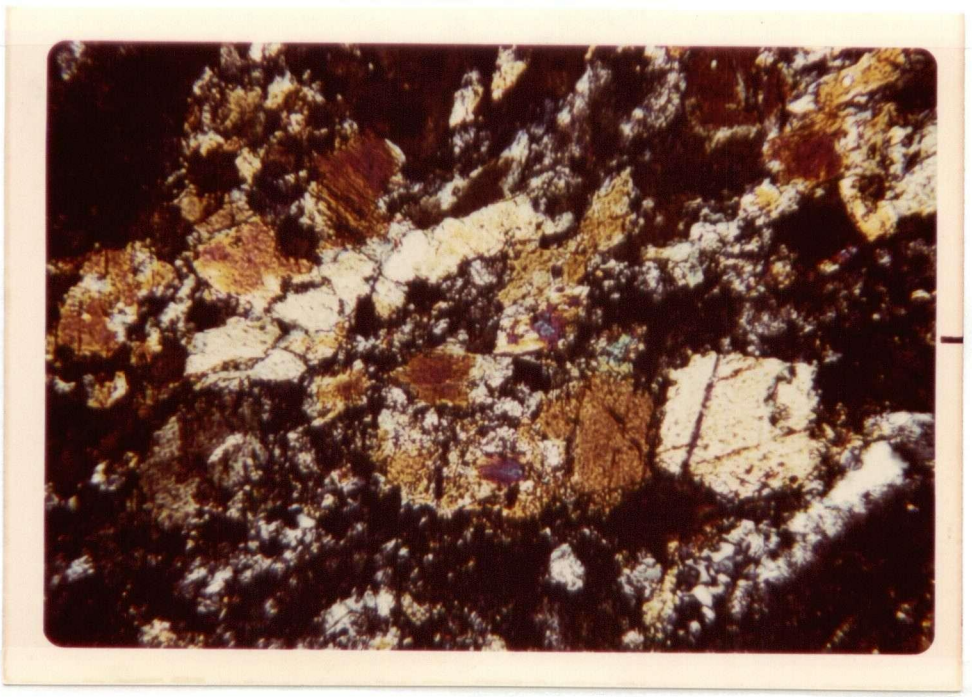

PLATE 3-3: Pale yellow brucite formed during pervasive, first main episode of serpentinization. (Crossed nicols.)

PLATE 3-4: Yellowish white brucite probably formed during second main episode of serpentinization, usually in fractures between picrolite. (Crossed nicols.)

is a little above 400°C at 2 kb (Figure 3-2). The stability of brucite is limited by the composition of the fluid phase, being stable only at very low CO_2 content, about 0.5 mole percent CO_2 at fluid pressure 2 kb and 400°C (Johannes, 1969). At higher CO_2 content of the fluid phase the breakdown of olivine occurs by the reaction (Figure 3-2):

Forsterite+Water+Carbon Dioxide →→→ Serpentine+Magnesite

$$2Mg_2SiO_4 + 2H_2O + CO_2 \rightarrow\rightarrow\rightarrow Mg_3Si_2O_7 \cdot 2H_2O + MgCO_3$$

Since both brucite and magnesite are common in the Clinton Creek ultramafic body, either the altering fluid changed and became richer in CO_2 during the process, or there were two separate epidoses of alteration, one yielding serpentine and brucite and the other serpentine and magnesite.

Orthopyroxene generally is replaced, without any sign of expansion, by bastite which preserves the morphological features of the original grain , and by minute crystals of magnetite arranged either along the cleavage planes or around the grain. From a chemical point of view, the serpentinization of orthopyroxene involves an increase in water, and, since the reaction apparently goes on at constant volume, a loss of silica, as well as small amounts of calcium and aluminum. A part of the silica released is probably incorporated in serpentine replacing the silica-poor olivine,

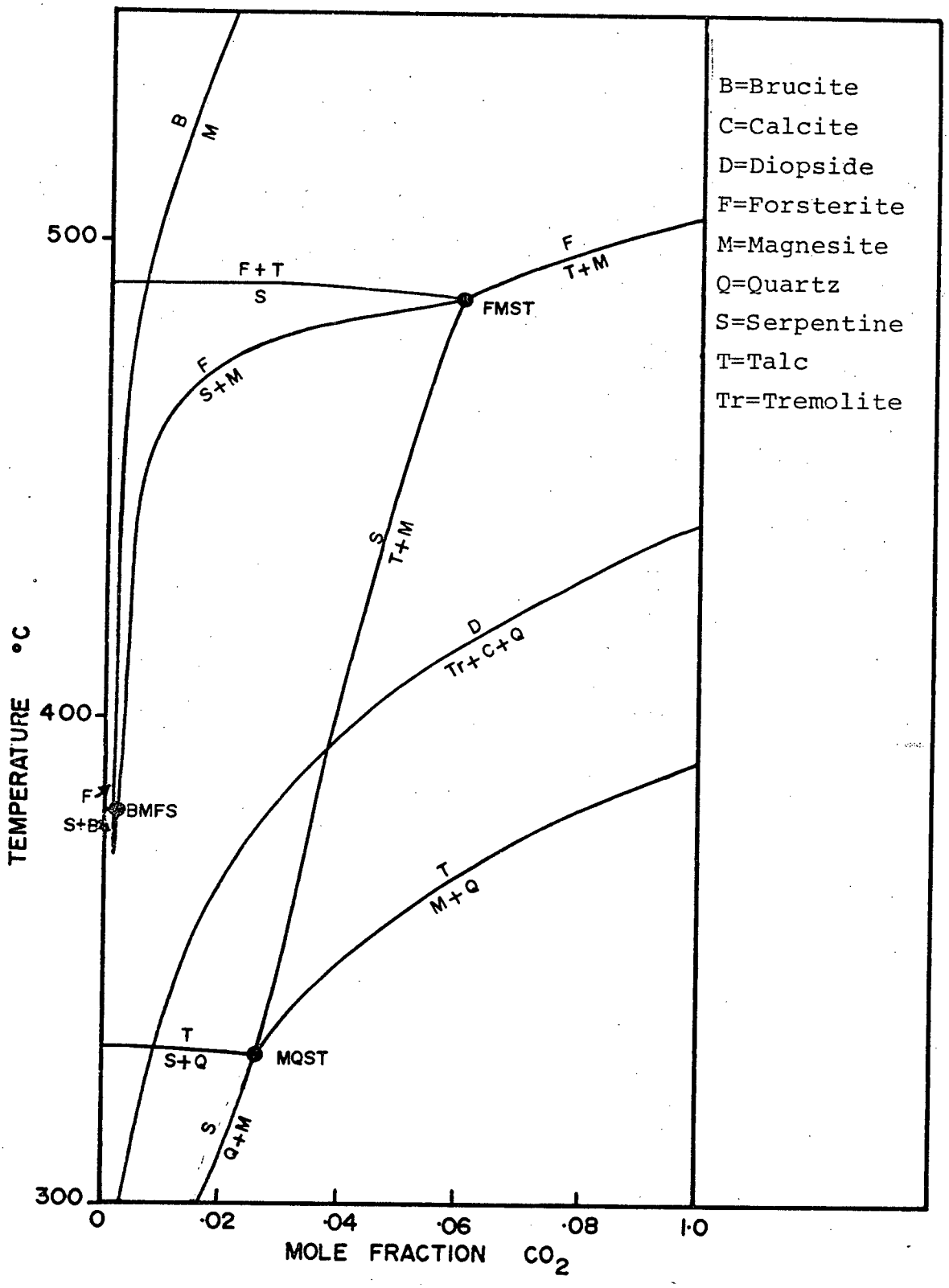

FIGURE 3-2: T-X DIAGRAM IN THE SATURATED SYSTEM MgO-SiO_2-H_2O-CO_2-CaO (after: Greenwood, 1967; Johannes, 1969; and Skippen, 1971).

whereas another part may be combined with calcium and aluminum to form calcium-rich alumino-silicates of rodingite (see below). Enstatite resists serpentinization and survives in rocks in which olivine is completely serpentinized. Experimentally enstatite is not stable below 700°C at 2 kb with low X_{CO_2} (Greenwood, 1963; Johannes, 1969; Evans and Trommsdorff, 1970), but breaks down to anthophyllite and forsterite.

Enstatite + Water Anthophyllite + Forsterite

$$9Mg_2Si_2O_6 + 2H_2O \quad 2Mg_7Si_8O_{22}(OH)_2 + 2Mg_2SiO_4$$

However, anthophyllite appears to be absent in the area. Therefore, it is assumed, at lower temperature and higher content of water, anthophyllite could break down to forsterite and talc (Figure 3-2).

Anthophyllite + Water $\rightarrow\rightarrow\rightarrow$ Forsterite + Talc

$$5Mg_7Si_8O_{22}(OH)_2 + 4H_2O \rightarrow\rightarrow\rightarrow 4Mg_2SiO_4 + 9Mg_3Si_4O_{10}(OH)_2$$

Eventually, with a drop of temperature and addition of water pressure, forsterite and talc may break down to serpentine (Evans and Trommsdorff, 1970) according to the following reaction:

Forsterite + Talc + Water $\rightarrow\rightarrow\rightarrow$ Serpentine

$$6Mg_2SiO_4 + Mg_3Si_4O_{10}(OH)_2 + H_2O \rightarrow\rightarrow\rightarrow 5Mg_3Si_2O_7.2H_2O$$

around 450°C at 2 kb.

The degree of alteration of chromite is apparently not related to the degree of serpentinization. Unaltered chromite is translucent dark reddish brown. Some chromite is replaced by an opaque black material usually magnetite (Plate 3-5), which may form a rim or completely replace the grain. Most chromite grains or magnetite after chromite grains are rimmed by a thin fine-grained halo of radiating chlorite which merges with the surrounding serpentine. It is found only around chromite grains with black rims but not around unaltered chromite. This suggests that both magnetite and chlorite are alteration products of chromite. Large chromite grains commonly have two generations of fractures: an early one filled with chlorite and bordered by magnetite, and later antigorite-filled fractures cross cutting the chlorite halo (Plate 3-5), this antigorite veinlet may or may not be adjacent to a black margin. This may suggest that alteration producing chlorite and magnetite occurred before pervasive serpentinization. Alteration of chromite to magnetite and chlorite occurs at temperatures above the stability limit of serpentine (Cerny, 1968).

Several different kinds of serpentinite are distin-

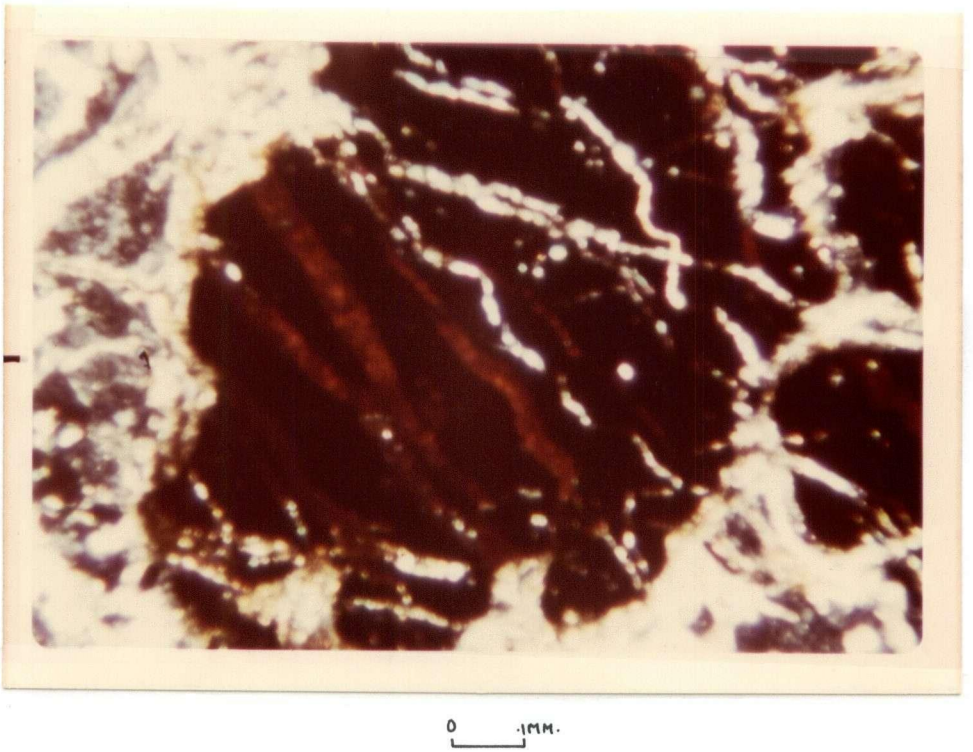

PLATE 3-5: Brownish red, trunsluscent chromite with black magnetite and pale colour chlorite. (PPL.)

guished in the Clinton Creek area. Generally, fibre-bearing serpentinite consists of antigorite, bastite, serpophite, chrysotile, picrolite, prochlorite and magnetite. Ordinarily it is dark green, compact and has a somewhat sugary texture. Very fine grained, dark green compact serpentinite normally consists of antigorite, serpophite, chlorite, magnetite and brucite in which chlorite forms as much as 40 percent of the rock. Fine-grained, flaky antigorite is replaced by bructie in part. Chlorite and brucite veins are quite common. Network serpentinite contains more than 80 percent of serpophite. This is very dark, nearly black rock with a few veinlets of talc and chrysotile and magnetite. Fish-scale serpentinite consists mainly of antigorite, some serphopite and chlorite. This occurs along sheared zone. Slab-like blocks of fist size to a metre size are coated with shining, polished antigorite. Slabs of serpentinite are arranged in an overlapping manner analogous to fish-scales. One of the characteristics of fish-scale serpentinite is lack of chrysotile fibre.

The age of serpentinization is not possible to determine. However, the initial serpentinization would probably have occurred when the ultramafic body first came in contact with hydrous rock units. Pervasive serpentinization could have taken place in Permian time during the main phase of metamorphism of the Clinton Creek area (Table 2-1).

b. Rodingitization

Rodingite is exposed only in the Porcupine and Snow Shoe pits. Two groups of rodingite are distinguished on the basis of age determined by relict minerals, stage of alteration, degree of deformation and nature of contacts. The older group consists of isolated tabular bodies (Plate 3-6) that range in length from three metres to twelve metres with thicknesses of 1 to 1.5 metres (Plate 2-3).

The older rodingite, in thin section, consists of garnet, idocrase, prehnite, chlorite, diopside, actinolite and epidote (Plate 3-7). Lack of primary relict minerals, except pyroxene, makes it impossible to precisely define the original rock. However, presence of pyroxene, the tabular form, intensity of shearing and deformation that are similar to those in the surrounding serpentinite, and absence of metamorphism of adjacent serpentine (Plate 3-8), suggest that the bodies were basic dykes emplaced before serpentinization. Original ferro-magnesium silicates were probably uralitized (actinolite) and chloritized (Plate 3-9), and calcic plagioclase was replaced by idocrase, prehnite, epidote and hydrogarnet. According to Coleman (1967) the replacement process could occur according to the following reactions:

$$3\ \text{Anorthite} + Ca^{2+} + 2H_2O \rightarrow\rightarrow\rightarrow \text{Zoisite} + 2H^{+}$$

PLATE 3-6: Older rodingite. Generally tabular, intensely deformed and usually coloured puplish on fracture surfaces. Exposed in Snow Shoe pit.

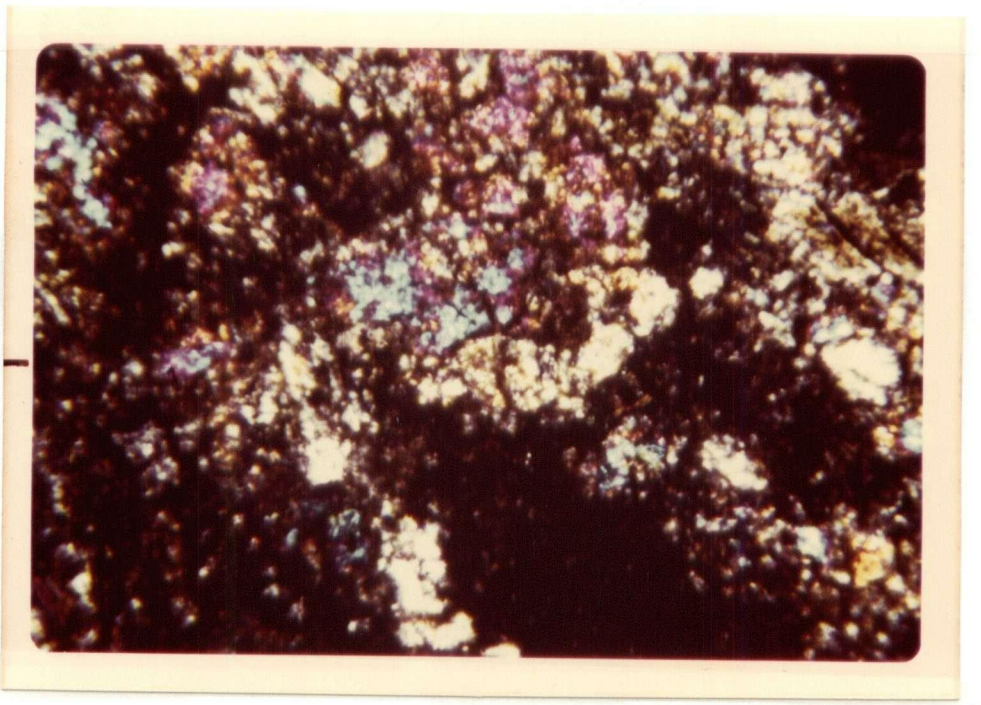

PLATE 3-7: Older rodingite: isotropic grossular garnet; blue idocrase; purplish and golden epidote; pale or whitish chlorite. (Crossed nicols.)

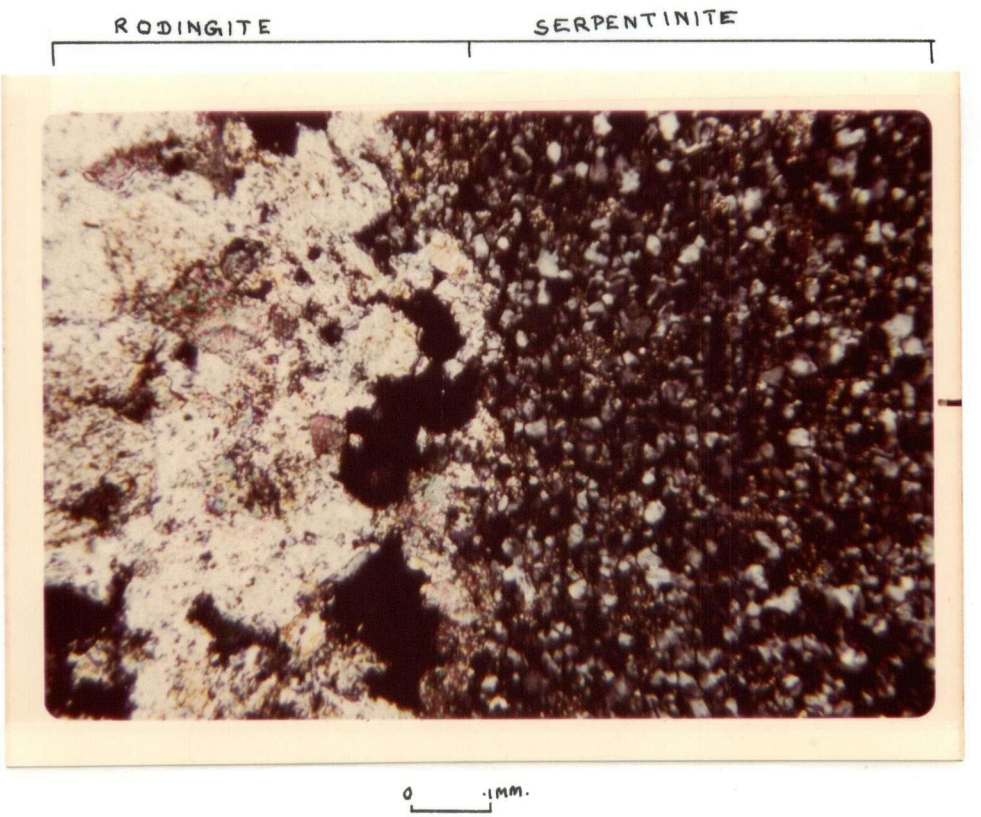

PLATE 3-8: Older rodingite showing absence of metamorphism at contact with serpentine. (Crossed nicols.)

PLATE 3-9: Uralitization and chloritization in rodingite. Yellowish green pyroxene at left top corner was replaced by adjacent pale colour chlorite and prismatic actinolite. The rest isotropic and gray minerals are serpentine. (Crossed nicols.)

$$4\ \text{Zoisite} + 0.5\ Ca^{2+} + 13H_2O \rightarrow\rightarrow\rightarrow \text{Hydrogarnet} + 10H^{+}$$

or

$$1.5\ \text{Anorthite} + 0.5Ca^{2+} + 1.5H_2O \rightarrow\rightarrow\rightarrow 1\ \text{Prehnite} + 0.5Al_2O_3 + H^{+}$$

$$2\ \text{Prehnite} + 4Ca^{2+} + Al_2O_3 + 6H_2O \rightarrow\rightarrow\rightarrow 2\text{Hydrogarnet} + 8H^{+}$$

Decomposition of ferro-magnesium minerals could yield iron for the formation of prehnite, epidote and idocrase, and magnesium for idocrase. Therefore, during rodingitization only calcium and water need to be added. Calcium for rodingite could be derived from clinopyroxene of ultramafic rocks during serpentinization (Barnes and O'Neil, 1969). Calcium has been shown to be released during serpentinization of ultramafic rocks (Poldervaart, 1955).

The younger group of rodingites is mainly distinguished by the development of thermal metamorphism at contacts with serpentine, less pronounced foliation and non-pervasive rodingitization. The central parts of the bodies are slightly altered gabbro but the margins consist of hydrogarnet, epidote, talc and chlorite. At the contacts serpentine has been dehydrated and converted into diopside and locally into talc and chlorite (Plate 3-10). Thus it appears that probably dykes of gabbro were intruded into already serpentinized peridotite.

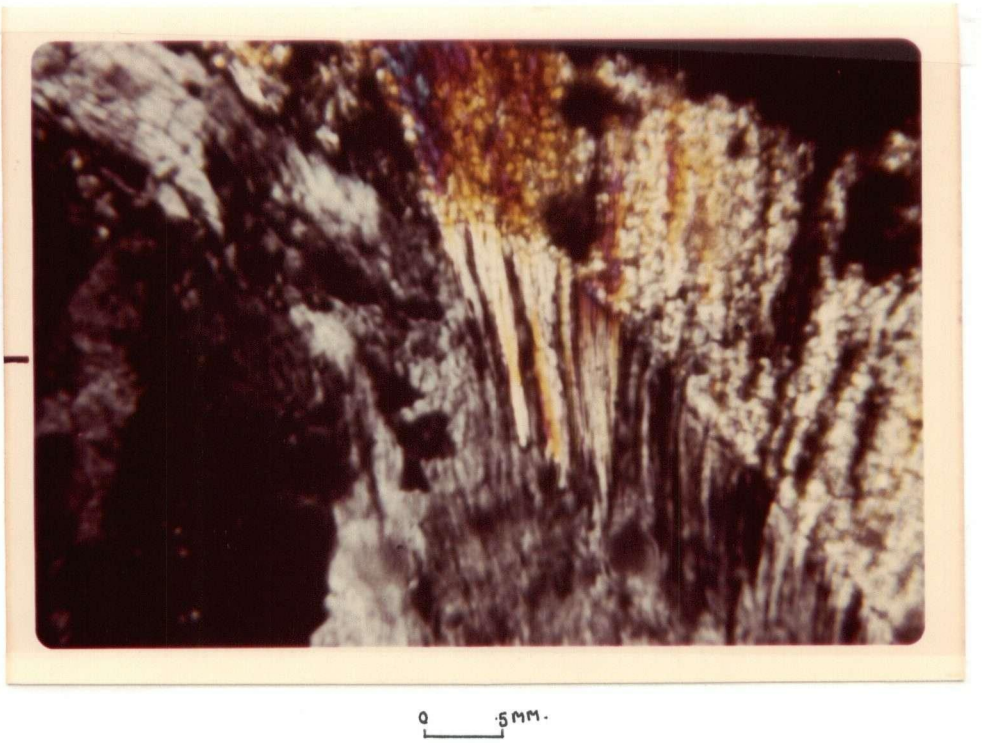

PLATE 3-10: Serpentine dehydrated into pyroxene. Grayish, greenish and isotropic minerals are serpentine. Second order interference colour minerals are pyroxene. (Crossed nicols.)

c. Blackwall and talc-carbonate alteration

Blackwall alteration[1] was found only at the margin of the Air Field ultramafic body (Figure 2-2) where it is exposed over an area four metres by ten metres. The marginal zone is moderately sheared. Blackwall alteration zone is succeeded towards the interior of the ultramafic body by a talc-carbonate zone. In both zones, serpentine co-exists with the alteration minerals.

Blackwall alteration, a zone about 0.5 metres thick, consists of gray to greenish black rock characterized by coarsely crystalline chlorite (1 mm to 5 mm) and tremolite (4 mm to 20 mm). It has replaced highly fractured serpentinite. The contact with the adjacent talc-carbonate zone or serpentinite is sharply defined. It has also a sharp and abrupt boundary with the country rock which is calcareous-quartz-muscovite schist. In thin section, the blackwall alteration consists of chlorite, tremolite, talc, serpentine and opaque minerals. Three textural varieties of chlorite are found. One occurs as band of flaky chlorite crystals, and another as smaller grains mixed with serpentine. The third type forms veins in adjacent serpentinite. Tremolite occurs as veins in fractures, and is restricted to a zone close to the contact with country rock. The silica required for

---

1: Blackwall alteration zone consists of highly foliated to almost massive, mainly dark coloured chlorite-rich rocks that form thin, sharply defined, and nearly continuous rinds about ultramafic bodies.

its production may have come from the quartz-muscovite schist and magnesium from the ultramafic rocks.

A talc-carbonate zone which lies adjacent to the blackwall alteration zone is about 0.3 metres thick, moderately sheared, and buff to pale greenish. It is more or less gradational with serpentinite. The gradual transition occurs through the development, in the serpentinite, of talc and talc-carbonate veins (Plate 3-11) mostly in shear surfaces of serpentinite. Pure talc-carbonate is rare other than in veins. In thin section the average mode of talc-carbonate zone is magnesite 50 percent, antigorite 25 percent, talc 20 percent with minor chlorite and chromite.

Talc-carbonate could be derived directly from peridotite or from serpentinite. Preservation of serpentine mesh texture in talc-carbonate and lack of peridotite textures or any primary minerals suggest that it was more probably derived from serpentinite. The source of CO_2 for the formation of talc-carbonate seems to have been calcareous country rocks. Abundance of veins of talc-magnesite in serpentinite might result from a local increase in X_{CO_2} along fractures.

3-2-C Late Stage Alteration

a. Silica-carbonate alteration

Silica-carbonate rock is made largely of varying amounts

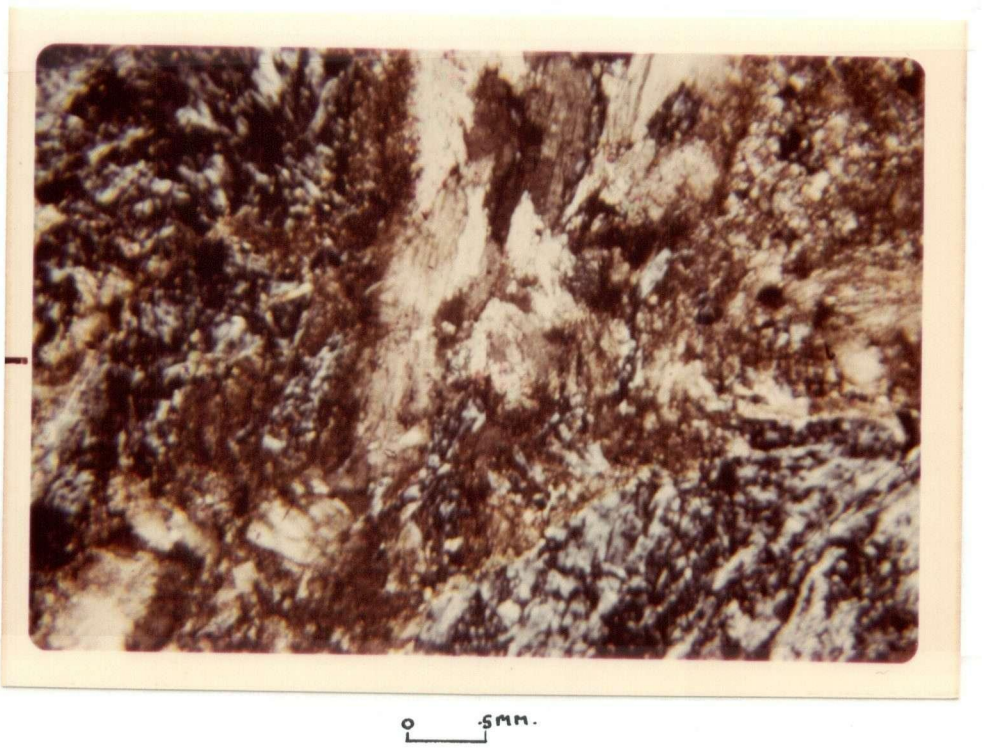

PLATE 3-11: Brownish and greenish talc-carbonate veins in grayish and isotropic serpentines. (Crossed nicols.)

of quartz, chalcedony, opal and magnesite with less ankerite, dolomite, chromite and picotite and rare mariposite, clacite and huntite $\{MgCa(CO_3)_4\}$. Opal is not as common as quartz. The rock forms an alteration zone along the margin of the serpentinite bodies (Figure 3-3, 3-4, Plate 3-12). Some small sheared serpentinite bodies are completely replaced, but thicker,more massive ones are generally replaced only along their sheared margins. The rock is easily recognized by its pseudomorphic character after serpentine and its frequent relationship with serpentinite. Its variation in appearance depends upon differences in mineralogy of the original rocks, the intensity of shearing, the grain size of replacing minerals and the relative abundances of quartz and carbonate minerals. Silica-carbonate rock derived from sheared serpentinite retains a lenticular nature. The different lenses and streaks are generally gray and green of various shades; the sheared texture may be accentuated by veining with light-coloured magnesite, dolomite or quartz.

Weathering generally alters the appearance of silica-carbonate rock, because ferroan-magnesite or dolomite is altered by weathering, leaving surface coatings of hydrated ferric-oxides and silica. A rock with more carbonate than silica usually gives rise to an ocherous soil (Figure 3-3 around 2 N, 9 W) containing only a few silicious fragments, one with more silica than carbonate weathers to a white and brown rock.

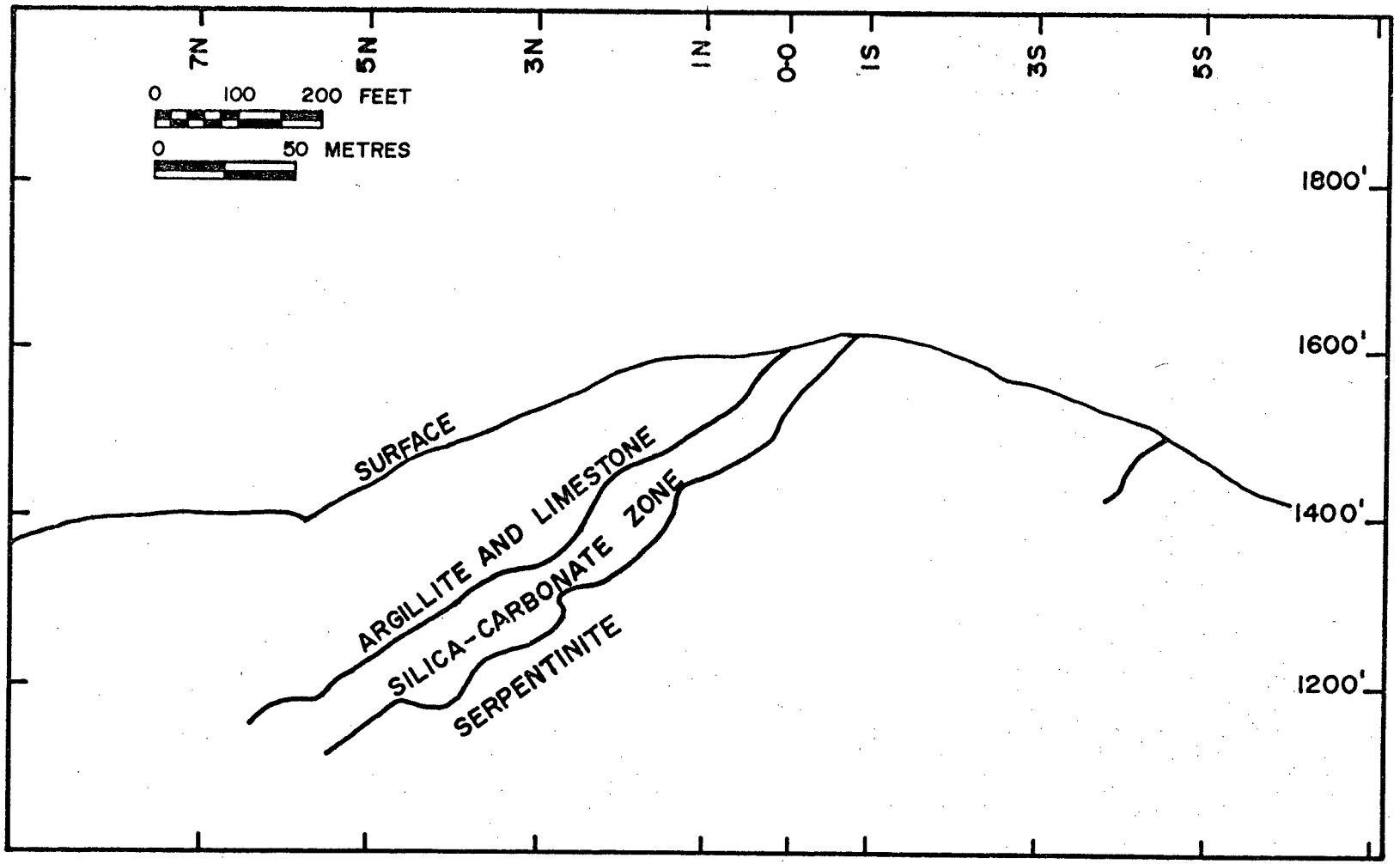

FIGURE 3-4: CROSS SECTION OF THE PORCUPINE SERPENTINITE BODY ALONG 12W. Note silica-carbonate zone dipping 45°. (See location at Figure 3-3.)

PLATE 3-12: North-western fault contact of the Porcupine ultramafic body is well marked by rusty looking quartz-carbonate zone dipping 45° tpwards northwest. (Photograph taken looking northeast.)

Stages of replacement from serpentine to silica-carbonate rock can be generalized. In the earliest stage antigorite and chrysotile veins are replaced by quartz and less abundant magnesite, rarely calcite in cracks giving a network of irregular veinlets (Plate 3-13). The replacement process is found to be easier for chrysotile than for antigorite. Secondly, bastite and serpophite in the core (away from fractures) are replaced with quartz, magnesite and dolomite. Finally quartz and minor magnesite replace the remaining serpentine minerals. These stages partially overlap. It seems possible that during alteration, the alteration products were not necessarily deposited together. It is thus clear that the development of the silica-carbonate rock is later than serpentinization and chrysotile vein formation.

There are two stages of quartz formation. The early stage quartz in thin section is fine-grained with rather rounded outlines and in hand specimen has a milky appearance. The second stage quartz is coarse-grained and generally clear. In some specimens, carbonate grains appear to have been broken off and isolated within patches of the second stage quartz indicating that clear variety quartz crystallized later than most of the magnesite and it is probable that this late stage of silicification is unrelated to silica-carbonate alteration.

Secondary magnetite formed during serpentinization is

PLATE 3-13: First stage of silica-carbonate alteration occurred along chrysotile veins. White veins consist of quartz and magnesite pseudomorphs after chrysotile. Chrysotile veins are light green.

incorporated in ferro-magnesite and is also transformed into hydrous-iron oxide. Chromite remains mostly unaltered but locally is altered to mariposite. The preservation of chrysotile veins, and larger textures and structures indicate that there has been no appreciable change in volume.

The average silica-carbonate rock consists of about 60 percent of carbonates, 35 percent of quartz with some chromite, iron oxides and mariposite. The process of replacement is mainly dehydration of serpentine and carbonatization (Figure 3-5).

The silica-carbonate zone is itself zoned. From core to margin, the sequence of altered rock is: serpentinite with some carbonates, talc-carbonate rock, and silica carbonate rock. It is considered that alteration proceeds by transporting CO_2 inward from surrounding rocks along fratures and grain boundries. It is possible that limestone and calcareous rocks in adjacent formation were the source of CO_2.

Quartz and magnesite are formed from the reaction of serpentine and CO_2 according to the following equation in an open system (Figure 3-2, 3-5):

Serpentine + Carbon Dioxide $\rightarrow\rightarrow\rightarrow$ Quartz + Magnesite + Water

$$Mg_3Si_2O_7.2H_2O + 3CO_2 \rightarrow\rightarrow\rightarrow 2SiO_2 + 3MgCO_3 + 2H_2O$$

Even very low CO_2 values of the fluid phase can lead

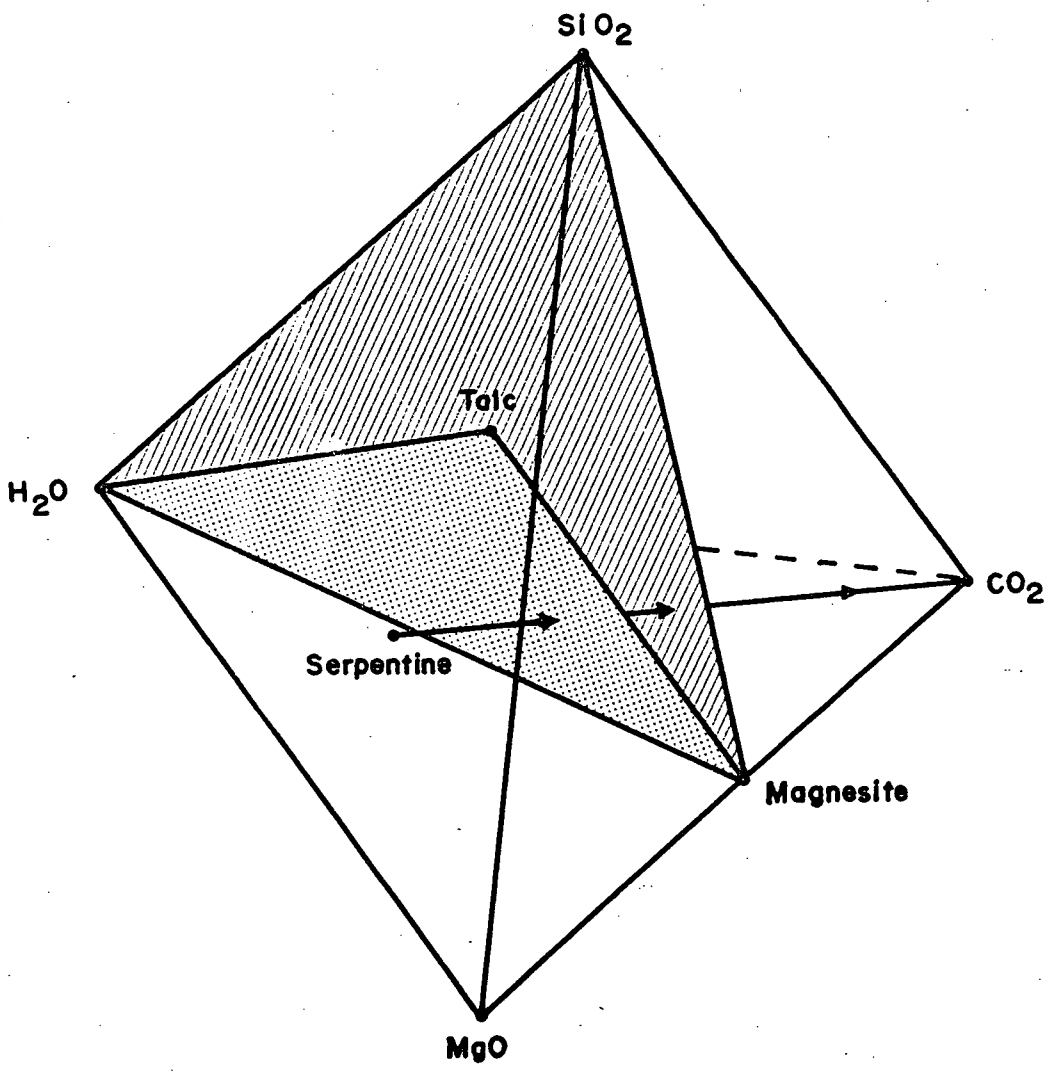

FIGURE 3-5: DEHYDRATION, CARBONATIZATION AND SILICIFICATION OF SERPENTINE DURING SILICA-CARBONATE ALTERATION SHOWN ON SiO_2-CO_2-MgO-H_2O TETRAHEDRON.

to formation of magnesite in serpentine (Johannes, 1969).

Magnesite and quartz could also be formed from serpentine, having talc as an intermediate step (Figure 3-2, 3-5).

Serpentine + Carbon Dioxide $\rightarrow\rightarrow\rightarrow$ Talc + Magnesite + Water

$$2Mg_3Si_2O_7.2H_2O + 8CO_2 \rightarrow\rightarrow\rightarrow Mg_3Si_4O_{22}.H_2O + 3MgCO_3 + H_2O$$

This reaction takes place at slightly higher CO_2 values and higher temperature than direct alteration to quartz and magnesite from serpentine (Greenwood, 1967; Johannes, 1969). Talc is unstable with increasing CO_2 values in the fluid phase, and yields magnesite and quartz according to the following reaction (Figure 3-2, 3-5):

Talc + Carbon Dioxide $\rightarrow\rightarrow\rightarrow$ Quartz + Magnesite + Water

$$Mg_3Si_4O_{22}.H_2O + 3CO_2 \rightarrow\rightarrow\rightarrow 4SiO_2 + 3MgCO_3 + H_2O$$

A big zone (14 metres across) of opal, rich in clay minerals and limonite (Plate 3-14), appears to be the result of present day weathering. These opaline masses are mainly restricted to near surface locations and were developed in the silica-carbonate zones.

PLATE 3-14: Black chunks of opal surrounded by limonitic iron-oxides give rise to a unique looking rusty zone at the highest level of the Porcupine pit. Adjacent gray zone is serpentinite.

b. Quartz-magnesite veins

Quartz-magnesite veins are the result of late silica-carbonate alteration and are found in shear zones or minor faults throughout the ultramafic bodies or at contacts with the country rock. They cut across the previously described quartz-carbonate zones. Magnesite, quartz and minor fibrous brucite, dolomite and serpentine are the chief minerals. The veins are 2 to 12 centimetres wide and mainly consist of coarse (4 to 50 mm) magnesite crystals and quartz. Many of them replace sheared veins (Plate 3-15) formerly filled with picrolite, braided antigorite, sheared chrysotile or sheared talcose gouge.

3-3 STRUCTURE

The ultramafic body, originally a single mass (1500 metres by 350 metres) has been faulted and now consists of three parts, the large western Porcupine body, the central Creek body and eastern Snow Shoe body (Figure 3-6). Faults separating the three parts strike northerly and dip nearly vertical (Plate 2-14). At each fault, the western block is down-thrown. These bodies are surrounded by limy-carbonaceous argillite and minor calcareous schist. The upper gently

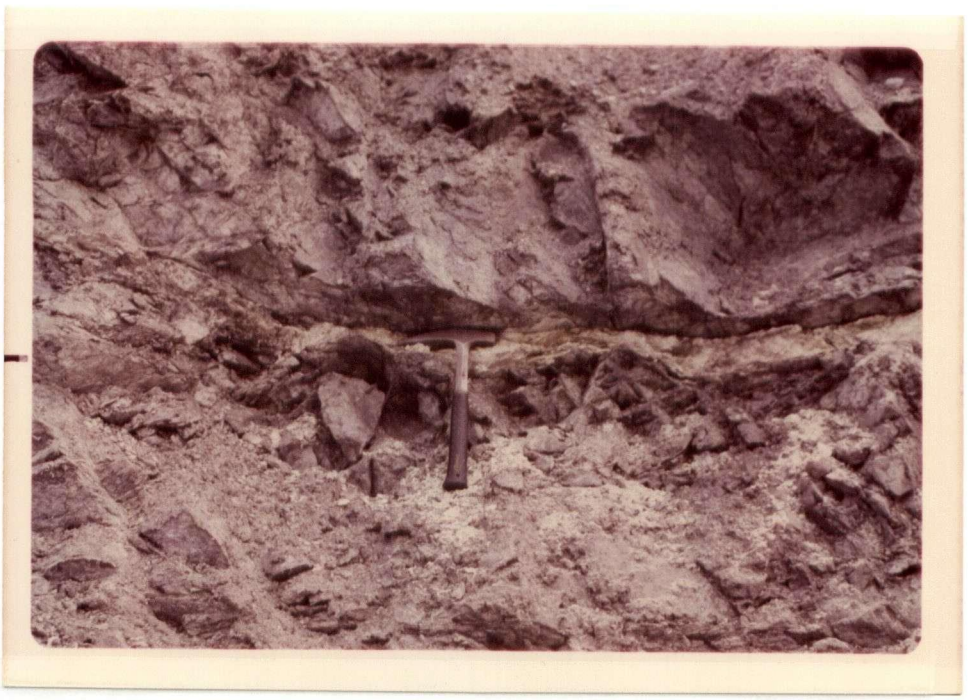

PLATE 3-15: Quartz-magnesite vein of late silica-carbonate alteration. These veins are always seen to replace serpentine along shear fractures in the Porcupine pit.

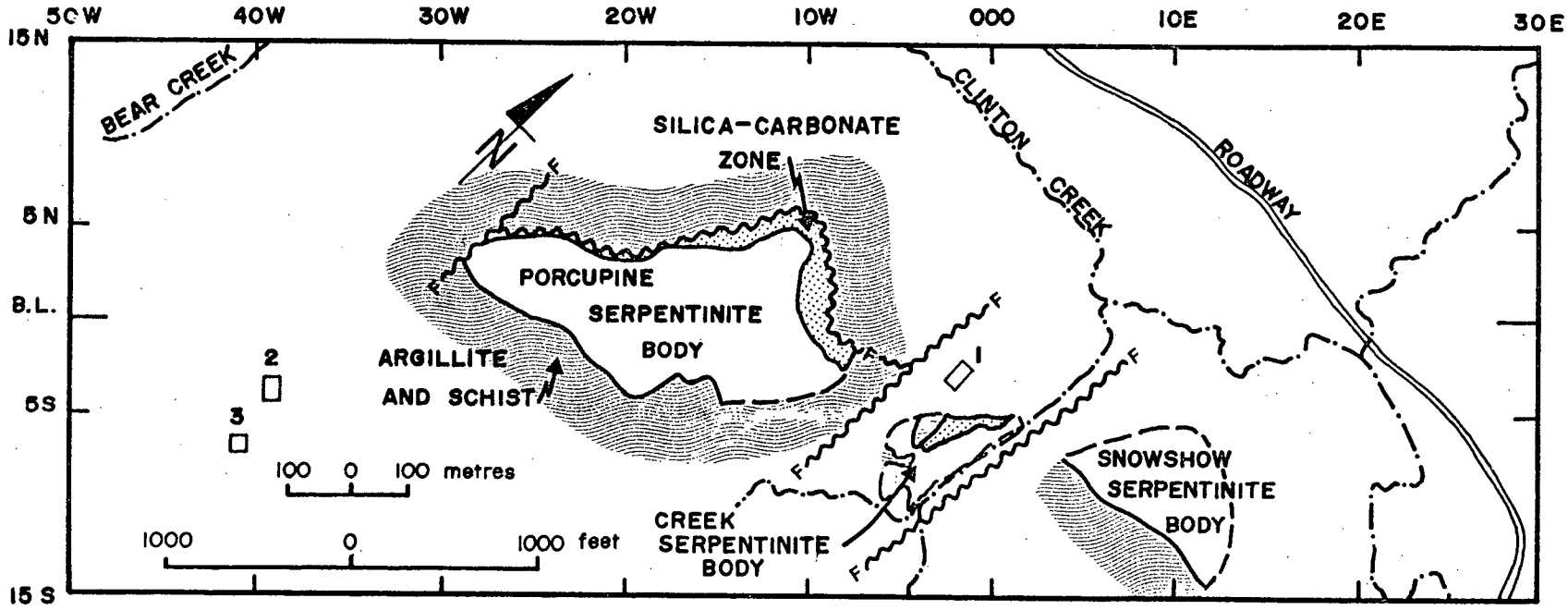

FIGURE 3-6: ORE BEARING PORCUPINE, CREEK AND SNOW SHOE SERPENTINITE BODIES. 1 = mine crusher. 2 = drill-core storage. 3 = drill storage. F-F = fault. B.L. = base line.

convex surface of the porcupine body plunges about 10° in a direction south 55°west (Plate 3-16). The northwestern contact of the Porcupine body is a fault that dips 45° northwesterly (Plate 3-12) and is almost parallel to bedding in the argillite in that vicinity (Figure 2-2). At the fault, argillite and serpentinite are highly sheared. The middle part of the southeasterly contact dips about 60° southeast as defined by diamond drilling (Figure 3-7, 3-8, 3-9). It is also a fault contact with a highly sheared serpentinite contact zone. Argillite and schist at this vicinity dips southerly.

Cross sections based on open pit exposures and partly on diamond drill data show that the outline of the upper part of the ultramafic mass curves and resembles an open fold (Figure 3-7, 3-8). Superimposed on this suggested fold are outlines that resemble recumbent folds of various styles (Figure 3-10, 3-11). Relatively small, tight, recumbent folds are distinct along the contact of silica-carbonate and argillite (Figure 3-12, 3-13). One can speculate that the recumbent folds belong to the first phase of deformation that affected the area, the northwest contact fault is probably related to the second phase of deformation.

3-4 ORIGIN

Most geologists recognize three broad kinds of ultra-

PLATE 3-16: Ore-bearing Porcupine ultramafic body plunging 10° towards 235°. (Photograph taken looking south-westerly.)

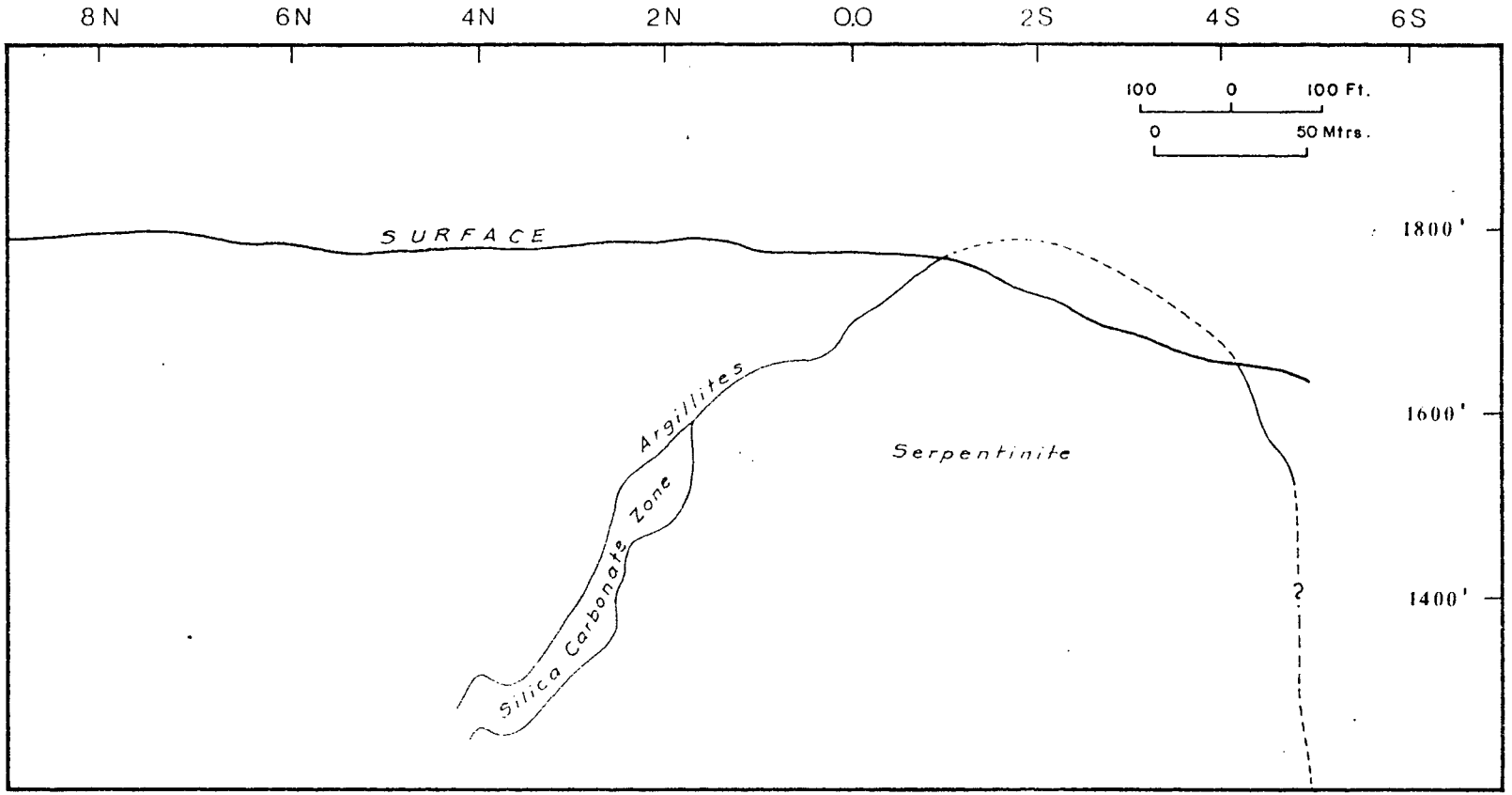

FIGURE 3-7: CROSS SECTION LOOKING NORTHEAST OF THE PORCUPINE SERPENTINITE BODY ALONG 19W. Note southeast contact dipping about 65°. (See location at Figure 3-3.)

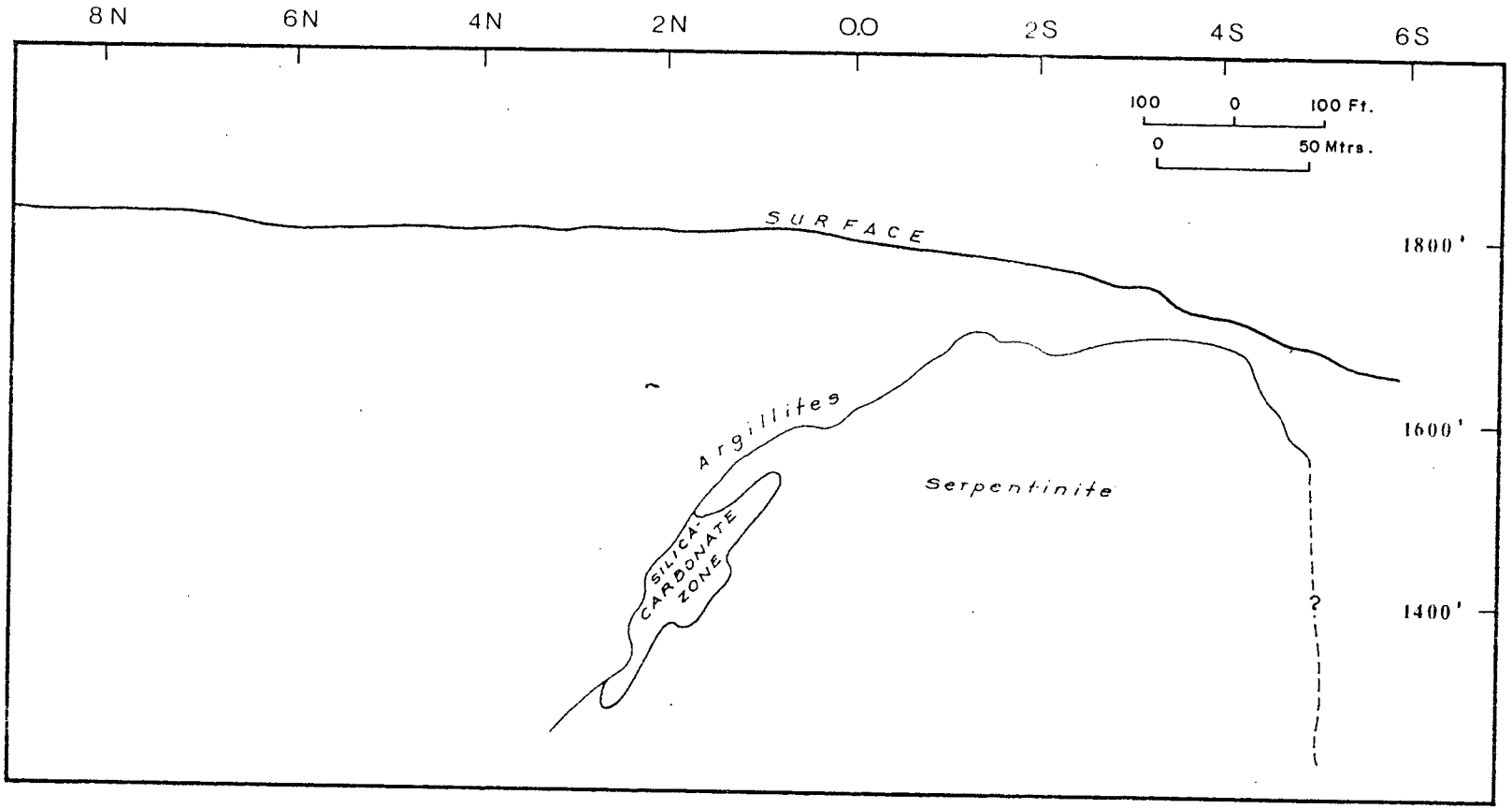

FIGURE 3-8: CROSS SECTION LOOKING NORTHEAST OF THE PORCUPINE SERPENTINITE BODY ALONG 20W. Note southeast contact dipping about 60°. (See location at Figure 3-3.)

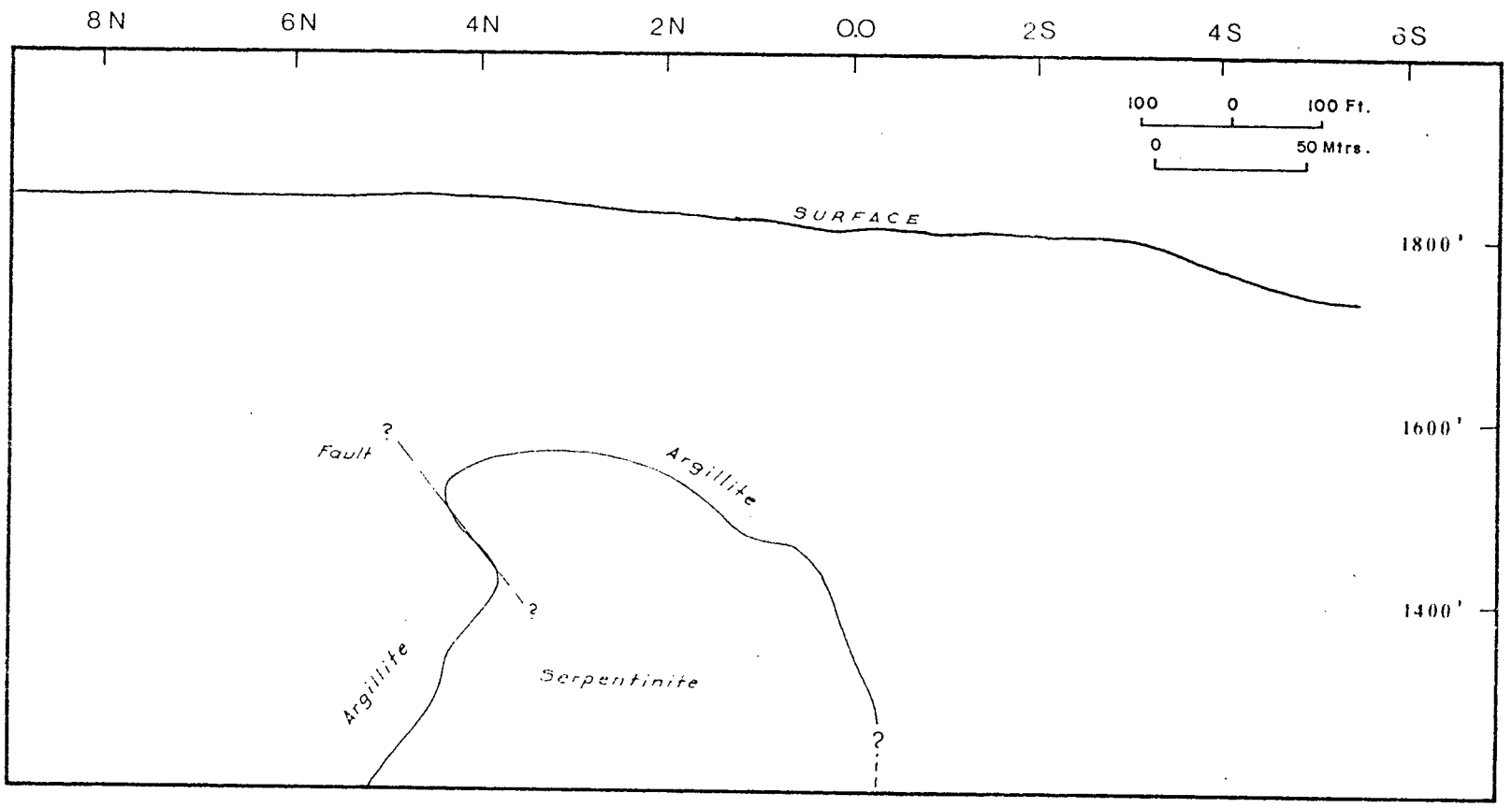

FIGURE 3-9: CROSS SECTION LOOKING NORTHEAST OF THE PORCUPINE SERPENTINITE BODY ALONG 26W. Note southeast contact dipping about 70°. (See location at Figure 3-3.)

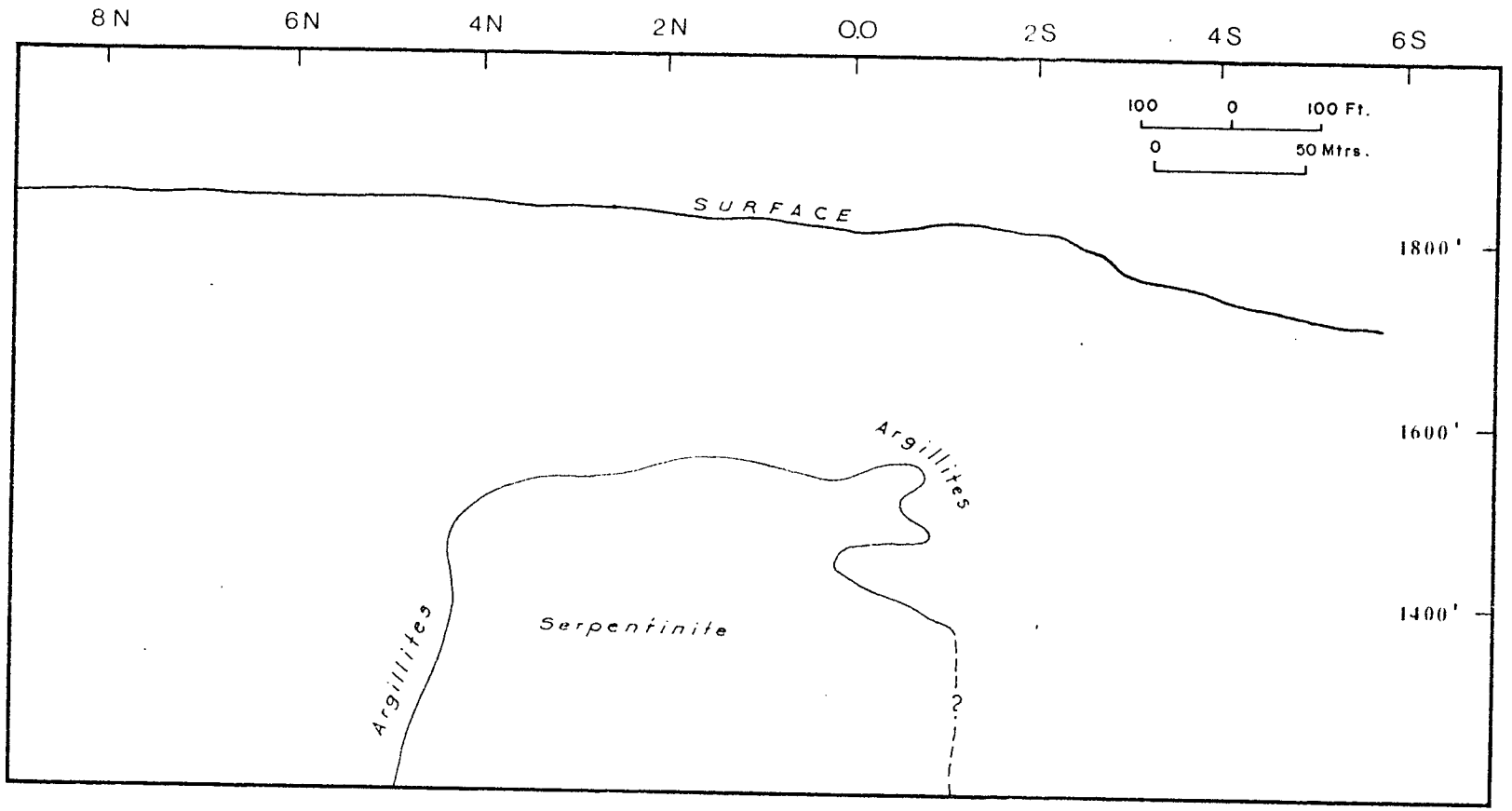

FIGURE 3-10: CROSS SECTION LOOKING NORTHEAST OF THE PORCUPINE SERPENTINITE BODY ALONG 24W. Note outline of contact resembles recumbent fold. (See location at Figure 3-3.)

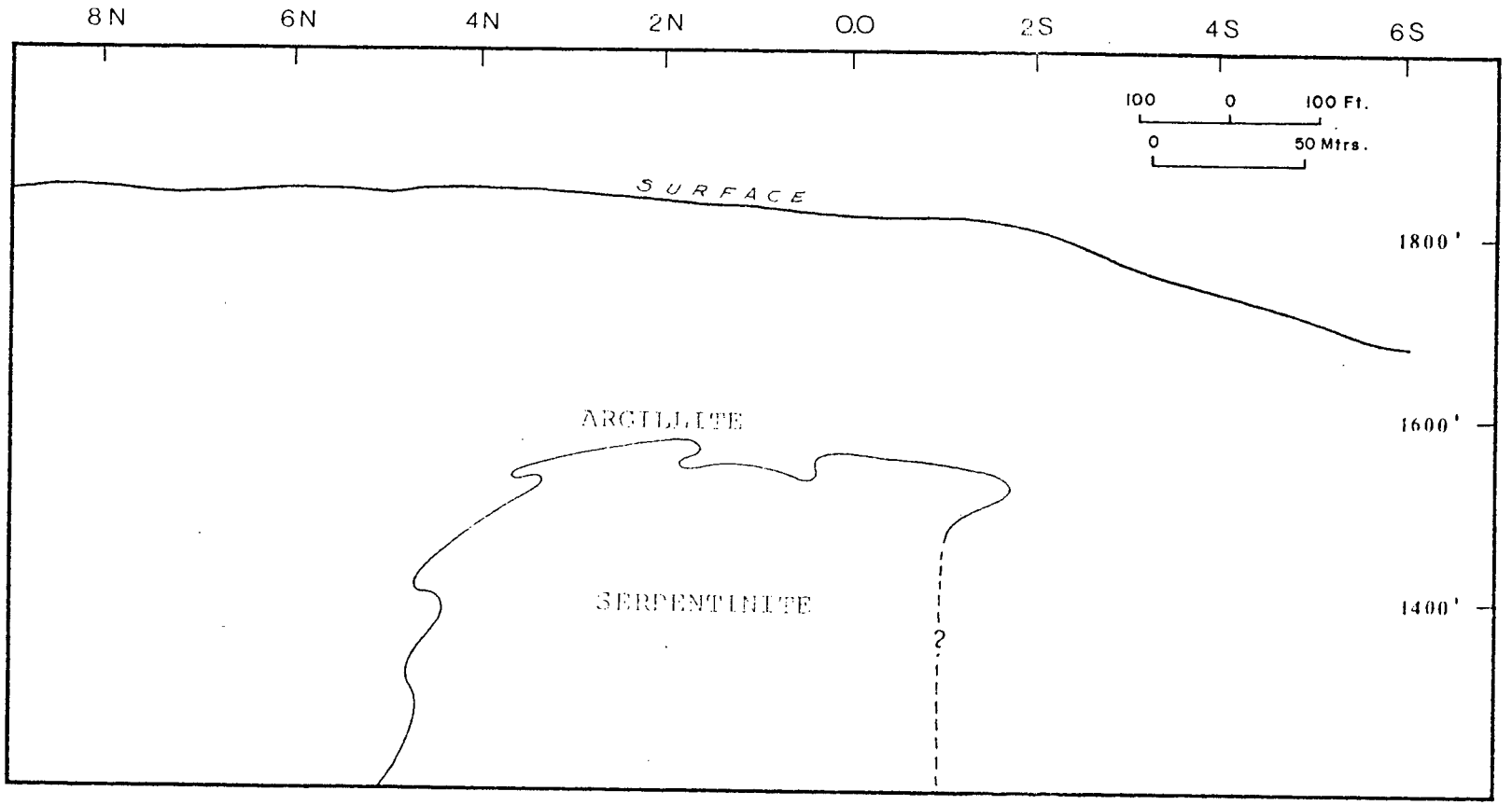

FIGURE 3-11: CROSS SECTION LOOKING NORTHEAST OF THE PORCUPINE SERPENTINITE BODY ALONG 23W. Note outline of contact resembles recumbent fold. (See location at Figure 3-3.)

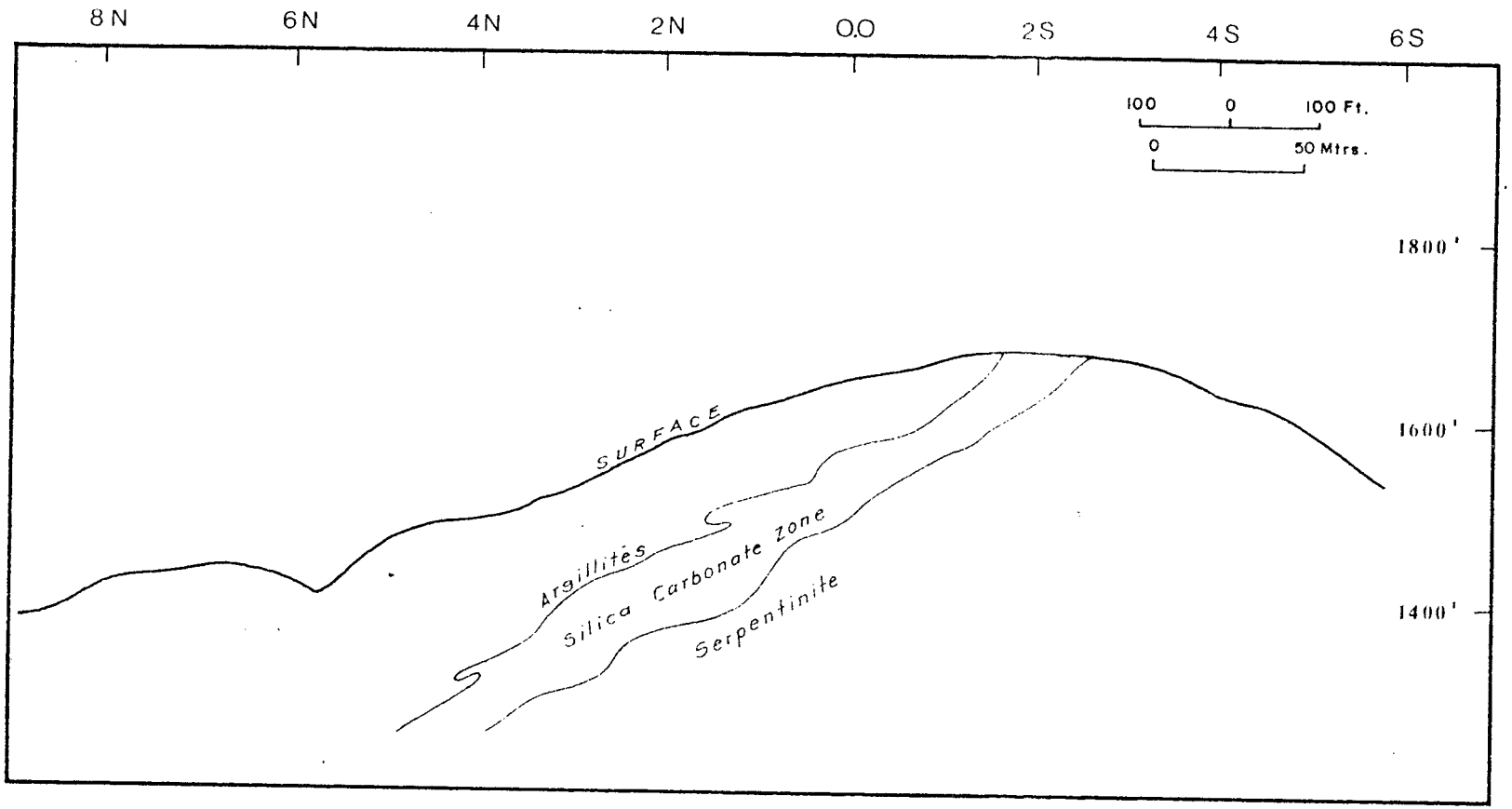

FIGURE 3-12: CROSS SECTION LOOKING NORTHEAST OF THE PORCUPINE SERPENTINITE BODY ALONG 10W. Note outline of contact of silica carbonate and argillite resembles recumbent fold. (See location at Figure 3-3.)

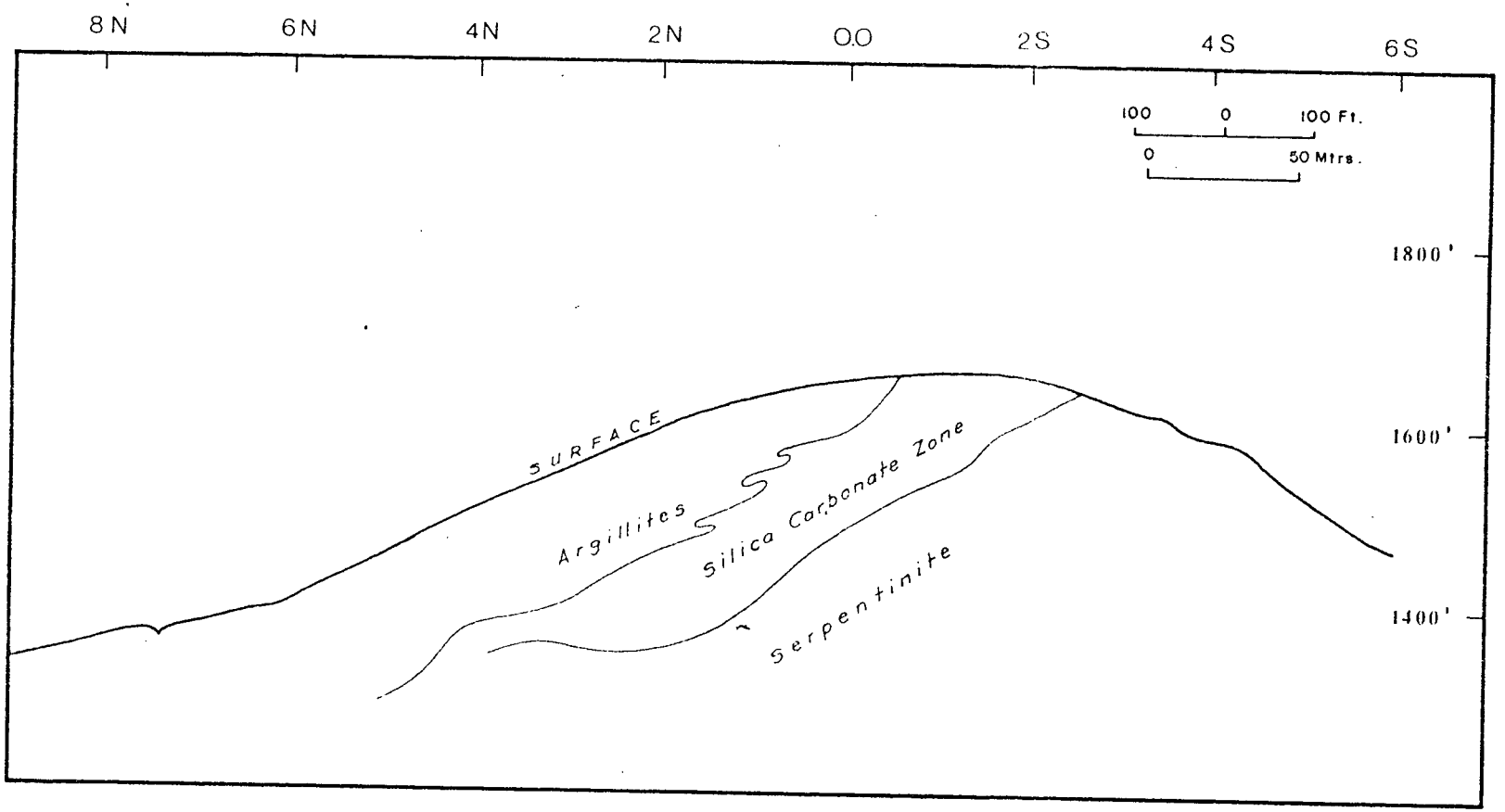

FIGURE 3-13: CROSS SECTION LOOKING NORTHEAST OF THE PORCUPINE SERPENTINITE BODY ALONG 9W. Note outline of contact of silica-carbonate and argillite resembles recumbent fold. (See location at Figure 3-3.)

mafic rocks. Layered ultramafic rocks are said to be due to magmatic differentiation and crystal settling (Wager and Brown, 1967), or perhaps, deformation and solid flow (Loney et al.,1971). The second kind, rocks of zoned ultramafic complexes have been explained in different ways by different researchers; some believe them to be magmatic, others metasomatic (Zavaritsky, 1928; Walton, 1951; Taylor and Noble, 1960; Bhattacharji and Smith, 1963; McTaggart, 1971). structures and textures such as cumulate textures,cryptic zoning, graded bedding, slump structures and channel fill structures are found in both layered and zoned ultramafic intrusions (Irvine, 1967; Wager and Brown, 1967). None of these features is recognized in the Clinton Creek ultramafic bodies. The author, therefore, believes the Clinton Creek ultramafic rocks to belong to the third kind of ultramafic body, the alpine type, which is discussed below.

Moores and MacGregor (1972) state that the emplacement of alpine type ultramafic bodies is due to the interaction of two or more lithospheric plates, at least one of which bears continental crust. They distinguish four types: (a) bodies with thermal aureoles suggesting intrusion at high temperature, (b) mantle slabs formed by diapiric upwelling of mantle material at spreading centres which were subsequently and independently emplaced onto the continental margins, (c) disrupted mantle slabs incorporated into melanges; and (d) conformable bodies in regionally metamorphosed terranes re-

presenting recrystallization and deformation of occurrences of types a, b and c. Certain features suggest that the ultramafic rocks of the Clinton Creek area fall into group c or d.

Pronounced mosaic textures in weakly serpentinized peridotite are said to result from syntectonic recrystallization (Ragan, 1969). Both mosaic texture and strained undulatory extinction are considered to be caused by solid state deformation in the pressure and temperature conditions of the upper mantle (Nicholas et al., 1972). Very low aluminium and calcium (Appendic C) are considered to be characteristic of crystalline mantle residue left after extration of basalt liquid (Dickey, 1970). Foliation may have developed during ascent of mantle material towards the surface. With release of pressure subsolidus reactions probably resulted in exsolution of clinopyroxene lamellae in orthopyroxene (Ragan, 1967; Loney et al., 1971; Himmelberg and Loney, 1963).

Original ultramafic rocks of the area are believed to have been lherzolite, harzburgite, pyroxenite and dunite. Country rocks consist of greenstone, some chert, argillite and limestone and with the ultramafic rocks, can be considered to form an ophiolite. Ultramafic bodies about 48 kilometres west of the Clinton Creek area in Alaska are interpreted as ophiolites by Foster (1974).

The absolute age of formation of the ultramafic bodies

is not known. However, their minimum age of emplacement can be determined. The oldest tight isoclinal folds with almost horizontal axial planes (F_1) seem to involve the margins of the ultramafic body (Figure 3-11). As this oldest known first phase deformation occurred with the main episode of metamorphism, in Permian time (see Table 2-1), the emplacement of the ultramafic rocks could not be younger than Permian.

A zone of ultramafic masses together with lenses of amphibolite and marble trend northwesterly close to and parallel to the Tintina fault where it crosses the Alaska-Yukon Territory border. These amphibolites and marbles are incorporated into and interlayered with low grade metamorphic rocks of greenschist facies. Occurrences of blue amphibole in quartzite and small bodies of eclogite are reported near Ross River along Tintina Trench (Foster, 1974). These data suggest that it is possible that the Tintina fault was an open rift in continental crust in early Permian time, and that ultramafic rocks and associated lenses of high grade metamorphites were emplaced tectonically when the rift closed. The rocks in question were thrust southwestward over Yukon Crystalline Plateau at the time of the closing of the trench (Tempelman-Kluit, 1976). Therefore the serpentinized ultramafic rocks might represent rocks that were thrust onto Yukon Crystalline Plateau before or during the main metamorphism (Permian) and which through subsequent deformation and metamorphism became intimately mixed with the rocks in which they were emplaced.

CHAPTER IV

THE CLINTON CREEK ASBESTOS DEPOSIT

4-1 INTRODUCTION

The Clinton Creek mine, about 225 kilometres south of the Artic Circle, was the most northerly open pit (Plate 4-1) operation in Canada. It is at an elevation of 535 metres on Porcupine Hill which overlooks Clinton Creek (Figure 2-2). The mill is situated on Trace Hill on the opposite side of Clinton Creek. and the ore was transported by a mile-long tramline. The ore to waste ratio average was 1:5 and the average chrysotile-fibre length between 1.5 mm and 3.0 mm. The three ore-bearing ultramafic bodies outlined by diamond drilling, was 270 metres wide and 1,400 metres long (Figure 3-6). The main Porcupine ore zone is 135 metres wide, and 535 metres long, and has been drilled to a depth of 900 feet (Figure 3-7).

4-2 CHRYSOTILE VEINS

PLATE 4-1: Clinton Creek open pit asbestos mine. Porcupine pit (right); Creek pit (middle); Snow Shoe pit (left). (Photograph taken looking towards southwest.)

4-2-A Textures and Structures

Two different types of chrysotile veins are distinguished: chrysotile-fibre veins and picrolite veins.

a. Chrysotile-fibre veins

Chrysotile fibre veins are of two types: cross-fibre and slip-fibre veins. The majority of the fibre veins in the Clinton Creek mine consist of cross-fibre chrysotile and are under six mm in width. In some, chrysotile fibres lie perpendicular to the vein wall, but in others the fibres form an acute angle with the wall (Plate 4-2). Figure 4-1, A and B show common variations of the first two types; and individual fibres pass from one wall of the vein to the other with perfect continuity. Many fibre-veins show partings. Those may be inclined (Figure 4-1-C) or parallel (Figure 4-1-D) to the vein wall. Both inclined and central partings are filled commonly with magnetite and less commonly with picrolite. In some specimens, partings divided the fibres into lenses (Figure 4-1-C), and in these there is no change in direction of fibres on each side of the parting. A few veins are made up of fibre lenses separated by antigorite, picrolite or magnetite (Figure 4-1-E). Slip-fibre veins (Figure 4-1-F) in which most of the chrysotile fibres are almost parallel to the vein wall, occur in conjunction with the cross-fibre or in zones where

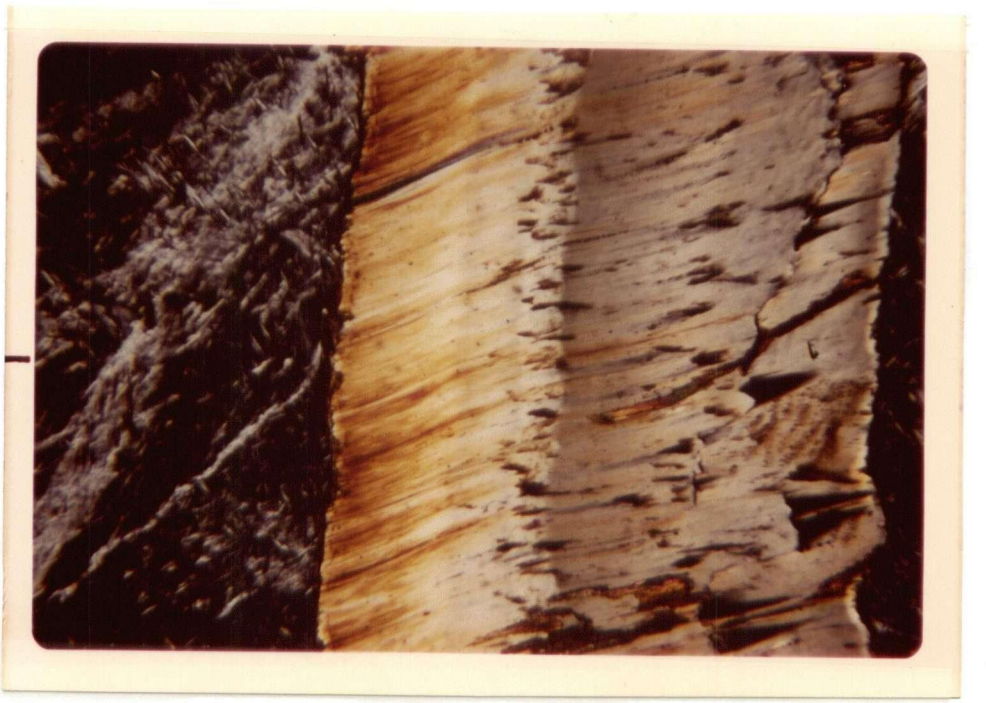

PLATE 4-2: Cross-fibre chrysotile vein in thin section. Fibres lie obliquely to the wall of the vein. Adjacent, gray and isotropic mineral is antigorite. (Crossed nicols.)

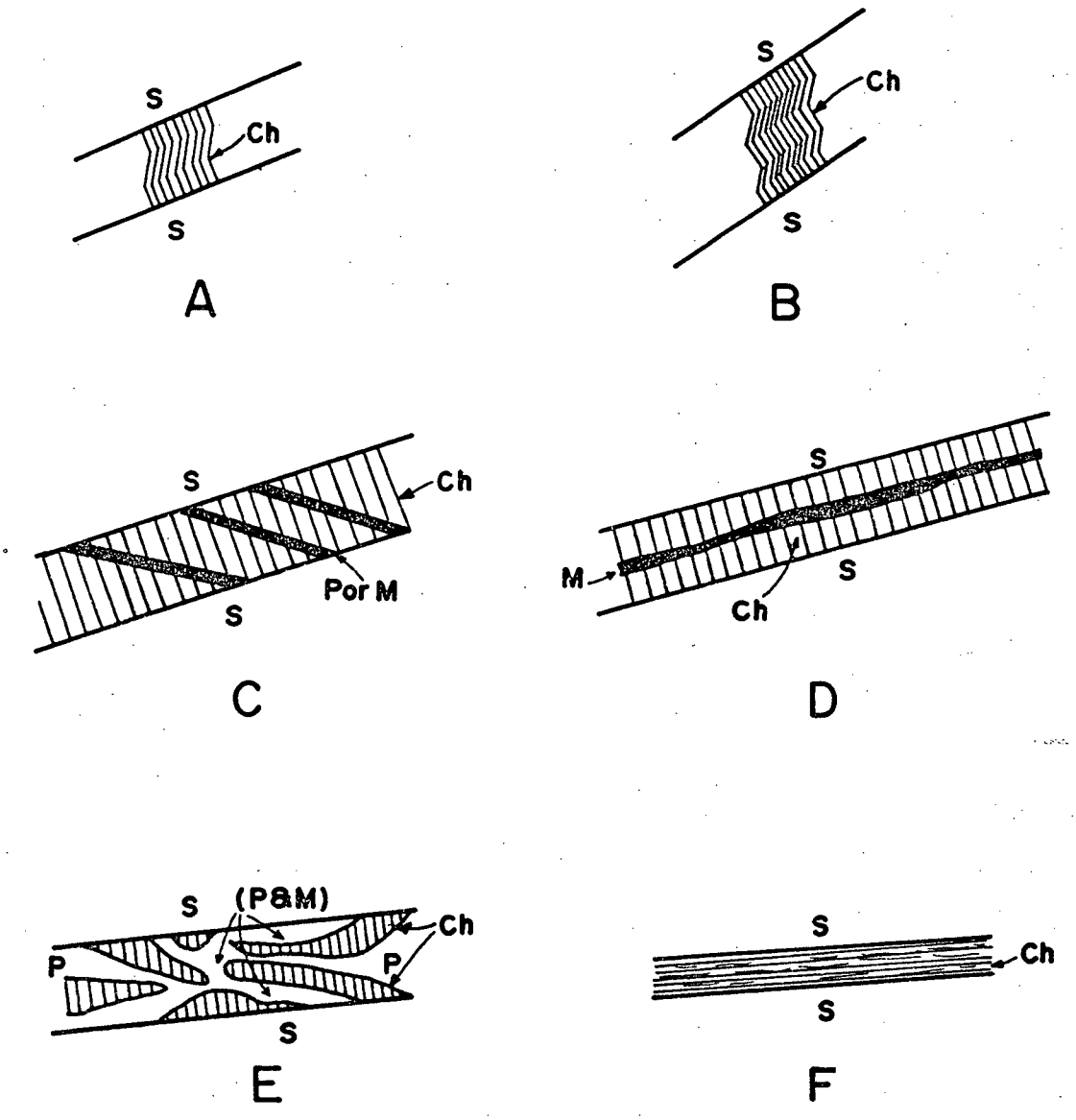

FIGURE 4-1: CHRYSOTILE-FIBRE VEINS.
A,B. Fibres oriented perpendicular and inclined to vein walls.
C. Inclined partings divided the fibres but the fibres do not change in direction on each side of the parting.
D. Central parting is usually filled with magnetite.
E. Composite vein is made up of fibre lenses separated by magnetite, picrolite or antigorite.
F. Slip-fibre vein.
(P = picrolite; M = magnetite; S = non-fibre serpentine; Ch = chrysotile-fibre.)

deformation has been intense.

Fibre veins may be straight or curved (Figure 4-2-A). Some intersect (Figure 4-2-B) or diverge (Figure 4-2-C). Colours of veins range from light green to dark green but individual veins are of only one colour. Most of the fibres separate readily and are soft like silk but some chrysotile veins are harsh and do not separate easily into fine fibres. Adjacent fibres are parallel. Some of them are perfectly straight but usually minute corrugations are present which give rise to a chatoyant and banded appearance of the vein (Figure 4-1-B). Fine-grained magnetite occurs as thin sheets or lenses which are oriented parallel or inclined to the wall, or parallel to fibres (Figure 4-2-D). Magnetite commonly fills the acute angle at low angle junctions (4-2-E). At some vein junctions there is a confused mixture of fibre, magnetite and serpentine. At other vein junctions the fibre of one vein will bend and become oriented parallel to the fibre of the other vein without any discontinuity (4-2-E and F). At some junctions fibres on one vein cut across the fibres of another vein completely (Figure 4-2-B).

b. Picrolite veins

Picrolite, non-fibrous chrysotile, compared to chrysotile fibre, is relatively hard, pale green to yellowish green, and has a splintery fracture. Picrolite veins occur

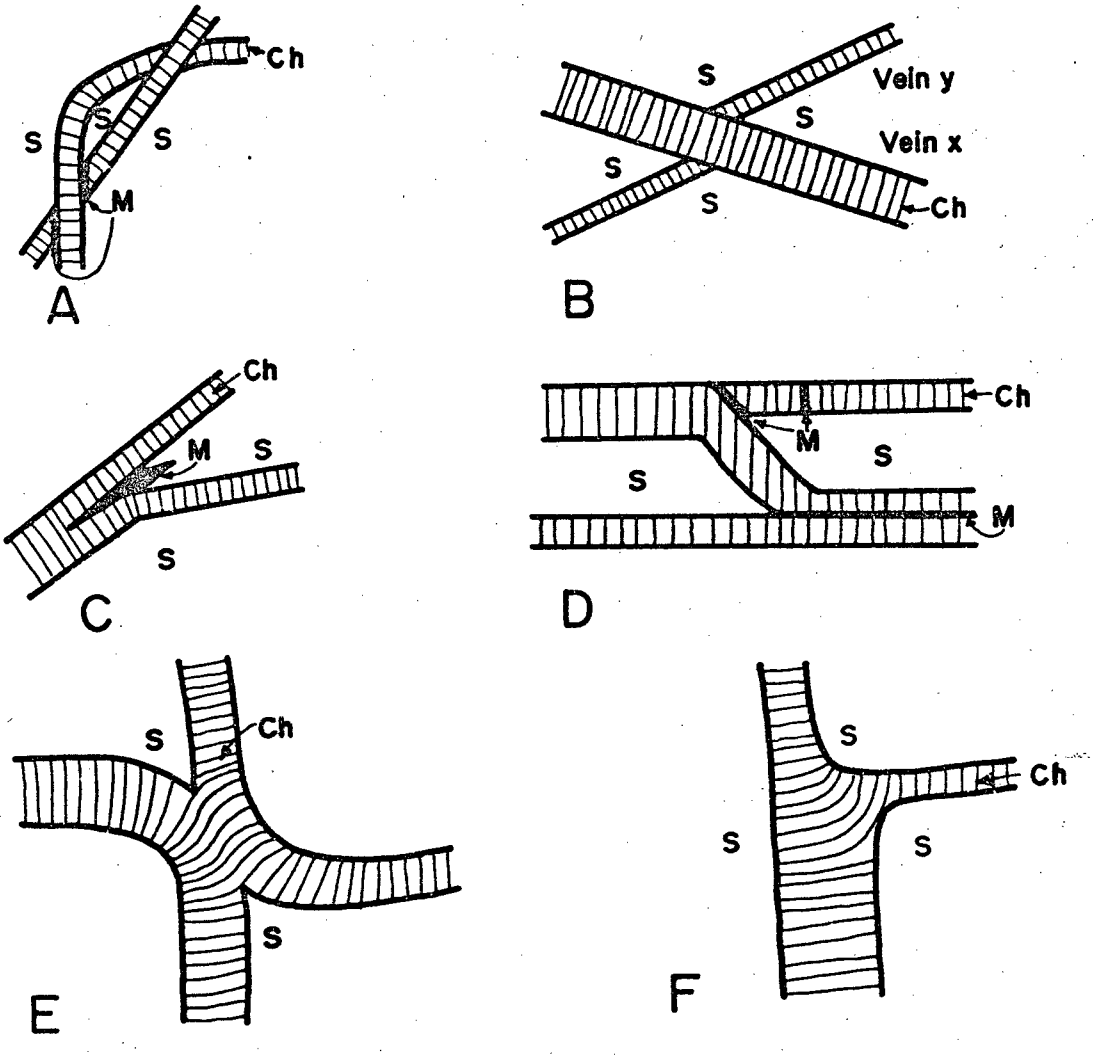

FIGURE 4-2: CHARACTERISTICS OF CHRYSOTILE-FIBRE VEINS.
A. Two fibre veins cut across each other at different points.
B. Fibre in vein X crystallized in an expansion fracture which separates vein Y perpendicularly.
C. Magnetite commonly fills acute angle at low angle junction.
D. Magnetite occurs as thin sheets or lenses in fibre-veins.
E,F. Fibre of one vein bands and becomes oriented parallel to the fibre of the other vein without discontinuity.
(Ch = chrysotile; M = magnetite; S = non-fibre serpentine).

mostly along fault surfaces, generally with fibre veins that are mostly of slip-fibre, and rarely as isolated fracture fillings. Picrolite appears to be contemparaneous with or later than chrysotile fibre. Veins range in width from microscopic to eight centimetres. Although some of the veins are hard and compact, others are soft due to a high content of uncombined water, for they tend to lose weight and crumble after brief exposure to the atmosphere.

Delicate bands or lenses of picrolite paralleling the walls of chrysotile veins are usually only a small fraction of a millimetre in thickness but may reach as much as several millimetres. The banding which is further emphasized by slight differences in colour and parting between successive bands is ordinarily sharp (Plate 4-3). Very few bands are perfectly straight; they mostly reflect the irregularities in the vein wall, which is slightly wavy. The banding does not extend across the full width of every vein, but is confined to one side of the vein.

Under microscope picrolite displays delicate banding parallel to the vein walls (Plate 4-3), and individual bands of picrolite are found to be composed of transverse fibres which occupy a position anywhere from normal to oblique to the margins of the bands (Plate 4-3). Variation in the position of extinction from band to band, is due to slight differences in orientation of the fibres in successive bands. The contact between the vein and wall rock may be sharp or

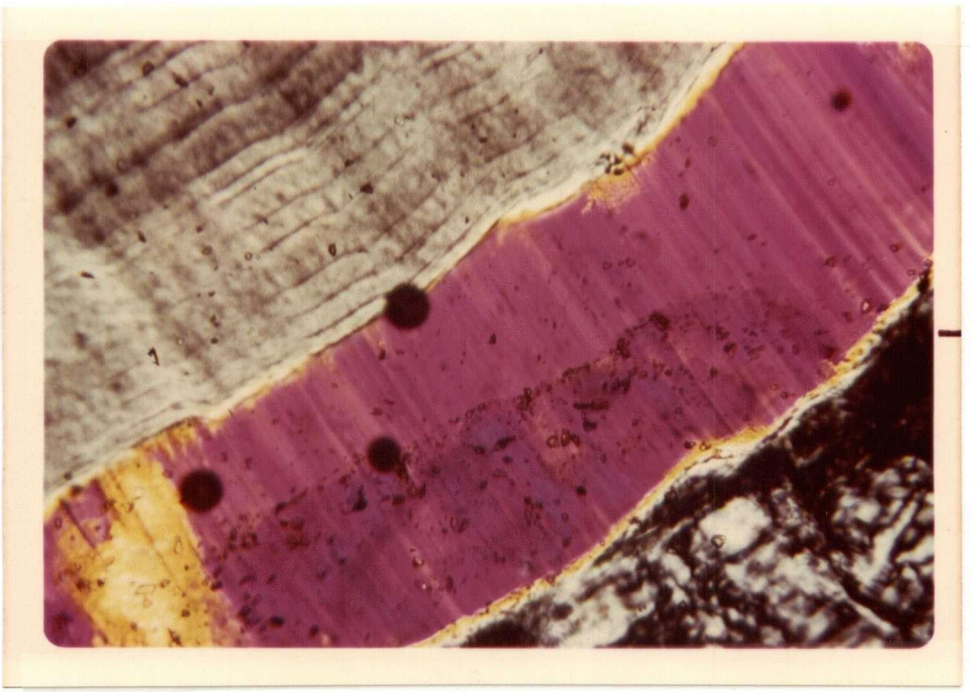

PLATE 4-3: light green, parallel, sharp banding of picrolite, at left hand top, displays fibre-like forms which are transverse to banding. Purple band is chrysotile-fibre. Gray and isotropic mineral at right hand bottom corner is antigorite. (Crossed nicols.)

gradual. Not all picrolite veins have a banded nature, some are amorphous or cryptocrystalline. Usually the smallest picrolite veins are amorphous. Unlike chrysotile-fibre veins, picrolite veins are devoid of magnetite. In places magnetite is found as inclined partings or coating in contrast to magnetite in fibre veins (Figure 4-3-A and B). Commonly fibre veins end abruptly at picrolite veins (Figure 4-3-C) and such picrolite veins are generally slickensided and lie along the direction of major shear planes. The sense of movement on such picrolite-bearing shears is generally normal rather than reverse. Chrysotile-fibres in contact with or close to picrolite veins are invariably brittle and brownish. Picrolite selvages on chrysotile-fibre veins are thick on one side of the fibre vein and thin or absent on the other side. This might be due to late deformation effects on the chrysotile vein, for there are some indications that chrysotile fibre has been deformed and altered to picrolite (Figure 4-3-D and E). Figure 4-3-F shows cross-fibre changed to slip-fibre and then to picrolite or directly to picrolite.

4-2-B Relationship with Serpentine Wall Rock

The contact of chrysotile-fibre and wall rock is sharp and generally planar, but minor crenulations are not uncommon. The wall may be in direct contact with fibre or coated with magnetite or slickensided picrolite. On a

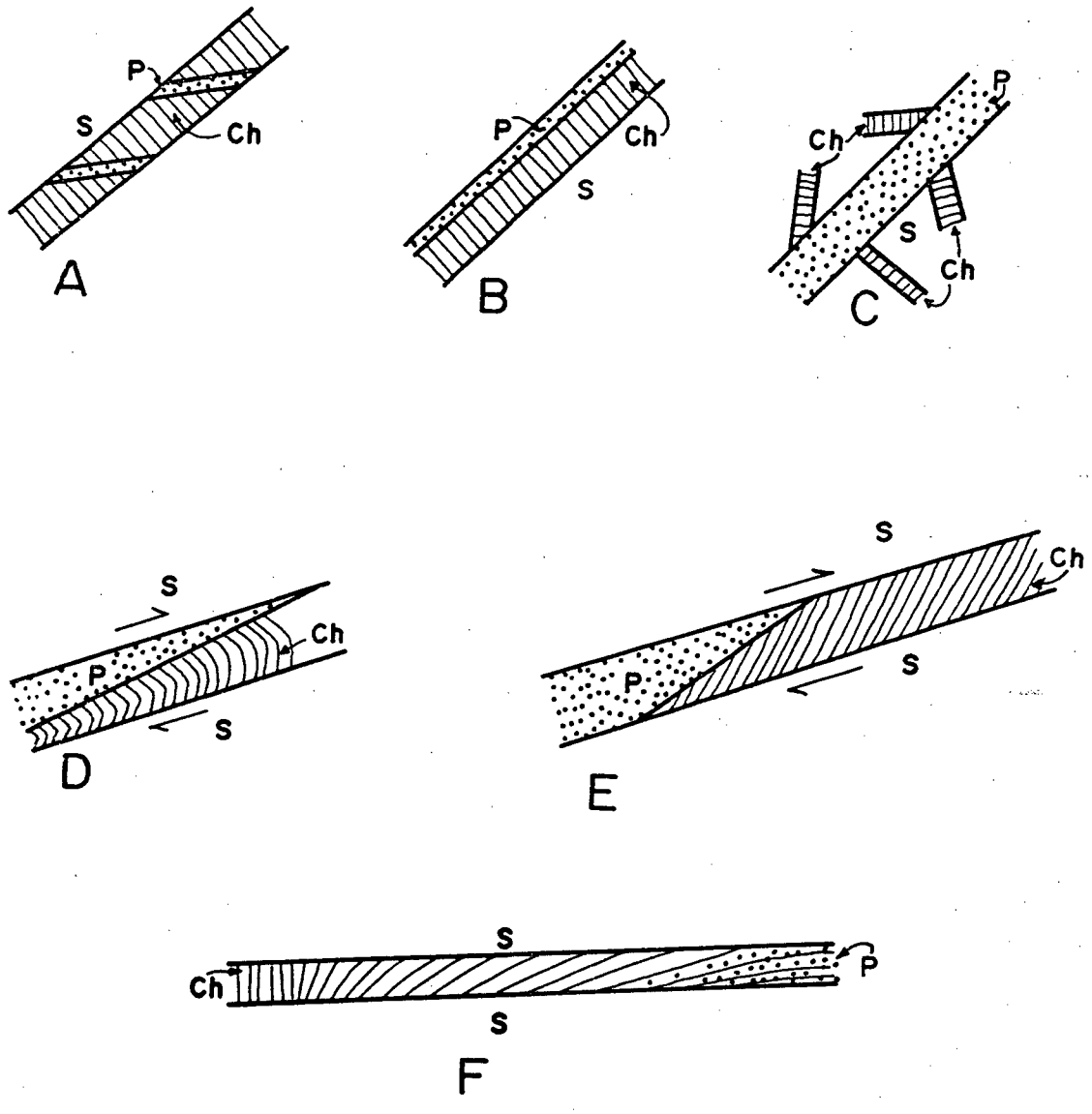

FIGURE 4-3: CHARACTERISTICS OF PICROLITE VEINS.
A. Picrolite occurs as parting in chrysotile-fibre vein.
B. Picrolite forms a coating on chrysotile-fibre vein.
C. Picrolite stops the continuation of some fibre vein.
D. Picrolite forms a pseudomorphs after deformed slip-fibre.
E. Picrolite occurs at an acute angle to fibre in same vein.
F. Successive change of cross-fibre to slip-fibre and then to picrolite. (P = picrolite; Ch = chrysotile-fibre; S = non-fibre serpentine).

macroscopic scale vein walls match, but under the microscope there are minor exceptions. Inclusions of wall rock in the veins are observed here and there and some of these fragments match the adjacent wall. Fibre veins that end abruptly against another vein do not taper in width. In a few cases veins taper and finally disappear (Plate 4-4).

4-2-C Chemistry of Chrysotile and Antigorite

A total of 97 specimens of chrysotile (33) and antigorite (64) were collected from the Clinton Creek area to study their respective chemistries. X-ray analysis showed that no other serpentine species were present. Chemical analysis of all samples were done using an ARL electron microprobe (Model-SEMQ) in the Department of Geological Sciences, University of British Columbia with assistance of Mr. G. Georgakopoulos. Samples were analyzed for eleven oxides (Na_2O, MgO, Al_2O_3, SiO_2, K_2O, CaO, TiO_2, Cr_2O_3, MnO, FeO, and NiO). Results are listed in Table 4-1.[1] Means, standard deviations and variances are given in a statistical summary (Table 4-2, 4-3). Figure 4-4 and 4-5 are histograms showing compositional variation of the major oxides that are different statistically in the two serpentine minerals. These histograms illustrate the limited composition-

---

1: See Appendix E

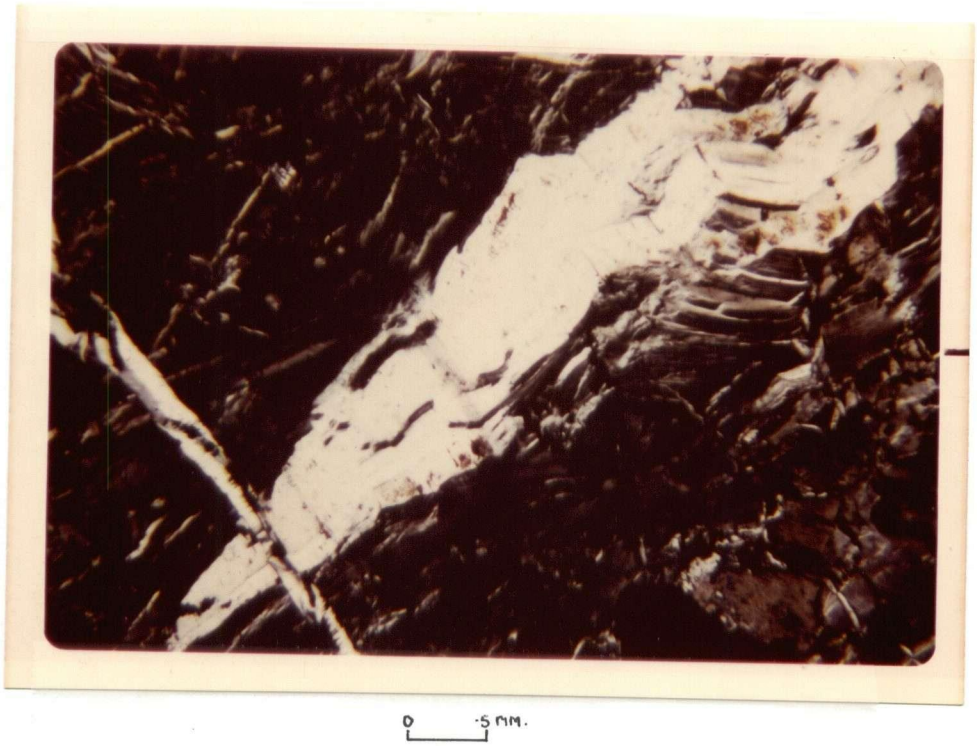

PLATE 4-4: Tapered, light gray chrysotile-fibre vein. Note cross-cutting vein, suggesting different periods of chrysotile-fibre formation. Also note matching walls. (Crossed nicols.)

TABLE 4-2

STATISTICAL SUMMARY OF ELEVEN OXIDES OF 33 CHRYSOTILE SAMPLES

Oxides	Arithmetic		
	Means($\bar{X}$)	Std. Deviation(S)	Variance(S^2)
Na_2O	0.0318	0.0101	0.0001
MgO	39.6417	0.4369	0.1909
Al_2O_3	0.8351	0.2676	0.0716
SiO_2	40.4060	0.8466	0.7168
K_2O	0.0306	0.0152	0.0002
CaO	0.0397	0.0230	0.0005
TiO_2	0.0336	0.0197	0.0004
Cr_2O_3	0.3379	0.3130	0.0980
MnO	0.0312	0.0192	0.0004
FeO	2.1297	0.6585	0.4336
NiO	0.2079	0.1255	0.0158

TABLE 4-3

STATISTICAL SUMMARY OF ELEVEN OXIDES OF 64 ANTIGORITE SAMPLES

Oxides	Arithmetic		
	Means ($\bar{X}$)	Std. Deviation (S)	Variance (S^2)
Na_2O	0.0208	0.0113	0.0001
MgO	38.0282	0.6792	0.4613
Al_2O_3	0.9456	0.3603	0.1298
SiO_2	41.9354	0.9900	0.9802
K_2O	0.0248	0.0148	0.0002
CaO	0.0300	0.0225	0.0005
TiO_2	0.0237	0.0174	0.0003
Cr_2O_3	0.2961	0.2266	0.0513
MnO	0.0487	0.0418	0.0017
FeO	2.9778	0.7924	0.6279
NiO	0.1961	0.1405	0.0198

MEAN ($\bar{X}$)	38·0282	0·9456	41·9354	2·9778
STD. DEVIATION (S)	0·6792	0·3603	0·99	0·7924
CLASS INTERVAL (C.I.)	1·65	0·0901	0·245	0·198

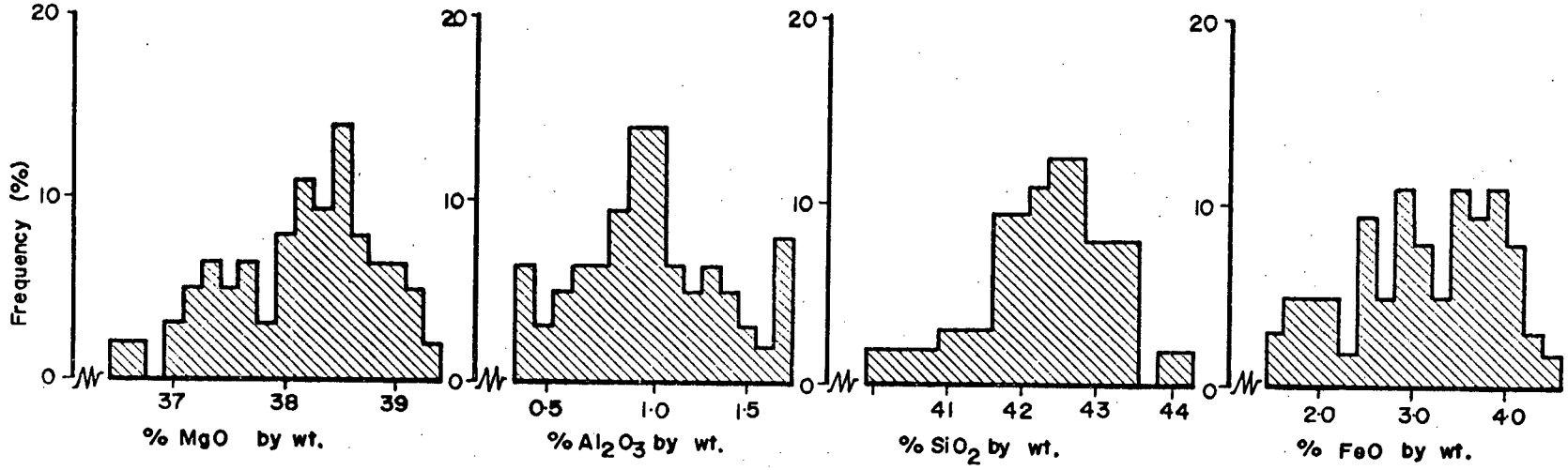

FIGURE 4-4: FREQUENCY DIAGRAMS OF MgO, Al_2O_3, SiO_2 and FeO (by wt. percent) OF 64 ANTIGORITE SAMPLES.

MEAN ($\bar{X}$)	39·6417	0·8851	40·4060	2·1297
STD DEVIATION (S)	0·4369	0·2676	0·8466	0·6585
CLASS INTERVAL (C.I.)	0·11	0·0669	0·21	0·165

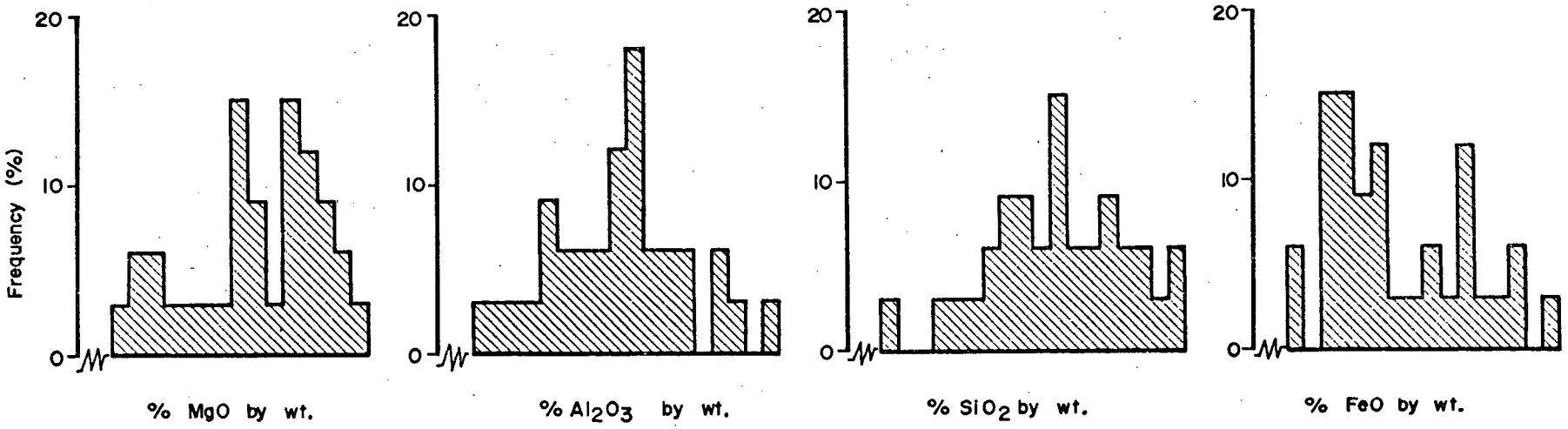

FIGURE 4-5: FREQUENCY DIAGRAMS OF MgO, Al_2O_3, SiO_2, and FeO (by wt. percent) OF 33 CHRYSOTILE SAMPLES.

al variation of the major oxides that are different statistically in the two serpentine minerals. The histograms illustrate the limited compositional ranges that are summarized in Table 4-2 and 4-3. Means and variances of each variable of the two serpentine minerals are compared by "t" test and "F" test to find whether or not the two minerals have the same chemical composition (tested at the 95 percent confidence level). These tests indicate that the means for MgO, Al_2O_3, SiO_2 and FeO are significantly different for the two minerals. Chemical difference between the two serpentine minerals could arise from several causes. Conditions of formation may be the principal explanation, in that temperature and fluid composition might have been the controlling factors. Certainly there would seem to be some control such as temperature necessary to explain the different chemical composition of the two minerals if they are in equilibrium.

4-3 FRACTURES AND DISTRIBUTION OF CHRYSOTILE FIBRE VEINS

Figure 4-6 shows a nearly random distribution of attitudes of fibre veins. This randomness is believed by the author to be mainly due to the curved nature of the veins along which attitudes in many directions can be measured.

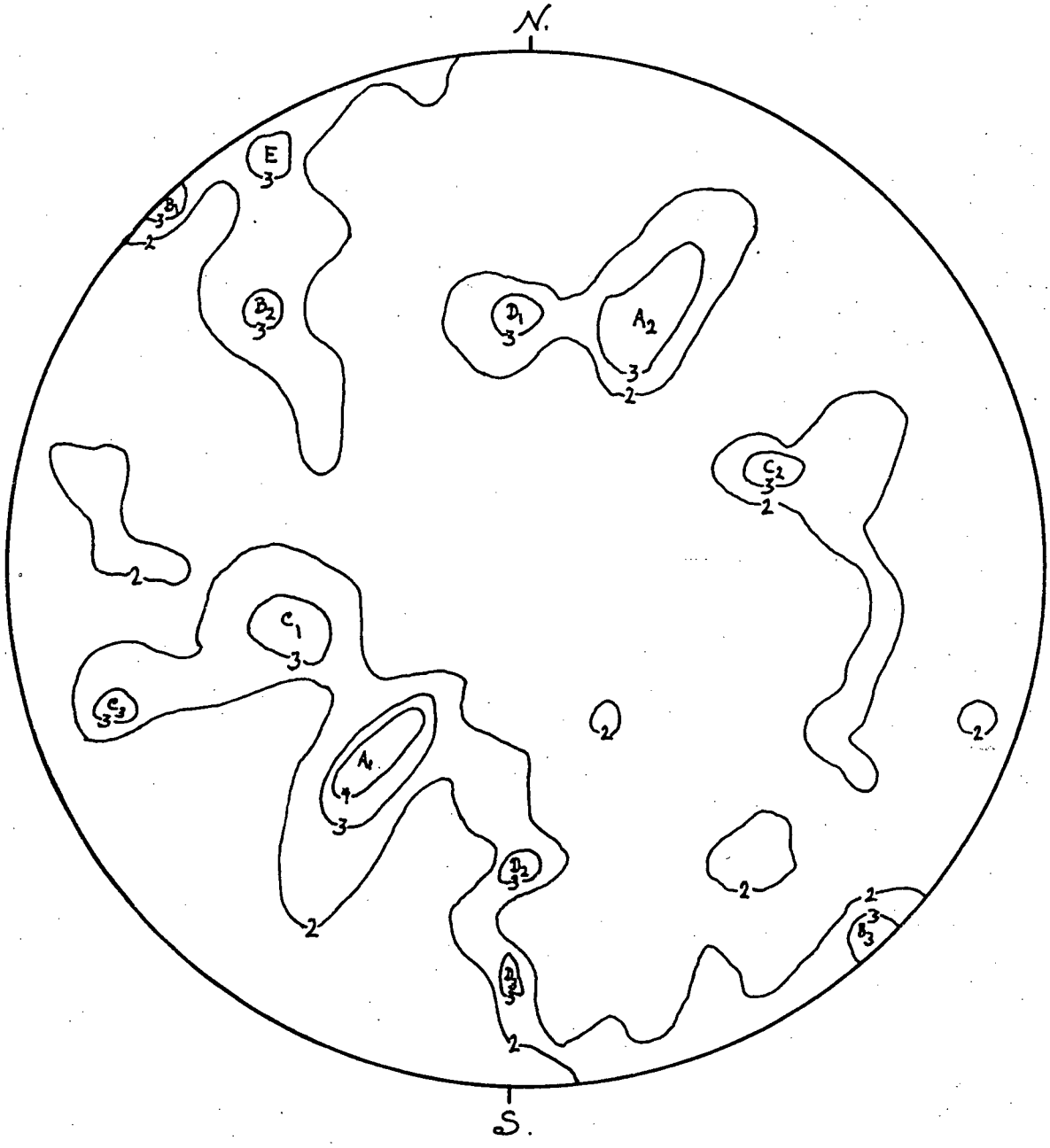

FIGURE 4-6: POLES TO 264 CHRYSOTILE-FIBRE VEINS.

Nevertheless, if concentrations of only three or four percent are considered, five distinct groups can be seen (Figure 4-6): A. 305°/35° to 60° - NE and SW; B. 225°/70° to 90° - SE; C. 340°/40° - NE and SW; D. 270°/45° to 70° - N and S; and E. 240°/80° - SE. Comparison of Figure 4-6 with Figure 4-7 and 4-8 shows that fibre-veins of groups A, B and C occur in shear zones and group D and E occur in joints. Ore grade zones of the Porcupine pit (Figure 4-9, 4-10) show the elongation of the high grade ore zones are in accord with the trends of groups B and D. A cross-section (Figure 4-11) of the Porcupine pit also reveals that the dips of different ore grade zones vary from 45° to 70°.

Fibres in steeply dipping veins are generally longer and thicker than those of low dips. Fracture spacing of 7 to 27 centimetres seems to be associated with longest average fibre (Plate 4-5). With higher fracture density, fibres become shorter.

Massive unsheared serpentinite contains very little fibre. Zones of polished fish-scale serpentinite are devoid of fibre. Also, finely crushed zones where serpentinite disintegrates on exposure and can be broken between the fingers are barren, even if it occurs within ore zones. Rare serpentinite breccias (Plate 4-6) mostly adjacent to rodingite, are devoid of chrysotile-fibre.

An attempt was made to correlate different kinds of fractures in the country rocks (Figure 2-11) as well as

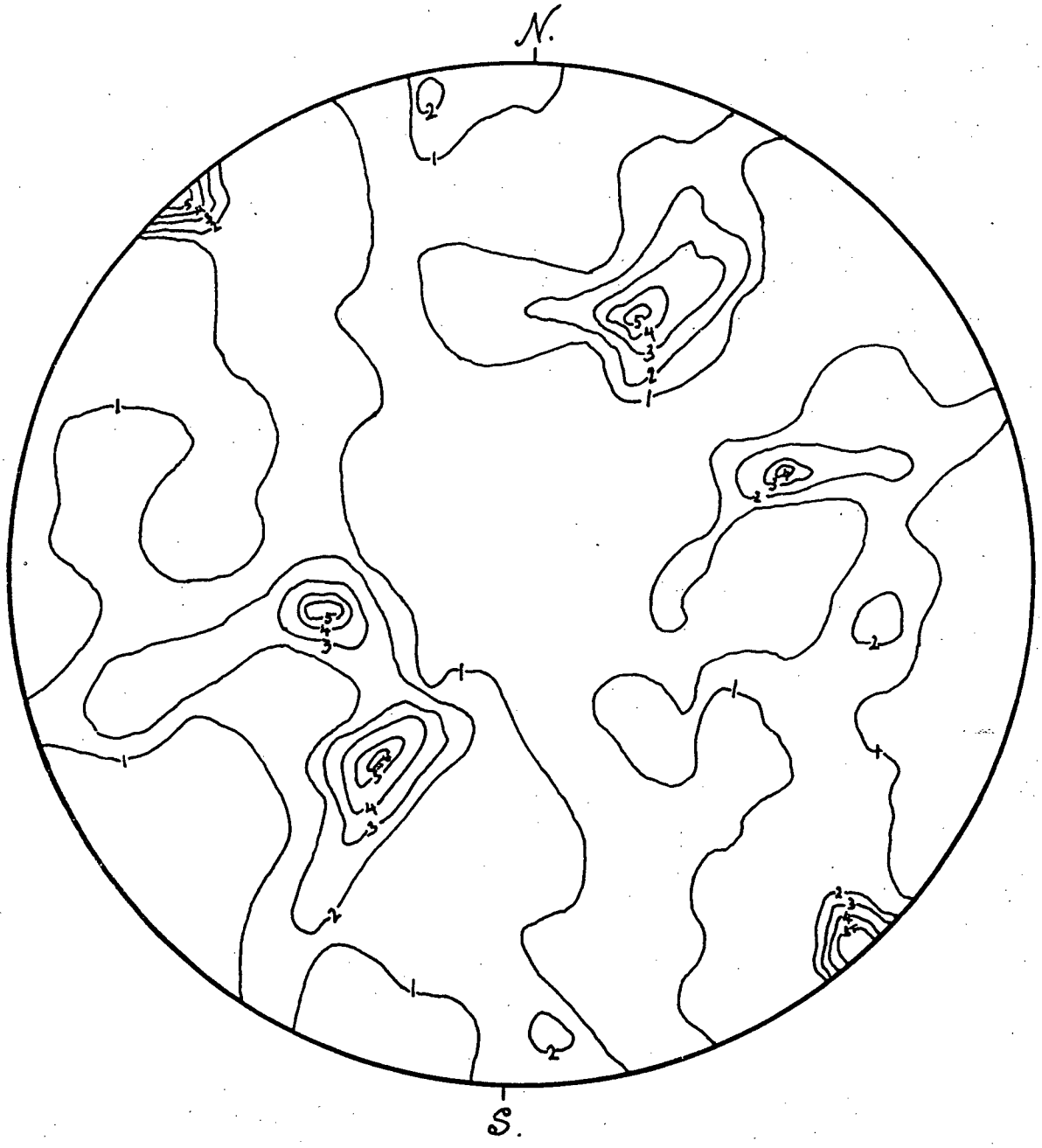

FIGURE 4-7: POLES TO 125 CHRYSOTILE-FIBRE VEINS SHOWING DISPLACEMENT ALONG THE CONTAINING FRACTURE.

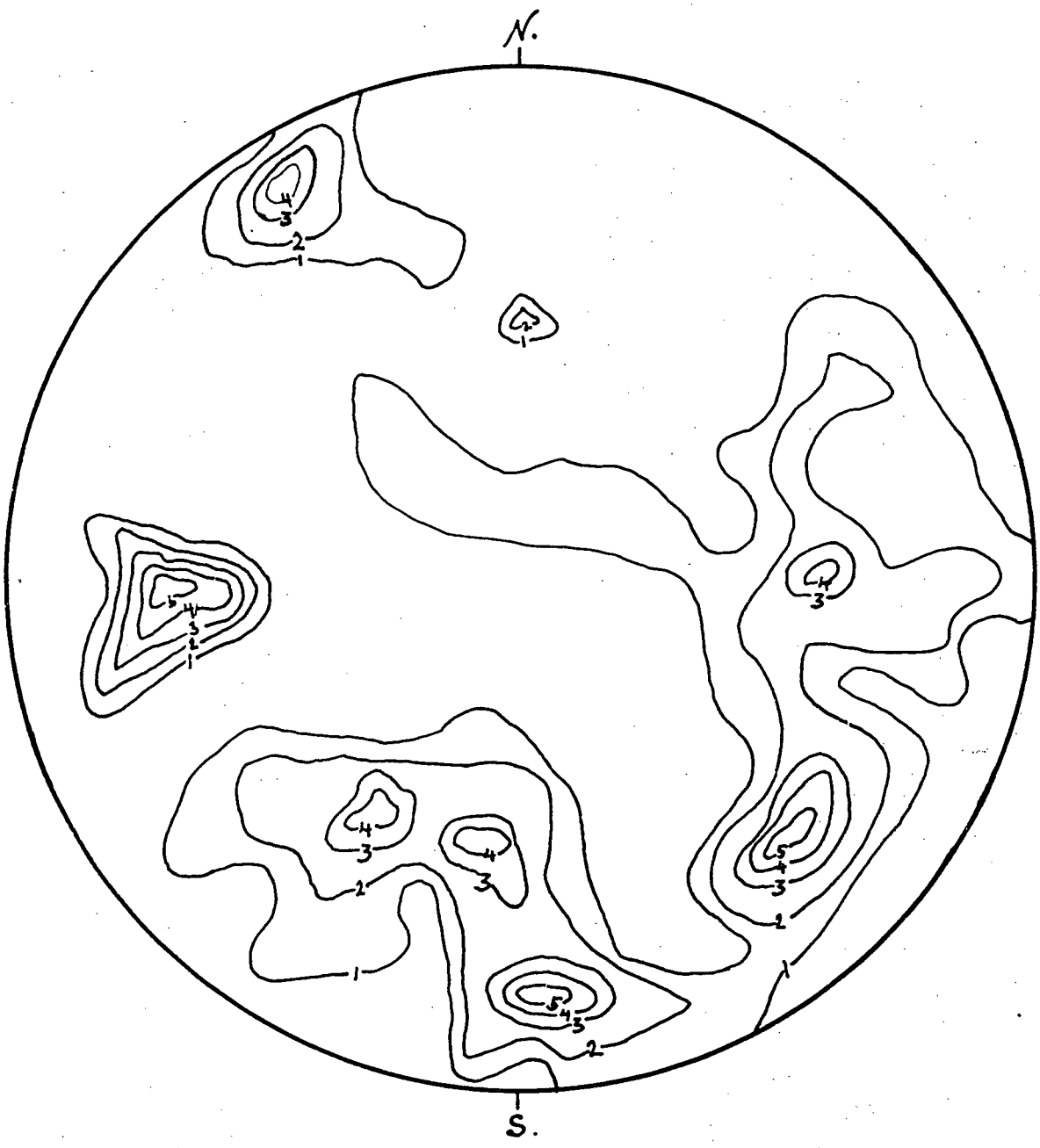

FIGURE 4-8: POLES TO 139 CHRYSOTILE-FIBRE VEINS IN JOINTS.

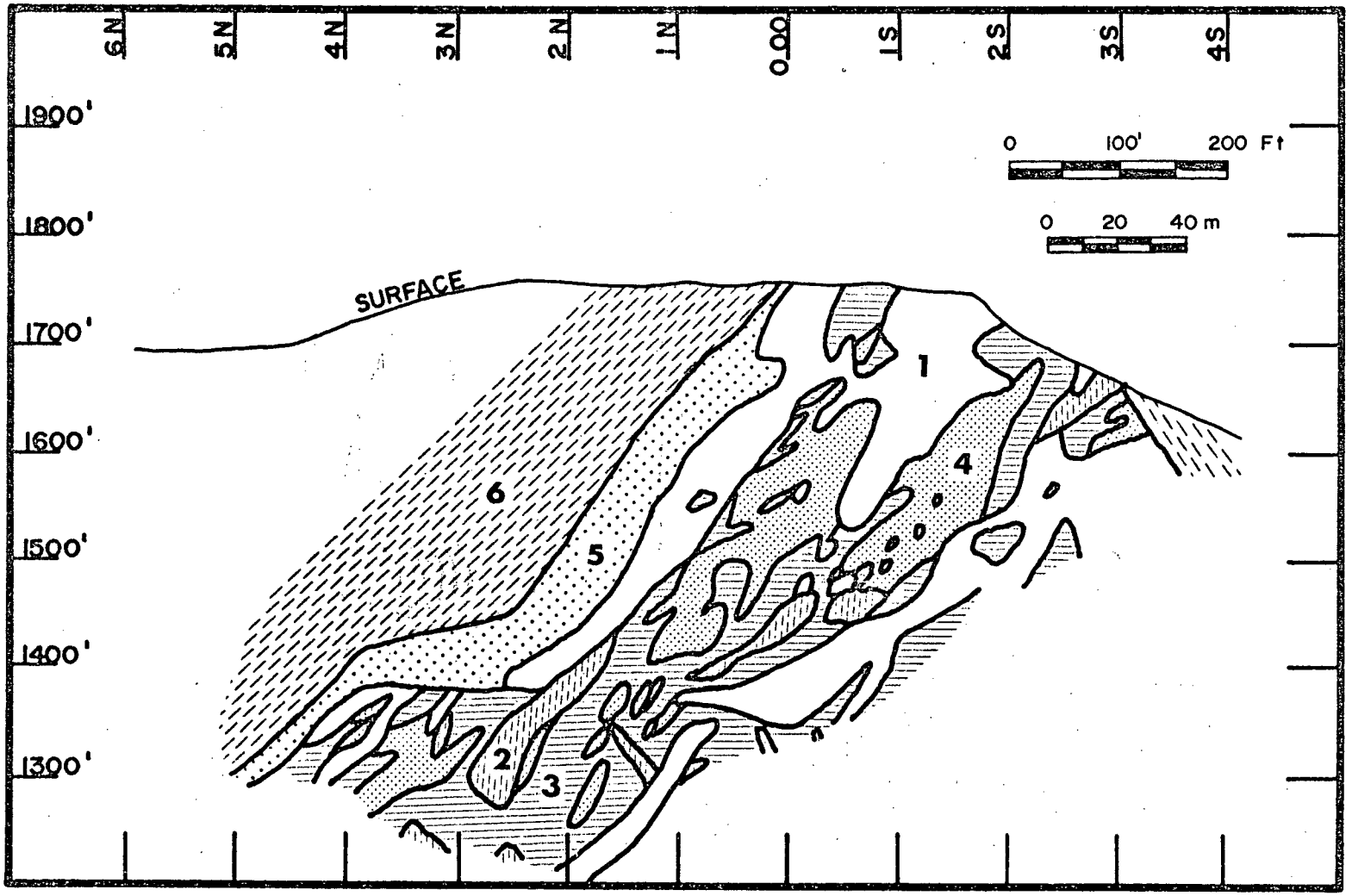

FIGURE 4-11: CHRYSOTILE-FIBRE ORE GRADE ZONES IN CROSS SECTION ALONG 17W. (See Figure 3-3 for location.) 1= Serpentinite with 0 to 1 percent fibre; 2= Serpentinite with 1 to 3 percent fibre; 3= Serpentinite with 3 to 7 percent fibre; 4= Serpentinite with more than 7 percent fibre; 5= Silica-carbonate rock; 6= Argillite.

PLATE 4-5: Long-fibre chrysotile veins in widely spaced fractures. This kind of vein is planer and has a consistant attitudes. Usually the length of fibres is longer than the length of the fibres in shear zones.

PLATE 4-6: Serpentinite breccia in Snow Shoe pit. It occurs usually in crushed serpentinite zone or adjacent to rodingite.

fractures adjacent to the Porcupine ultramafic body (Figure 4-12) with five concentrations of chrysotile-fibre-veins (Figure 4-6) previously mentioned. Fibre-veins of group D_2, D_3 and E closely parallel some of the joint concentrations shown in Figure 2-11. Fibre-veins of group A_2 and B_1 parallel some of the fault concentrations shown in Figure 4-12. Group A, the highest concentration of fibre-veins generally coincides with foliations F_2 (Figure 2-8) which strike northwest and dip northeast. Some groups of fibre-veins are not quite parallel to sets of fractures but differ by five to ten degrees both in strike and dip. This may be due to the difference in physical properties of the ultramafic rock and the country rock. Some of the fibre-veins cannot be correlated with any of the fractures described above and it is possible that these vein-fractures developed during serpentinization.

The above facts lead the writer to believe that although chrysotile-fibre chrystallized in many kinds of fractures, the main commercial concentration of fibre is controlled by joints and faults noted above.

4-4 ORIGIN OF CHRYSOTILE VEINS

4-4-A Temperature of Formation of Serpentine Minerals

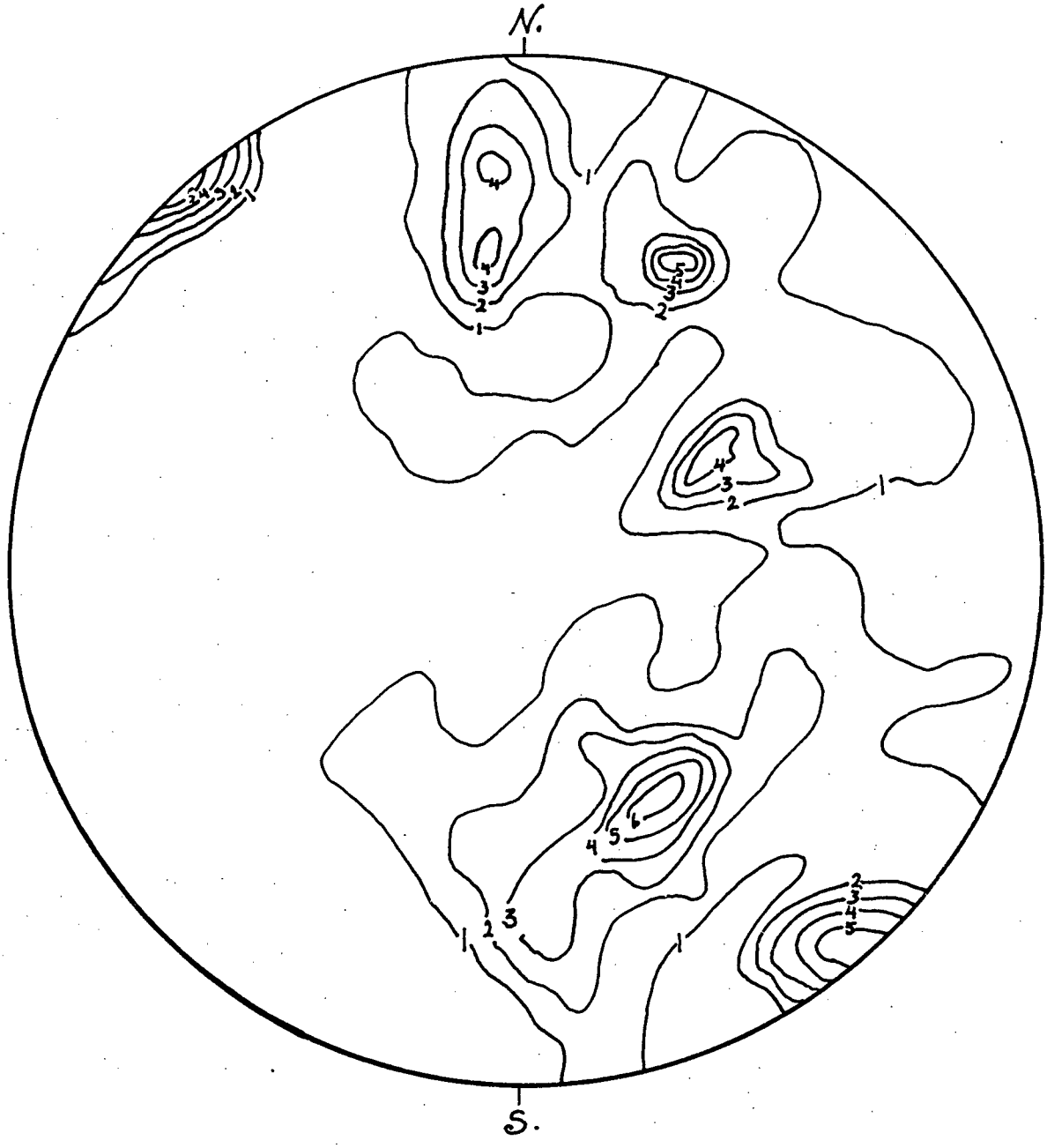

FIGURE 4-12: POLES TO 105 FAULTS IN AND ADJACENT TO THE PORCUPINE ULTRAMAFIC BODY.

Temperatures of serpentinization are reported to range from about 400°C to 100°C. Cashman and Whetten (1976) proposed that formation of serpentine occurred under P - T conditions probably less than 100°C, based on field evidence. Wenner and Taylor (1971) suggested a temperature range of 85°C to 185°C from the equilibrium of the assemblage lizardite and chrysotile and argue for antigorite formation as low as 220°C. This is based on $^{18}O/^{16}O$ fractionation data between co-existing serpentine and magnetite. This low temperature formation of chrysotile is probably due to its chemical difference from other serpentine minerals. However, serpentinization of ultramafic rocks at the Mid-Atlantic ridge is believed to have taken place at 480°C, (Aumento and Laubat, 1971). Experiments indicate serpentinization temperature of olivine (Fo_{90}) at a water pressure of 1000 atmospheres, is around 400°C (Bowen and Tuttle, 1949; Yoder, 1952; Hostetler et al., 1967).

4-4-B Formation of Chrysotile Veins

a. Previous ideas

The formation of chrysotile asbestos has been the subject of many discussions. The principal hypotheses of origin are open space filling and replacement. Fracture filling may occur in two ways:

i. Fluids deposit chrysotile in open fractures or in fractures that are opening as they are filled (Keep, 1929; Bain, 1932; Badollet, 1947; Gabrielse,1960; Tatarinov, 1967; Laliberte, 1972).

ii. The veins are formed as crystal growth pushes the wall apart and the crystals grow from solutions introduced at the central parting of the fibre-veins (Taber, 1924).

Two types of replacement are distinguished:

i. Veins crystallized during serpentinization of the rock. Chrysotile-fibre forms outward from pre-existing fractures, through which waters passed during serpentinization (Dresser, 1917; Harvie, 1923; Graham, 1944).

ii. Veins formed by replacement of already serpentinized wall rock by solutions that passed along tight cracks (Hendry, 1956; Grubb, 1962).

Riordon (1955) believed that, at Thetford, both replacement and fracture filling played major roles in chrysotile-fibre vein formation.

b. Evidence from Clinton Creek

Evidence from the Clinton Creek deposit mainly supports the fracture filling hypothesis. Most of the veins have straight clean-cut walls which are not characteristic of replacement veins. Most of the fibre veins have matching walls on a megascopic scale (Figure 4-13-A). It thus appears that

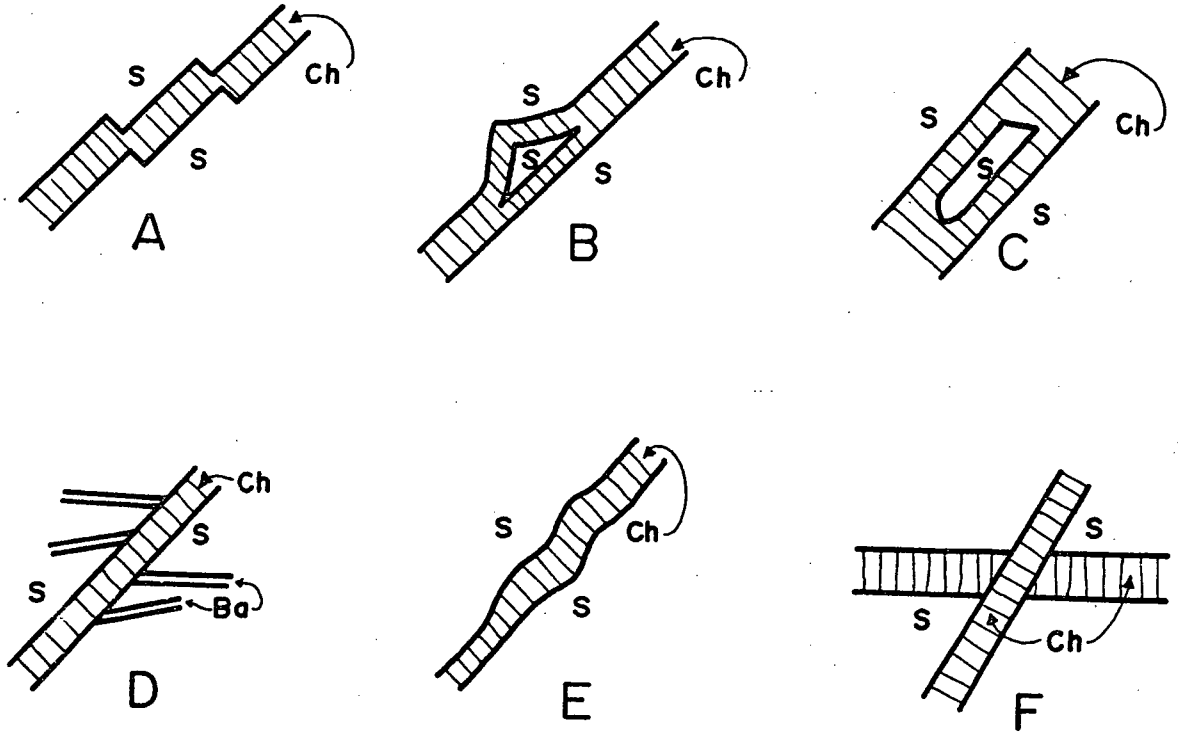

FIGURE 4-13: MECHANICS OF ORIGIN OF CHRYSOTILE VEINS. A. Matching walls. B. Matching re-entrant. C. Straight border inclusion. D. Barren fractures intersected by chrysotile-fibre vein. E. Miss-match walls(only on microscopic scale). F. Directly replaced intersecting veins. (Ch = chrysotile; S = non-fibre serpentine; Ba = barren fracture).

the fibres filled pre-existing openings. Some fibres seem to have the shape of tension gashes of S shaped fractures. Such veins are more easily explained as fracture fillings than as replacements. Some veins carry inclusions of wall-rock which match the re-entrants of similar shape in the adjacent wall-rock (Figure 4-13-B). Some inclusions, although lacking a matching re-entrant, still show relatively straight borders (Figure 4-13-C) which supports fracture filling. Most intersections of cross cutting veins do not show widening, characteristic of replacement, but show matching walls (Figure 4-2-B). Fibres split cleanly from the vein walls and this suggests fracture filling rather than replacement. Tight fractures, which are contemporaneous with or earlier than fibre formation contain no chrysotile (Figure 4-13-D) and thus argue against replacement. Dilation off-set at intersecting veins (Figure 4-2-B) suggests open space filling. Tapered veins (Plate 4-4) also supoorts fracture filling.

Although evidence of fracture filling rather than replacement seems convincing and exists on a wide scale, veins in a few specimens have mismatched walls (Figure 4-13-E), and few intersecting veins show possible replacement characteristics (Figure 4-13-F).

4-4-C Chrysotile Forming Solutions and Chrysotile Deposition

The writer believes that the chrysotile fibres were

deposited in fractures, in serpentinite, that was formed during the early pervasive serpentinization. Chrysotile at the Clinton Creek deposit has not been observed directly in contact with olivine or pyroxene or country rock but it is invariably separated from these minerals by a layer of serpentine (Figure 4-14). Therefore, it seems that chrysotile fibre was precipitated only on the walls of fractures in previously formed serpentine. This leads to the hypothesis that serpentine walls are a requirement for chrysotile deposition explains why there was no chrysotile formed in fractures in the adjacent country rock.

Chrysotile fibre at the Clinton Creek asbestos deposit has different phases of formation as indicated by some of the cross-cutting relationship of the fibre veins. It has been suggested that serpentine minerals, especially chrysotile could be dissolved and redeposited at temperatures as low as 85°C (Wenner and Taylor, 1971). The required warm aqueous solution would seem to be widely available from a number of sources. However, the main source and phase of mineralization probably could have taken place at the end of the Cretaceous when the acid intrusive rocks intruded the vicinity of the Clinton Creek area. Intrusive rocks, however, are unknown around the deposit. The nearest, but small, exposed granodiorite is about five kilometres west of the mine and a large body (30 sq. kilometres) is about thirteen kilometres northwest of the deposit. These intrusions are believed to

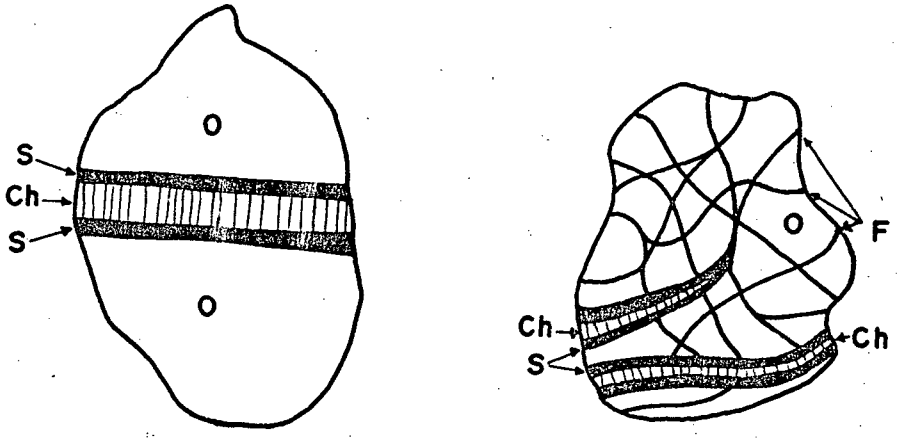

FIGURE 4-14: CHRYSOTILE FORMS ADJACENT TO SERPENTINE, BUT NOT TO OLIVINE. (Ch = chrysotile; F = fracture; O = Olivine; S = non-fibre serpentine).

have provided a heat source to generate thermal waters. The reaction of warm aqueous solution with the existing serpentine along fractures gave rise to deposition of chrysotile fibre in an essentially closed system. Warm aqueous solution only reacted as an agent in the formation of chrysotile fibre, but neither added new element or subtracted hardly any of the pre-existing elements of the serpentinite in any detectable amount.

CHAPTER V

EXPLORATION FOR CHRYSOTILE ASBESTOS IN THE NORTHERN CORDILLERA

5-1 INTRODUCTION

The writer visited, for periods ranging from two days to two weeks, the following asbestos occurrences. Cassiar and Kutcho deposits in the British Columbia, Canex, Caley and Tincup Lake deposits in Yukon Territory and Dahl Creek and Eagle deposits in Alaska, U.S.A. (Figure 5-1). Of these, the Cassiar deposit is the only one from which there has been production. The writer, in addition, examined some barren ultramafic bodies. These reconnaissance visits were carried out in an attempt to define guides for asbestos exploration.

5-2 FEATURES OF CHRYSOTILE ASBESTOS BEARING ULTRAMAFIC BODIES

5-2-A Cassiar, B.C.

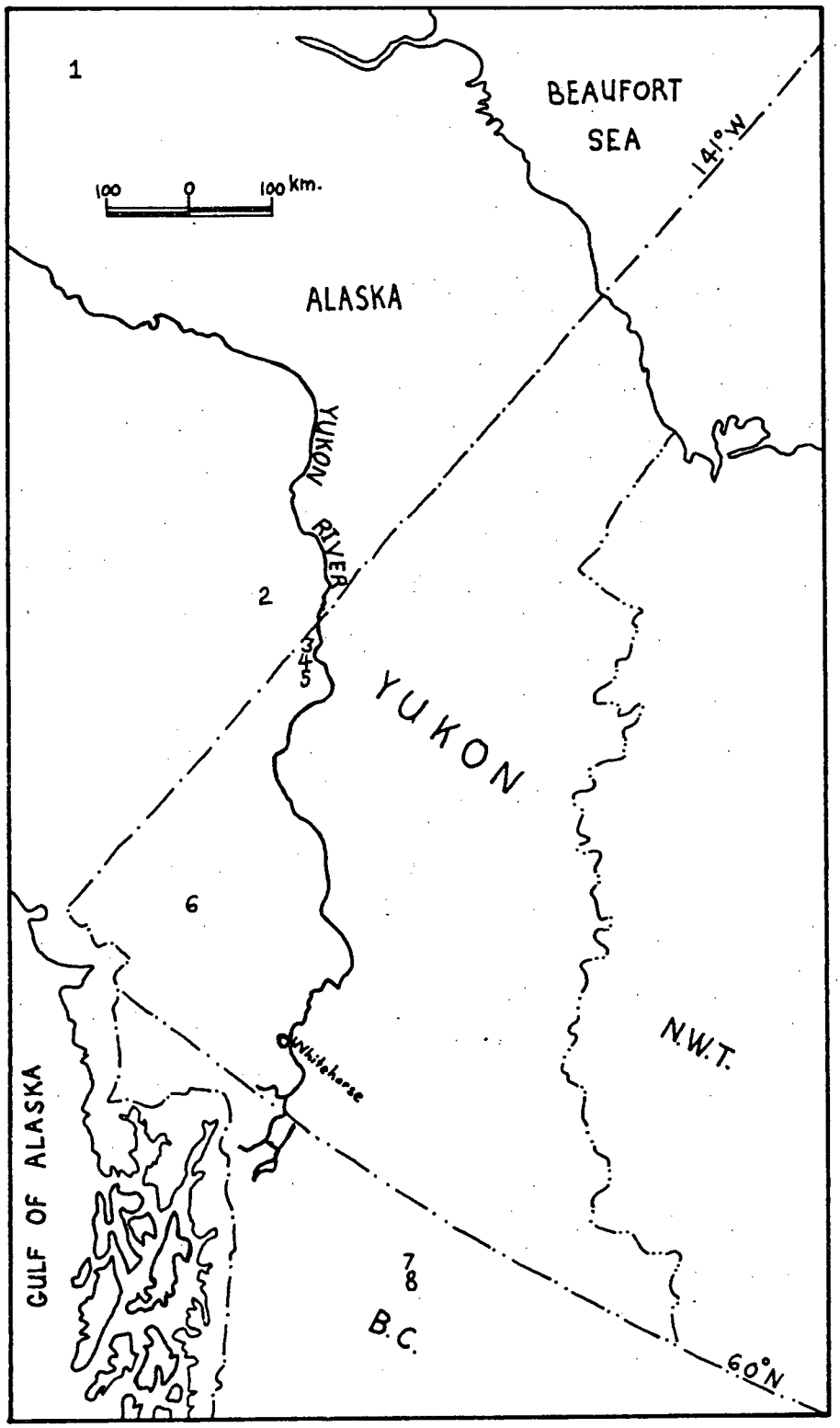

FIGURE 5-1: ASBESTOS BEARING ULTRAMAFIC BODIES IN B.C., Y.T. AND ALASKA. 1=Dahl Creek; 2=Eagle; 3=Canex; 4=Clinton Creek; 5=Caley; 6=Tin-cup; 7=Kutcho; 8=Cassiar.

Cassiar asbestos deposit (59°23'N, 129°46'W; Figure 5-1) is situated in northern British Columbia, 65 kilometres south of Yukon Border and 160 kilometres southwest from Watson Lake. An ore-bearing ultramafic body was emplaced into the Devonian-Mississippian Sylvester Group composed of several hundred feet of alternating, thin bedded black argillites and argillaceous quartzite, and interbedded volcanic flows and tuff. The ore body occurs within a lenticular slab of completely serpentinized peridotite folded conformably with the enclosing rocks and dipping 30° to 45° east. The ultrabasic body and enclosing strata form the eastern limb of a northerly trending syncline. The slab is 3.2 kilometres long, and the southern two-thirds is narrow, sheared and barren. The ore body is in the northern 460 metres of the slab and has a width of 210 metres. Depth of the fibre-bearing zone is not known. The orebody is divided into a series of lenses by shear zones of low dip. Chrysotile occupies conjugate fractures in the relatively competent blocks of serpentine between these shears. Both hanging and footwall contacts of the serpentinite body are highly sheared. The hanging-wall contact consists of a zone of indurated argillite locally referred to as "alteration zone", composed of zoisite-quartz-tremolite rock with local irregular bodies of nephrite jade and uvarovite garnet (Hewett, 1978). The footwall contact, mask by a zone of crushed argillite and graphitic schists, is a reverse fault trending 135° and dipping

northeast. The contact of the Cassiar batholith is within 2.5 kilometres of the deposit.

5-2-B Kutcho, B.C.

Kutcho mountain (59°33'N, 129°58'W; Figure 5-1) is underlain by a eugeosynclinal assemblage of marine sedimentary rock (argillite, sandstone, limestone) and interbedded volcanic flows (greenstone) correlative with the Sylvester Group of Devonian-Mississippian age (Gabrielse, 1963). These enclose an ultramafic body at least 19 kilometres long and 1.6 kilometres wide, composed of serpentinized peridotite and dunite. The body strikes northwesterly and dips gently to the east. Dykes and irregular intrusions of diorite with some gabbro cut the serpentinite body or are marginal to it. The Cassiar batholith lies nine miles east of the area, but a granitic spur comes within one mile of the serpentinite body. Parts of the body are partly serpentinized but the other parts are wholely serpentinized. Three enechelon fibre-bearing zones have been located so far. These are separated by shear zones which are parallel to the footwall contact. Fibres occupy conjugate joint systems. Silica-carbonate alteration is present.

5-2-C Canex, Y.T.

The Canex ultramafic (Figure 5-1, Figure 2-2) with some chrysotile asbestos occurrence is a serpentinized peridotite body located about 4 kilometres west of the Clinton Creek Porcupine ore body. It is surrounded mostly by limy argillite and in part by greenstone. The area was surveyed by Cassiar Asbestos Corporation with a Sharpe's MF-1 vertical intensity fluxgate magnetometre in 1964. The result of this magnetic survey and geological mapping indicate that the serpentinized ultramafic mass is a sheet about 80 metres thick and about 600 metres long, striking easterly and dipping about 30° southerly. It is probably conformable with the overlying limy argillites on the west and is near the crest of a major anticlinal structure. Visual estimates of the fibre content do not exceed three percent and most fibre-veins are short, rarely exceeding six millimetres. A silica-carbonate alteration zone lies between the serpentinite and argillite at the southern contact.

5-2-D Caley, Y.T.

The Caley asbestos occurrence (64°18'N, 140°12'W; Figure 5-1) is situated about 32 kilometres southeast of Clinton Creek. The deposit lies in a serpentinized peridotite that is surrounded by quartz-carbonate rock. It strikes northerly and dips gently eastward. The body is bordered on the north by quartz-sercite schists and on the

south by black, argillaceous limestone and slate which appear to trend north-easterly. The body is about 1000 metres long and 400 metres wide, most of which is composed of quartz-carbonate alteration with an unaltered central remnant (400 metres by 130 metres) of serpentinite with chrysotile fibre. The body is trough-like and was found to bottom within 100 metres of the surface. A large granitic stock lies five kilometres to the north.

5-2-E Tincup Lake, Y.T.

The Tincup Lake asbestos occurrence (61°18'N, 135°15'W; Figure 5-1) is along the northern border of a serpentinized peridotite body. The body is about 1.6 kilometres wide and appears to dip at a very high angle probably conformably with the surrounding rock units. The ultramafic body is composed of dunite, peridotite and pyroxenite. It is enclosed in country rocks consisting of greenstone, quartzite, limestone and argillaceous rocks. The large northwest-trending Ruby Range batholith lies just to the south of the ultramafic body.

5-2-F Dahl Creek, Alaska

The Dahl Creek asbestos occurrence (66°56'N, 156°54'W; Figure 5-1) is in a serpentinized ultramafic body. The

ore body has prominent shear zones trending 320° to 330° and dipping 10° to 28° and 60° to 90° northeast. Longest fibres occur in joints adjacent to shear zones. The ultramafic body is mostly in contact with black argillaceous limestone and minor schist. Country rock consists of limestone, mica-schist, graphite-mica-schist, and chlorite-schist all of probable early Paleozoic age. Structural relationship of the country rock to the ultramafic body seems conformable. Alteration was not observed.

5-2-G Eagle, Alaska

The Eagle asbestos occurrence (64°35'N, 142°30'W; Figure 5-1) is about 90 kilometres west of the Clinton Creek asbestos mine. An asbestos-bearing, highly serpentinized peridotite body is cut by widely spaced joints. The body appears to extend about 1,000 metres in an east-west direction. The fibre-bearing zone is exposed over a length of about 500 metres, but mineralization within this zone is erratic. The north and south ends of the mineralized part appear to contain the highest concentrations of chrysotile-fibre. A zone in the centre approximately 80 metres long contains little or no fibre. Generally, fibre-veins are spaced 25 to 50 centimetres apart, although in some places more closely spaced fibre-veins are observed. Average fibre length is about 6 millimetres and the longest fibre observed

is 20 millimetres. The serpentinite body is emplaced in country rock of similar lithology to that of the Clinton Creek area and is probably of middle Paleozoic age. Alteration zones were not observed. Granodiorite bodies were noted in the vicinity of the ultramafic body.

5-3 FEATURES OF BARREN ULTRAMAFIC BODIES

Barren ultramafic bodies within the Clinton Creek area, in adjacent parts of Yukon, northern B.C. and Alaska, visited by the writer, differ in some respects from those that contain asbestos. These barren bodies have been emplaced wholely in greenstone or in quartz-mica schist, rather than at or near contacts of argillite and greenstone or in argillite. In addition, most of the barren ones are extremely large or small compared to the fibre-bearing bodies. Larger bodies are generally relatively unsheared; and smaller bodies commonly are composed completely of fish-scale serpentine, the result of intensive shearing. Generally larger ultramafic bodies are not highly fractured and the degree of serpentinization does not seem to be more than fifty percent.

5-4 GUIDES IN THE SEARCH FOR CHRYSOTILE ASBESTOS

a. Exposures of ultramafic bodies are indicated by lack of heavy vegetation and dark green to orange weathering blocky talus they produce. Both characteristics can easily be seen from a distance or from the air.

b. All fibre-bearing serpentinized bodies discussed here are emplaced along the contact of argillaceous metasediments and greenstone or schist, or wholely in argillaceous metasediments. All of these interbedded greenstone and argillaceous partly metamorphosed sediments seem to be of Devonian-Mississippian age. On the contrary, barren ultramafic bodies are situated within greenstone or quartz-mica schist.

c. All deposits occur within one to nine miles of granitic intrusions of probably Jurrassic or Cretaceous age. These intrusions are believed to have contributed a heat source for asbestos formation.

d. Significant concentrations of chrysotile asbestos are confined to ultramafic bodies which are at least 75 percent serpentinized.

e. Ultramafic lenses whose elongation is perpendicular or at high angle to the directions of regional fold axes seem to be most favorable sites for development of a chrysotile asbestos deposit.

f. Known commercial deposits and occurrences of chrysotile-fibre lie in relatively small (1,000 to 2,000 metres) ultramafic bodies compared to large bodies which are widespread in B.C., Y.T. and Alasaka. unfortunately depth cannot be estimated from outcrop area. It is probable that there is an optimum size, relative to deforming stress, that will allow the serpentine body to be fractured sufficiently to form an orebody.

g. Relatively unsheared ultramafic bodies have low potentials for the development of concentrations of good quality chrysotile-fibre. Also fish-scale shearing, if a dominant characteristic, is a negative criterion for the occurrence of economic concentrations of chrysotile-fibre. The great majority of small serpentinite bodies are composed of fish-scale serpentinite. In all cases, fibre-veinlets occupy fractures, in more or less massive serpentinite blocks bounded by lenticular shear zones.

h. Fracturing must be fairly intense to provide adequate openings for chrysotile-fibre formation in ore grade concentrations. Structural mapping in surrounding country rocks may indicate particular intensities of regional fractures whose extensions across ultramafic masses may indicate potential for high grade quality-fibre.

i. Silica-carbonate alteration is commonly associated with serpentinized ultramafic masses, and in certain cases may be a useful guide for such masses. However, this is usually

an alteration that post-dates chrysotile-fibre formation and if superimposed on chrysotile-fibre can reduce its quality or destroy it completely.

CHAPTER VI

SUMMARY AND CONCLUSION

The most abundant rocks of the Clintin Creek area belong to the Yukon Metamorphic Complex which are originally an alternate sequence of marine sedimentary and volcanic rocks. The writer obtained a model age for these rocks of 470 Ma(Ordovician) by whole rock Rb-Sr dating. Fossil evidence, documented by others from an area just west of the Yukon River near Alaska border indicated a Paleozoic age, probably Devonian. The main episode of metamorphism occurred in Permian. It appears, therefore, that the rocks of the area were formed in the middle Paleozoic(Ordovician to Devonian).

Intensity and style of deformation in the country rocks and ultramafic bodies suggest that the ultramafic rocks of the area were emplaced in the country rocks probably during the Permian period, the time of main metamorphism. It is probable that the Tintina fault a few kilometres away from the study area reflects a zone of weakness along which the alpine-type ultramafic bodies of the Clinton Creek area and probably some of the others along and close to the Tintina Trench were em-

placed tectonically. These were later folded and metamorphosed with the country rocks. The area was intruded by acid intrusive rocks in latest Cretaceous-earliest Tertiary time. Columnar jointed basalt of Selkirk volcanics equivalent is the youngest, undeformed, fresh rock of the area. These Selkirk volcanic rocks were extruded at Holocene or Pleistocene (Bostock, 1966).

Three main phases of deformation were delineated. Probably the oldest and most complex phase occurred during the Permian, along with the initial movement of the Tintina fault. Small, tight, isoclinal folds are characteristic of this phase. The structural trend (300° to 315°) is roughly parallel to the direction of the Tintina Trench. Due to later deformation of the folds of this phase, local change in axial trends up to 010° is common. Direction of vergence varies from 030° to 100°. The second phase of deformation gave rise to large recumbent and isoclinal folds with trends varying from 270° to 290° with southerly vergence. The third phase of deformation gave rise to antiform structure of regional scale.

Eighteen lenses of serpentinized ultramafic bodies have been mapped. Two of these, the Porcupine and Snow Shoe ultramafic bodies are mined for asbestos. A few of other bodies contain appreciable amount of chrysotile-fibre but apparently not of adequate quantity to be mined. Most of the ultramafic bodies are essentialy devoid of known chrysotile-fibre and these were excessively sheared or very massive without much fractures. Again, if serpentinization is less

than 75 percent there is practically no chance for commercial mineralization. Fracturing is one of the most important factors in control of mineralization. Fairly intense fractures are essential to provide adequate openings for chrysotile-fibre formation in ore grade concentrations. Chrysotile-fibre bearing serpentinized ultramafic masses within argillite unit or at the contact of argillite unit and other rock units seem to carry ore grade or substential amount of chrysotile-fibre.

BIBLIOGRAPHY

Anhaeusser, C.R., 1976, The Nature of Chrysotile Asbestos Occurrences in Southern Africa: A Review: Ec. Geol., v. 71, p. 96-116.

Armstrong, R.L., 1978, Pre-Cenozoic Phanerozoic Time Scale-Computer File of Critical Dates and Consequences of New In-Progress Decay-Constant Revisions: in Cohee, G.V., and M.F. Glaessner, ed., Contributions to the Geologic Time Scale: Am. Assoc. Petrol. Geologist, Studies in Geology, No. 6, p. 73-91.

Aumento, F., 1970, Serpentine Mineralogy of Ultrabasic Intrusions in Canada and on the Mid-Atlantic Ridge: Geol. Surv. Canada, Paper 69-53, 51 p.

——— 1972, The Oceanic Crust of the Mid-Atlantic Ridge at 45° N: Canada Dept. Energy, Mines and Resources, Earth Physics Branch Pub., 42, No. 3, p. 71-85.

——— B.D. Loncarevic, and D.T. Ross, 1971, Hudson Geotraverse: Geology of Mid-Atlantic Ridge at 45° N Royal Soc. London Philos. Trans., v. A268, p. 623-650.

——— and H. Loubat, 1971, The Mid-Atlantic Ridge Near 45° N, IV: Serpentinized Ultramafic Intrusions: Cana. Jour. Earth Sci., v. 8, p. 631-663.

Badgely, P.C., 1959, Structural Methods for the Exploration Geologist: Harper Bros. New York.

Badollet, M.S., and C. Faessles, 1947, The Epignesis of the Minerals and rocks of the Serpentine Belt, Eastern Townships, Quebec: Cana. Mining Jour., v. 67, p. 157-167.

Bain, G.W., and S.B. Keith, 1932, Chrysotile Asbestos: Ec. Geol., v. 27, p. 169-188.

Barnes, I., V.C. LaMarche Jr., and G. Himmerlberg, 1967, Geochemical Evidence of Present-Day Serpentinization: Science, v. 156, p. 830-832.

——— and J.R. O'Neil, 1969, The Relationship Between Fluid-Type Ultramafics and Possible Modern Serpentinization, Western United States: Geol. Soc. America Bull., v. 80, p. 1947-1960.

——— J.B. Rapp, and D.H. White, 1973, Silica-Carbonate Alteration of Serpentine: Wall Rock Alteration in Mercury Deposits of the California Coast Ranges: Ec. Geol.,v. 68,

p. 388-398.

Bostock, H.S., 1936, Carmacks District, Yukon: Geol. Surv. Cana., Memoir 189, 67 p.

——— 1948, Physiography of Canadian Cordillera, with Special Reference to the Area North of Fifty-Fifth Parallel: Cana. Geol. Surv. Memoir 247, 106 p.

——— 1966, Notes on Glaciation in Central Yukon Territory: Cana. Geol. Surv. Paper 65-36, 18 p.

Bowen, N.L., and F. Tuttle, 1949, The System $MgO-SiO_2-H_2O$: Geol. Soc. Am. Bull., v. 60, p. 439-460.

Brooks, A.H., 1900, A Reconnaissance in the Tantana and White River Basins, Alaska, in 1898: U.S. Geol. Surv. Ann. Rept. 20, pt. 7.

Brooks, C., S.R. Hart, and I. Wendt, 1972, Realistic Use of Two-Error Regression Treatments as Applied to Rubidium-Strontium Data: Reviews Geophys. Space Phys., v. 10, No. 2, p. 551-577.

Budinski, D.R., 1969, Sept., Geology of the Clinton Creek Orebody: Western Miner.

Cairnes, D.D., 1914, The Yukon-Alaska International Boundary Between Porcupine and Yukon Rivers: Cana. Geol. Surv. Memoir 67, 161 p.

Campbell, R.B., 1967, Geology of Glenlyon Map-Area, Yukon Territory: Cana. Geol. Surv. Memoir 352, 92 p.

———and H.W. Tipper, 1971, Geology of Bonaparte Lake Map-Area, British Columbia: Cana. Geol. Surv. Memoir 363, 100 p.

Cashman, S.M., and J.T. Whetten, 1976, Low-Temperature Serpentinization of Peridotite Fanglomerate on the West Margin of the Chiwaukum Graben, Washington: Geol. Soc. Am. Bull., v. 87, p. 1773-1776.

Cerney, P., 1968, Comments on Serpentinization and Related Metasomatism: Am. Mineral., v. 53, p. 1377-1385.

Church, W.R., 1972, Ophiolite: Its Definition, Origin as Ocean Crust and Mode of Emplacement in Orogenic Belts, with Special Reference to the Appalachians; Cana. Dept. Energy, Mines and Resources, Earth Physics Branch Pub., v. 42, No. 3, p. 71-85.

Cockfield, W.E., 1921, Sixty-mile and Ladue Rivers Area, Yukon: Cana. Geol. Surv. Memoir 123, 60 p.

Coleman, R.G., 1967, Low-Temperature Reaction Zones and Alpine Ultramafic Rocks of California, Oregon and Washington: U.S. Geol. Surv. Bull. 1247, 49 p.

——— 1971, Plate Tectonic Emplacement of Upper Mantle Peridotites Along Continental Edges: Jour. Geophys. Research, v. 76, p. 1212-1222.

Davies, H.L., and L.E. Smith, 1971, Geology of Eastern Papua: Geol. Soc. Am. Bull. v. 82, p. 3299-3312.

Deer, W.A., R.A. Howie, and J. Zussman, 1963, Rock-forming Minerals: New York, John Wiley and Sons Inc.

Dewey, J.F. and J.M. Bird, 1970, Mountain Belts and New Global Tectonics: Jour. Geophys. Research, v. 75, No. 14, p. 2625-2647.

——— 1971, Origin and Emplacement of the Ophiolite Suite: Appalachian Ophiolites in Newfoundland: Jour. Geophys, Research, v. 76, p. 3179-3206.

Diekey, J.S. Jr., 1970, Partial Fusion Products in Alpine-Type Peridotites: Serrania de la Ronda and Other Examples: Min. Soc. Am. Spec. Paper 3, p. 33-50.

Douglas, R.J.W., H. Gabrielse, J.O. Wheeler, D.F. Scott and H.R. Belyea, 1970, Geology of Western Canada, in Douglas, R.J.W., ed., Geology and Economic Minerals of Canada: Geol. Surv. Cana., Econ. Geol. Rept. 1, p. 366-488.

Dresser, J.A., 1913, Preliminary Report on the Serpentine and Associated Rocks of Southern Quebec: Geol. Surv. Cana., Memoir 22.

Eckstrand, O.R., 1975, The Dumont Serpentinite: A Model for Control of Nickeliferous Opaque Mineral Assemblages by Alteration Reactions in Ultramafic Rocks: Ec. Geol., v. 70, p. 183-201.

Evans, B.W., and V. Trommsdorff, 1970, Regional Metamorphism of Ultramafic Rocks in the Central Alps: Paragenesis in the System $CaO-MgO-SiO_2-H_2O$: Schweiz. Min. Pet. Mitt., v. 50, No. 3, p. 481-492.

Faure, G., and J.L. Powell, 1972, Strontium Isotope Geology: Springer-Verlag, New York, 188 p.

Faust, G.T., and J.J. Fahey, 1962, The Serpentine-Group Minerals: U.S. Geol. Surv. Prof. Paper 384-A, 87 p.

Foster, H.L., 1969, Asbestos Occurrence in the Eagle C-4 Quadrangle, Alaska: U.S. Geol. Surv. Circ. 611, 7 p.

——— and T.E.C. Keith, 1974, Ultramafic Rocks of the Eagle Quadrangle, East-Central Alaska: Jour. Research U.S. Geol. Surv., v. 2, No. 6, p. 657-669.

——— F.R. Weber, R.B. Forbes, and E.E. Brabb, 1973, Regional Geology of Yukon-Tantana Upland, Alaska, in Arctic Geology: Am. Assoc. Petroleum Geologists Memoir 19, p. 388-395.

Gabrielse, H., 1960, The Genesis of Chrysotile Asbestos in the Cassiar Asbestos Deposit, Northern British Columbia: Ec. Geol., v. 55, p. 327-338.

——— 1963, McDame Map-Area, Cassiar District, B.C.: Cana. Geol. Surv. Memoir 319, 139 p.

——— and J.O. Wheeler, 1960, Tectonic Framework of the Southern Yukon and Northwestern British Columbia: Geol. Surv. Cana. Paper 60-24.

Godwin, C.I., 1975, Imbricate Subduction Zones and their Relationship with upper Cretaceous to Tertiary Porphyry Deposits in the Canadian Cordillera: Cana. Jour. Earth Sci., v. 12, No. 8, p. 1362-1378.

——— Alternative Interpretations for the Casino Complex and Klotassin Batholith in the Yukon Crystalline Terrane: Cana. Jour. Earth Sci., v. 12, No. 11, p. 1910-1916.

Graham, R.P.D., 1944, Serpentine Belt, Eastern Townships, in Geology of Quebec, Que. Dept. Mines, Geol. Dept. 20, p. 413-447.

Green, L.H. 1972, Geology of Nash Creek, Larsen Creek, and Dawson Map-Areas, Yukon Territory: Cana. Geol. Surv. Memoir 364 157 p.

——— and J.A. Roddick, 1962, Dawson, Larsen Creek, and Nash Creek Map-Areas, Yukon Territory: Geol. Surv. Cana. Paper 62-7, 20 p.

Greenwood, H.J., 1963, The Synthesis and Stability of Anthrophyllite, Jour. Pet., v. 4, p. 317.

——— 1967, Mineral Equilibria in the System $MgO-SiO_2-H_2O-CO_2$: in Abelson, P.H., ed., Researches in Geochemistry, v. 2, John Wiley and Sons, New York, London Sydney, p. 542.

Grubb, P.L.C., 1962, Serpentinization and Chrysotile Formation in the Matheson Ultrabasic Belt, Northern Ontario: Ec. Geol., v. 57, p. 1228-1246.

Hart, S.R., 1964, The Petrology and Isotopic Mineral Age Relations of a Contact Zone in the Front Range, Colorado: Jour. Geol., v. 72, p. 493-525.

Harvie, R., 1923, Thetford Map-Area: Geol. Surv. Cana., unpublished rept.

Hendry, N.W., and H.K. Conn, 1956, The Ontario Asbestos Properties of Canadian Johns-Manville Company Limited: Geology of Canadian Industrial Mineral Deposits, 6th Commonwealth Mining and Metallurgical Cong., p. 36-45.

Hewett, F.G., 1978, April, The Cassiar Story: Geology: C.I.M. Bull.

Himmelberg, G.R., and R.A. Loney, 1973, Petrology of Vulcan Peak Alpine-Type Peridotite, Southwestern Oregon: Geol. Soc. Am. Bull., v. 84, p. 1585-1600.

Honnorez, J. and P. Kirst, 1975, Petrology of Rodingites from the Equatorial Mid-Atlantic Fracture Zones and their Geotectonic Significance: Contrib. Mineral. Petrol., v. 49, p. 233-257.

Hostetler, P.B., and C.L. Christ., 1968, Studies in the System $MgO-SiO_2-CO_2-H_2O$ (I): the Activity Product Constant of Chrysotile: Geochimica et Cosmochimica Acta, v-32, p. 485-497.

——— R.G. Coleman, F.A. Mumpton, and B. Evans, 1966, Brucite in Alpine Serpentinites: Am. Mineral., v. 51, p. 75-98.

Htoon, M., 1976, Mineral Industry Report 1975, Yukon Territory: Indian Affairs and N. Devel., Pub. No. QS-8127-000-EE-A1, p. 8-13.

Irvine, T.N., 1967, The Duke Island Ultramafic Complex South-Eastern Alaska: in Wyllie, P.J., ed., Ultramafic and Related Rocks: Wiley and Sons Inc., New York, p. 84-97.

——— and T.C. Findley, 1972, Alpine-Type Peridotite with Particular Reference to the Bay of Islands Igneous Complex: Cana. Dept. Energy, Mines and Resources, Earth Physics Branch Pub., v. 42, No. 3, p. 97-107.

Jackson, E.D., 1968, The Character of the Lower Crust and Upper Mantle Beneath the Hawaiian Islands: XXIII Int. Geol. Cong., Prague, v. 1, p. 135-150.

Johannes, W., 1969, An Experimental Investivation of the System $MgO-SiO_2-H_2O-CO_2$: Am. Jour. Sci., v. 267, p. 1083.

Keep, F.E., 1929, Geology of the Shabani Mineral Belt, Belingwe District: Geol. Surv. South. Rhod. Bull., v. 12.

Laliberte, R., 1972, The Jeffrey Mine, Asbestos Quebec: Quebec Asbestos Mining Region of Southeastern Quebec, p. 19-26.

Laurent, R., 1975, Petrology of the Alpine-Type Serpentinites of Asbestos and Thetford Mines, Quebec: Schweiz. Min. Petr. Mitt., v. 55, No. 3.

——— Occurrences and Origin of the Ophiolites of Southern Quebec, Northern Appalachians: Cana. Jour. Earth Sci., v. 12, p. 443-455.

LePichon, X., 1969, Models and Structure of Oceanic Crust: Tectonophysics, v. 7, p. 385-401.

Lockwood, J.P. 1972, Possible Mechanisms for the Emplacement of Alpine-Type Serpentinite: Geol. Soc. Am. Memoir 132, p. 273-287.

Loney, R.A., G.R. Himmerlberg, and R.G. Coleman, 1971, Structure and Petrology of the Alpine-Type Peridotite at Burro Mountain, California, U.S.A.: Jour. Petrol., v. 12, p. 245-310.

McConnell, R.G., 1905, Report on Gold Values in the Klondike High-Level Gravels; Summary Report, Geol. Surv. Cana. also in Bostock, H.S., 1957: Yukon Territory, Selected Field Reports of the Geological Survey of Canada, 1898 to 1933; Geol. Surv. Cana., Memoir 284, 650 p.

McIntyre, G.A., C. Brooks, W. Compston, W., and A. Turek, 1966, The Statistical Assessment of Rb-Sr Isochrons: Journ. Geophys. Res., v. 71, No. 22, p. 5459-5468.

McTaggart, K.C., 1971, On the Origin of Ultramafic Rocks: Geol. Soc. Am. Bull., v. 82, p. 23-33.

Medaris, L. G. Jr., 1969, Partitioning of Fe^{++} and Mg^{++} Between Coexisting Synthetic Olivine and Orthopyroxene: Am. Jour. Sci., v. 267, p. 945-968.

Mertie, J.B. Jr., 1937, The Yukon-Tantana Region, Alaska: U.S. Geol. Surv. Bull. 872, 276 p.

Monger, J.W.H., J.G. Souther, and H. Babrielse, 1972, Evolution of the Canadian Cordillera: A Plate-Tectonic Model: Am. Jour. Sci., v. 272, No. 7, p. 577-602.

Moores, E.M. and I.D. MacGregor, 1972, Types of Alpine Ultramafic Rocks and their Implications for Fossil Plate Interactions: Geol. Soc. Am. Memoir 132, p. 209-223.

Mossman, D.J., 1970, Fracture Phenomena in and around Serpentinized Dunite in Ultramafic Rocks from the Greenhills Complex, Southland, New Zealand: Geol. Soc. Am. Bull., v. 81, p. 3753-3756.

Mulligan, R., 1963, Geology of Teslin Map-Area, Yukon Territory (105C): Cana. Geol. Surv. Memoir 326, 96 p.

Nicholas, A., 1969, Une vue unitaire concernant l'origine des massifs ultrabasiques des Alpes occidentales internes: Acid sci. Paris Comptes rendus, v. 269, p. 1831-1834.

——— J.L. Bouchez, F. Boudier and J.C.Mercier 1971, Textures Structures and Fabrics Due to Solid State Flow in Some European Lherzolites: Tectonophysics, v. 12, p. 55-86.

Noble, J.A. and H.P. Taylor Jr., 1960, Couelation of the ultramafic Complexes of Southeastern Alaska with Those of Other Parts of North America and the World: in Petrographic Provinces, Igneous and Metamorphic Rocks: Internat. Geol. Cong., 21st, Norden 1960, pt. 8 p. 188-197.

Obradovich, J.D., and W.A. Cobban, 1975, A Time Scale for the Late Cretaceous of the Western Interior of North America: Geol. Assoc. Cana. Spec. Paper 13, p. 31-54.

Page, N.J., 1967, Serpentinization Considered as a Constant Volume Metasomatic Process: A Discussion: Am. Mineral., v. 52, p. 545-549.

——— 1968, Chemical Differences Among the Serpentine "Polymorphs": Am. Mineral., v. 53, p. 201-215.

Pearson, W.N., 1977, April, The Minto Copper Deposit, Yukon Territory: A Metamorphosed Orebody in the Yukon Chrystalline Terrane: M.Sc. Thesis, Queen's University, Kingston, Ontario.

Poldevaart, A., 1955, Chemistry of the Earth's Crust: Geol. Soc. Am. Spec. Papers, 145 p.

Prest, V.K., D.R. Grant, and V.N. Rampton, 1968, Glacial Map of Canada: Geol. Surv. Cana., Map 125-A.

Ramsay, J.G., 1967, Golding and Fracturing of Rocks: McGraw-Hill, New York, 568 p.

Ragan, D.M., 1967, The Twin Sisters Dunite, Washington: in Wyllie, P.J., ed., Ultramafic and Related Rocks: John Wiley, New York, p. 160-166.

——— 1969, Olivine Recrystallization Textures: Mineral. Mag., v. 37, p. 238-240.

Riordon, P.H., 1955, The Genesis of Asbestos in Ultrabasic Rocks: Ec. Geol., v. 50, p. 67-81.

——— 1962, Geology of the Asbestos Belt in Southeastern Quebec: Cana. Ins. Mining Metal. Bull., v. 55, No. 601, p. 311-313.

——— and R. Laliberte, 1972, Asbestos Deposits of Southern Quebec: in Guidebook to excursion B-08: Internat. Geol. Cong. 24th, Montreal 1972, 21 p.

Roddick, J.A., 1967, Tintina Trench: Jour. Geology, v. 75, No. 1, p. 23-33.

Scarfe, C.M., and P.J. Wyllie, 1967, Serpentine Dehydration Curves and Their Bearing on Serpentinite Deformation in Orogenesis: Nature, London, v. 215, p. 945-946.

Sinclair, A.J., 1976, Applications of Probability Graphs in Mineral Exploration: Assoc. Explor. Geochem., Sp. v. 4, 95 p.

Skippen, G.B., 1971, Experimental Data for Reactions in Siliceous Marbles: Jour. Geol., v. 79, p. 457.

Steinmann, F., 1905, Geologische Beobachtungen in den Alpen II: Die Schardt'sche Uberfaltungs theorie und die geologishe Bedautung der Tiefseeabsatze und der opthiolithischen Massengesteine. Ber. Nat. Ges. Freiburg, I, Bd. 16, 44-65.

Taber, S., 1924, The Origin of Veins of Fibrous Minerals: Ec. Geol., v. 19, p. 475-486.

Tatarinov, P.M., and B.R. Artemov, 1967, Chrysotile Asbestos Deposits of the U.S.S.R.: Ministry of Geology, U.S.S.R.

Tempelman-Kluit, D.J., 1972, Geology and Origin of the Faro, Vangorda, and Swim Concordant Zinc-Lead Deposits, Central Yukon Territory: Cana. Geol. Surv. Bull. 208, 73 p.

——— 1974, Reconnaissance Geology of Aishihik Lake, Sang and Part of Stewart River Map-Areas, West Central Yukon: Cana. Geol. Surv. Paper 73-41, 97 p.

——— 1976, The Yukon Crystalline Terrane: Enigma in the Canadian Cordillera: Geol. Soc. Am. Bull., v. 87, p. 1343-1357.

——— and R.K. Wanless, 1975, Potassium-Argon Age Determinations of Metamorphic and Plutonic Rocks in the Yukon Crystalline Terrane: Cana. Jour. Earth Sci., V. 12, p. 1895-1909.

Thayer, T.P., 1966, Serpentinization Considered as a Constant-Volume Metasomatic Process: Am. Mineral., v. 51, p. 685-709.

Turner, F.J. and J. Verhoogen, 1960, Igneous and Metamorphic Petrology: 2nd ed., McGraw-Hill, New York, 694 p.

Vance, J.A., and M.A. Dungan, 1977, Formation of Peridotites by Deserpentinization in the Darrington and Sultan Areas, Cascade Mountains, Washington: Geol. Soc. Am. Bull., v. 88, p. 1497-1508.

Varne, R., and M.J. Rubenach, 1972, Geology of Macquarie Island and Its Relationship to Oceanic Crust: in Hayes D.E., ed., Antarctic Oceanology 11: Antarctic Research Ser. Australian-New Zealand Sector, v. 19, p. 98-109.

Veach, N.J., 1972, Aeromagnetic Survey, East Alaska Range, Eagle, Alaska: Alaska Dept. Nat. Resources, Geol. and Geophys. Surveys 24 map, scale 1:63,360.

Wager, L.R. and G.M.Brown, 1968, Layered Igneous Rocks: Oliver and Boyd, Edinburgh and London, 588 p.

Wahrhaftig, C., 1965, Physiographic Divisions of Alaska: U.S. Dept. Interior, Geol. Surv. Prof. Paper 482,52 p.

Wenner, D.B. and H.P.J. Taylor, 1971, Temperatures of Serpentinization of Ultramafic Rocks Based on O^{18}/O^{16} Fractionation Between Coexisting Serpentine and Magnetite: Contr. Mineral. and Petrol. v. 32, p. 165-185.

White, W.H., G.P. Erickson, K.E. Northcote, G.E. Dirom, and J.E. Harakal, 1967, Isotopic Dating of the Guichon Batholith, B.C.: Cana. Jour. Earth Sci., v. 4, p. 677-690.

Wicks, F.J., 1977, Serpentine Textures and Serpentinization: Cana. Mineral., v. 15, p. 459-488.

——— and E.J.W. Whittaker, 1975, A Reappraisal of the Structures of the Serpentine Minerals: Cana. Mineral., v. 13, p. 227-243.

——— E.J.W. Whittaker, and J. Zussman, 1977, An Idealized Model for Serpentine Textures After Olivine: Cana. Mineral., v. 15, p. 446-458.

———and J. Zussman, 1975, Microbeam X-ray Diffraction Patterns of the Serpentine Minerals: Cana. Mineral., v. 13, p. 244-258.

Williams, H., and J. Malpas, 1972, Sheeted Dykes and Brecciated Dyke Rocks within Transported Igneous Complexes, Bay of Islands, Western Newfoundland: Cana. Jour. Earth Sci., v. 9, p. 1216-1229.

——— and W.R. Smyth, 1973, Metamorphic Aureoles Beneath Ophiolite Suites and Alpine Peridotites: Tectonic Implications with Western Newfoundland Examples: Am. Jour. Sci., v. 273, p. 594-621.

Winkler, H.G.F., 1974, Petrogenesis of Metamorphic Rocks: 3rd ed., Springer-Verlag, New York Inc., 237 p.

Yoder, H.S. Jr., 1952, The MgO-Al_2O_3-SiO_2-H_2O System and the Related Metamorphic Facies: Am. Jour. Sci., Bowen Vol., p. 569-627.

York D., 1967, The Best Isochron: Earth Pla. Sci. Lett., v. 2, p. 479-482.

——— 1969, Least Square Fitting of a Straight Line with Correlated Errors: Earth Pla. Sci. Lett., v. 5, p. 320-324.

——— and R.M. Farquhar, 1972, The Earth's Age and Geochronology: Pergamon, 178p.

APPENDIX A

Definition of Greenstone

Greenstone used in this thesis is derived from mafic volcanic rocks and pelitic sedimentry rocks. These are formed in the lower temperature part of the metamorphic conditions. Hornblende has been replaced by actinolite, chlorite, and epidote. Quartz, albite and minor biotite, muscovite and calcite are also present. Greenstone of volcanic origin and sedimentary origin are distinguished by the relative amount of minerals they contain. Greenstone derived from sedimentary origin contains more quartz and muscovite, less chlorite, albite, and epidote, and generally no actinolite.

APPENDIX B

THE OPHIOLITE ASSEMBLAGES

The definition and interpretation of ophiolite has undergone considerable evolution since the term was first used by Steinmann (1905) in referring to an association of peridotite (serpentinite), gabbro, diabase, spilite and related rocks (Church, 1972). A recently proposed definition (G.S.A. Penrose Conference on Ophiolites, 1972) is:

A completely developed ophiolite consists of mafic to ultramafic rocks in the following sequence from the bottom working up:

Ultramafic complex consisting of harzburgite, lherzolite and dunite, usually with a metamorphic tectonite febric.

Gabbroic complex ordinarily with cumulus textures and usually less deformed than the ultramafic complex.

Mafic sheeted dike complex.

Mafic volcanic complex, commonly pillowed.

Associated rock types:

-ribbon cherts, shale, minor limestone

-sodic felsic intrusive and extrusive rocks.

Most recent interpretations (Church, 1972; Coleman, 1971; Dewey and Bird, 1971) view ophiolite suites as being

transported oceanic crust and mantle, based on the following considerations, as summerized by Williams and Smyth (1973):

1. Similarities in gross physical characteristics of ophiolite suites with geophysical models of oceanic crust and mantle (LePichon, 1969).

2. Transported on-land ophiolite is rooted in oceanic lithosphere at Papua, New Guinea (Davies and Smith, 1971).

3. Strong lothologic similarities between ophiolites and rocks of MacQuarie Ridge(Varne and Rubenach, 1972).

4. Lothological and chemical similarities of oceanic tholeiites and pillow lavas of ophiolite suites (Aumento et al., 1971).

5. Models relating sea floor spreading to the formation of sheeted dike complexes (Williams and Malpas, 1972).

6. High pressure mineralogy of peridotites requiring mentle depths for conditions of crystallization (Medaris, 1972).

7. Common occurrence of metamorphic tectonites in ophiolite peridotites, displaying textures like those exprementally reproduced under conditions representative of the mentle (Nicolas, 1969).

8. Similar metamorphic mineral assemblages in oceanic rocks at mid-ocean ridges compared with those of ophiolites (Williams and Malpas, 1972; Aumento, 1972).

According to Plate Tectonic theory (eg. Coleman,1971) fragments of oceanic crust and upper mantle are emplaced along

continental edges by a process of obduction, whereby oceanic lithosphere is overthrust onto the continental margin.

APPENDIX C

MICROPROBE ANALYSES OF PYROXENES AND OLIVINE

ORTHOPYROXENE (Enstatite)

Sample No.	SiO_2	Al_2O_3	FeO	MgO	Total	Number of ions on the basis of 6 oxygens					En
						Si	Al^4	Al^6	Fe	Mg	
MHP 14	55.30	3.00	5.2	34.50	98.50	1.91	0.09	0.03	0.16	1.77	91.7
MHP 33	56.74	0.31	5.7	37.14	99.89	1.95	0.01	-	0.16	1.91	91.9

APPPNDIX C (Cont.)

CLINOPYROXENE (Diopside)

Sample No.	SiO_2	Al_2O_3	FeO	MgO	CaO	Total	No. of ions on the basis of 6 oxygens						En	Di
							Si	Al^4	Al^6	Fe	Mg	Ca		
MHD 39	53.91	2.32	2.11	17.7	23.10	99.14	1.96	0.04	0.06	0.06	0.96	0.90	49.9	46.7
MHD 99	52.52	4.07	1.83	16.7	24.23	99.35	1.91	0.09	0.08	0.06	0.90	0.94	47.5	49.6

OLIVINE (Fosterite)

Sample No.	SiO_2	FeO	MgO	Total	No. of ions on the basis of 4 oxygens			(Fo) $\frac{100\ Mg}{Mg + Fe}$
					Si	Fe	Mg	
MHO 31	41.56	11.19	47.76	100.41	1.014	0.228	1.738	88.3
MHO 66	40.9	7.4	50.8	99.1	0.997	0.151	1.846	92.4

In all calculations total iron is taken as FeO.

APPENDIX D

DEFINITION OF DIFFERENT SERPENTINE MINERALS USED HERE

Two different species of serpentine minerals, antigorite and chrysotile are recorded in the Clinton Creek area. Under these two species different names are used by the writer on the basis of textures.

Antigorite

Antigorite = Antigorite pseudomorphs after olivine;
Feathery textured antigorite;
Mosaic textured antigorite.

Serpophite = Isotropic antigorite.

Bastite = Antigorite that retains pyroxene's texture (antogorite pseudomorphs after pyroxene).

Chrysotile

Chrysotile = Asbestiform chrysotile.

Picrolite = Non-asbestiform chrysotile.

APPENDIX E

MICROPROBE ANALYSES OF CHRYSOTILE AND ANTIGORITE

Chemical analyses of 33 chrysotile samples and 64 antigorite samples were done using an ARL electron microprobe (Model - SEMQ) at the Dept. of Geological Sciences, the University of British Columbia. Samples were analyzed for eleven oxides. The standards used were jaideite, forsterite, andalusite, wallastonite, orthoclase, wallstonite, rutile, escoalite, spessartite, faylite and olivine for Na, Mg, Al, Si, K, Ca, Ti, Cr, Mn, Fe and Ni respectively. Results are listed in the following Table 4-1.

TABLE 4-1

ANALYTICAL DATA FOR ELEVEN OXIDES OF CHRYSOTILE AND ANTIGORITE

Sample No.	Na_2O	MgO	Al_2O_3	SiO_2	K_2O	CaO	TiO_2	Cr_2O_3	MnO	FeO	NiO
CH01	0.03	39.00	0.89	39.91	0.04	0.01	0.04	0.49	0.05	2.72	0.38
CH02	0.02	39.50	0.86	40.28	0.02	0.05	0.06	0.23	0.01	2.71	0.38
CH03	0.03	38.87	0.88	41.36	0.04	0.09	0.02	0.29	0.04	3.08	0.27
CH04	0.02	39.89	0.79	39.48	0.05	0.01	0.03	0.03	0.07	2.77	0.45
CH05	0.03	38.99	0.86	41.99	0.01	0.07	0.01	0.48	0.02	2.87	0.52
CH06	0.02	39.68	0.30	41.13	0.03	0.02	0.01	0.21	0.02	3.62	0.29
CH07	0.01	39.77	0.98	39.24	0.01	0.04	0.06	0.35	0.03	2.42	0.54
CH08	0.02	38.84	0.54	41.79	0.03	0.07	0.01	0.90	0.03	3.28	0.27
CH09	0.03	40.07	0.35	40.00	0.01	0.03	0.04	0.72	0.05	3.21	0.24
CH10	0.03	39.54	0.41	41.17	0.01	0.05	0.01	0.69	0.04	2.88	0.20
CH11	0.04	39.69	0.59	41.59	0.03	0.07	0.07	0.74	0.02	1.42	0.06
CH12	0.04	38.77	0.88	41.24	0.03	0.05	0.05	0.63	0.01	1.19	0.11
CH13	0.03	40.08	0.89	41.01	0.02	0.06	0.04	0.09	0.02	1.62	0.15
CH14	0.03	39.89	0.81	40.59	0.06	0.02	0.05	0.05	0.01	1.58	0.19

Table 4-1 (continued):

Sample No.	Na_2O	MgO	Al_2O_3	SiO_2	K_2O	CaO	TiO_2	Cr_2O_3	MnO	FeO	NiO
CH15	0.02	40.22	0.86	40.89	0.02	0.06	0.05	0.07	0.02	1.63	0.19
CH16	0.03	39.27	0.87	40.11	0.06	0.03	0.05	0.07	0.04	1.65	0.11
CH17	0.04	40.07	0.62	39.77	0.03	0.04	0.04	0.11	0.04	1.53	0.01
CH18	0.03	39.45	0.73	40.72	0.03	0.01	0.01	0.07	0.06	1.51	0.12
CH19	0.04	39.89	0.76	40.41	0.04	0.03	0.03	0.07	0.01	1.65	0.21
CH20	0.06	39.56	0.68	40.83	0.03	0.03	0.02	0.06	0.01	1.49	0.04
CH21	0.03	39.57	0.64	40.42	0.03	0.06	0.03	0.57	0.01	1.77	0.16
CH22	0.05	39.52	0.49	41.38	0.05	0.07	0.02	0.82	0.07	1.97	0.18
CH23	0.05	39.69	0.58	40.97	0.05	0.07	0.02	0.59	0.03	2.12	0.18
CH24	0.04	39.99	1.41	40.06	0.04	0.02	0.06	0.04	0.04	2.27	0.17
CH25	0.03	40.19	1.01	40.35	0.03	0.02	0.02	0.03	0.07	1.99	0.13
CH26	0.03	39.84	1.08	40.34	0.02	0.01	0.02	0.04	0.01	2.58	0.19
CH27	0.04	39.83	1.05	39.44	0.01	0.03	0.01	0.04	0.03	2.52	0.07
CH28	0.03	39.17	1.22	39.84	0.02	0.02	0.08	0.07	0.04	2.02	0.12
CH29	0.02	39.12	1.23	39.74	0.01	0.01	0.05	0.04	0.01	1.92	0.21

Table 4-1 (continued):

Sample No.	Na_2O	MgO	Al_2O_3	SiO_2	K_2O	CaO	TiO_2	Cr_2O_3	MnO	FeO	NiO
CH30	0.03	40.00	0.91	39.61	0.04	0.05	0.03	0.89	0.02	1.80	0.27
CH31	0.04	39.98	0.99	38.29	0.06	0.06	0.04	0.90	0.05	1.22	0.12
CH32	0.03	39.97	1.08	39.02	0.03	0.04	0.02	0.19	0.01	1.86	0.07
CH33	0.03	40.26	1.32	40.43	0.02	0.01	0.01	0.58	0.04	1.40	0.17
PC01	0.01	37.19	0.86	42.83	0.01	0.01	0.01	0.02	0.06	3.58	0.01
PC02	0.01	37.93	0.53	42.34	0.01	0.01	0.01	0.02	0.11	3.81	0.02
PC03	0.01	37.65	0.85	42.56	0.01	0.01	0.05	0.02	0.12	4.09	0.02
PC04	0.01	38.20	0.52	42.81	0.01	0.01	0.02	0.03	0.12	3.56	0.01
PC05	0.04	37.15	1.29	41.74	0.01	0.01	0.02	0.69	0.03	2.77	0.33
PC06	0.03	37.92	1.38	41.45	0.01	0.01	0.08	0.81	0.02	2.90	0.33
PC07	0.02	38.78	0.75	42.62	0.04	0.05	0.03	0.26	0.10	1.95	0.20
PC08	0.02	37.40	0.94	42.71	0.01	0.02	0.04	0.41	0.03	2.84	0.16
PC09	0.03	38.12	0.97	42.13	0.01	0.06	0.08	0.35	0.01	2.91	0.24
PC10	0.01	37.58	1.15	41.81	0.06	0.04	0.03	0.27	0.06	3.18	0.14

Table 4-1 (continued):

Sample No.	Na_2O	MgO	Al_2O_3	SiO_2	K_2O	CaO	TiO_2	Cr_2O_3	Mno	FeO	NiO
PC11	0.01	38.40	1.08	42.52	0.04	0.07	0.04	0.31	0.03	3.31	0.28
PC12	0.02	38.57	1.08	41.47	0.03	0.08	0.01	0.30	0.02	2.95	0.26
PC13	0.01	38.25	0.95	41.96	0.01	0.06	0.02	0.30	0.05	2.78	0.30
PC14	0.01	37.60	0.38	42.15	0.01	0.02	0.01	0.28	0.10	3.73	0.16
PC15	0.04	38.55	0.62	43.75	0.01	0.07	0.02	0.07	0.05	2.71	0.09
PC16	0.02	39.12	0.62	43.09	0.03	0.02	0.01	0.09	0.03	1.76	0.17
PC17	0.03	38.57	1.13	40.93	0.01	0.01	0.01	0.36	0.08	2.79	0.11
PC18	0.03	38.71	1.34	38.90	0.02	0.04	0.01	0.39	0.04	2.57	0.03
PC19	0.01	38.34	0.36	41.68	0.03	0.02	0.02	0.02	0.07	2.90	0.12
PC20	0.04	38.11	1.25	41.60	0.04	0.01	0.02	0.65	0.02	1.62	0.02
PC21	0.05	38.96	1.11	39.78	0.05	0.03	0.01	0.48	0.02	2.36	0.10
PC22	0.05	38.07	1.15	41.54	0.06	0.01	0.03	0.43	0.03	1.57	0.07
PC23	0.04	38.13	0.72	41.70	0.05	0.02	0.01	0.49	0.03	3.30	0.08
PC24	0.01	38.10	0.97	43.21	0.01	0.01	0.01	0.31	0.16	3.21	0.22
PC25	0.01	36.28	0.99	42.52	0.01	0.5	0.01	0.260	0.16	4.45	0.21

Table 4-1 (continued):

Sample No.	Na_2O	MgO	Al_2O_3	SiO_2	K_2O	CaO	TiO_2	Cr_2O_3	MnO	FeO	NiO
PC26	0.01	37.08	0.87	42.10	0.03	0.05	0.02	0.37	0.03	3.14	0.47
PC27	0.03	37.25	0.94	42.43	0.02	0.06	0.02	0.45	0.03	3.43	0.56
PC28	0.01	38.85	0.99	43.25	0.01	0.01	0.01	0.61	0.01	1.64	0.41
PC29	0.03	38.51	1.03	41.48	0.02	0.09	0.03	0.55	0.03	2.60	0.31
PC30	0.01	38.11	1.18	41.90	0.02	0.02	0.08	0.63	0.04	2.43	0.31
PC31	0.02	38.40	0.89	42.32	0.04	0.01	0.01	0.60	0.01	3.20	0.36
PC32	0.01	38.80	0.63	43.86	0.01	0.07	0.01	0.47	0.01	1.31	0.53
PC33	0.02	38.37	0.93	42.87	0.01	0.01	0.01	0.60	0.02	2.11	0.37
PC34	0.01	37.79	1.95	40.76	0.04	0.06	0.02	0.25	0.02	2.47	0.10
PC35	0.01	37.14	0.52	42.14	0.01	0.02	0.02	0.45	0.07	3.65	0.04
PC36	0.02	37.49	0.40	41.89	0.02	0.03	0.04	0.06	0.08	3.56	0.03
PC37	0.03	37.35	0.58	41.45	0.03	0.04	0.06	0.08	0.12	3.46	0.01
PC38	0.02	37.47	0.29	42.16	0.02	0.01	0.02	0.18	0.12	3.30	0.06
PC39	0.02	36.99	0.34	41.58	0.01	0.02	0.02	0.24	0.18	3.89	0.05
PC40	0.01	37.78	0.34	42.82	0.01	0.01	0.02	0.24	0.12	3.36	0.07

Table 4-1 (continued):

Sample No.	Na_2O	MgO	Al_2O_3	SiO_2	K_2O	CaO	TiO_2	Cr_2O_3	MnO	FeO	NiO
PC41	0.01	37.09	1.21	41.22	0.02	0.02	0.03	0.62	0.04	2.83	0.38
PC42	0.04	37.38	0.70	41.94	0.04	0.02	0.05	0.24	0.03	3.91	0.16
PC43	0.03	38.21	0.77	43.08	0.03	0.02	0.01	0.51	0.04	2.29	0.41
PC44	0.03	36.84	0.77	42.44	0.02	0.01	0.01	0.58	0.04	3.78	0.40
PC45	0.02	38.74	0.85	43.22	0.01	0.07	0.02	0.59	0.01	2.38	0.32
PC46	0.03	38.81	0.72	42.36	0.03	0.01	0.01	0.29	0.02	1.90	0.18
PC47	0.01	38.59	0.73	42.06	0.04	0.07	0.02	0.03	0.07	3.33	0.13
PC48	0.02	38.68	0.87	42.66	0.03	0.01	0.01	0.08	0.03	1.42	0.14
PC49	0.02	38.30	1.07	42.19	0.04	0.01	0.04	0.10	0.02	1.78	0.21
PC50	0.02	37.94	0.81	41.86	0.05	0.02	0.02	0.05	0.02	3.68	0.17
PC51	0.03	38.40	0.82	42.49	0.03	0.03	0.02	0.07	0.05	1.95	0.12
PC52	0.03	39.22	0.81	41.31	0.03	0.07	0.02	0.04	0.03	3.76	0.15
PC53	0.02	38.37	0.83	41.43	0.02	0.02	0.01	0.07	0.01	2.67	0.12
PC54	0.01	37.72	0.69	40.12	0.02	0.04	0.03	0.23	0.02	3.61	0.14
PC55	0.01	39.09	1.59	40.35	0.05	0.01	0.02	0.02	0.02	4.22	0.11

Table 4-1 (continued):

Sample No.	Na_2O	MgO	Al_2O_3	SiO_2	K_2O	CaO	TiO_2	Cr_2O_3	MnO	FeO	NiO
PC56	0.01	38.37	1.57	40.87	0.02	0.03	0.02	0.06	0.03	3.78	0.18
PC57	0.01	38.40	1.58	40.76	0.02	0.04	0.03	0.07	0.01	4.00	0.12
PC58	0.02	39.03	1.59	39.17	0.01	0.02	0.01	0.03	0.01	4.04	0.14
PC59	0.01	38.03	1.59	42.66	0.02	0.03	0.03	0.03	0.03	2.45	0.12
PC60	0.02	38.22	1.48	42.89	0.02	0.02	0.03	0.01	0.03	1.71	0.13
PC61	0.01	38.07	0.87	41.88	0.04	0.01	0.01	0.33	0.03	2.81	0.37
PC62	0.04	38.02	0.94	41.86	0.03	0.02	0.01	0.17	0.02	3.58	0.17
PC63	0.02	36.42	1.24	40.05	0.06	0.01	0.05	0.60	0.04	3.92	0.49
PC64	0.02	36.81	1.37	42.27	0.02	0.05	0.01	0.74	0.01	3.81	0.33

All analyses done by electrin microprobe. Total iron is represented as FeO.
Sample no. with CH represents chrysotile. Sample no. with PC represents antigorite.

APPENDIX F

METHODS USED FOR RADIOMETRIC AGE DETERMINATIONS

Eleven samples from the Clinton Creek area have been dated by radiometric methods. Four samples were dated by the potassium-argon method and seven samples by rubidium-strontium whole rock method. Samples include: four of quartz-muscovite schist, three of greenstone, two of quartz-muscovite-biotite schist, one of granodiorite and one of amphibolite. All but the granodiorite sample was collected within the mapped area. Amphibolite was collected from an eight foot lens in quartz-muscovite schist. All samples were analysed in the K-Ar laboratory and the Rb-Sr laboratory of the University of British Columbia.

For mineral separation the rocks were crushed to a stage where individual minerals were free. A fast electromagnetic device was used to seperate quartz and felsic minerals from mafic minerals. Flaky micas and prismatic amphiboles were separated on vibrating table. Further separation of the residium was done on a slow electromagnetic separator. Finally, some samples were separated in heavy liquids. Hand picking was used for final cleaning.

Potassium analyses[1] were run in duplicate by atomic absorption using a Techtron AA4 spectrophotometer and argon analyses[2] by isotope dilution using an AEI MS - 10 mass spectrometer and purity ^{38}Ar spike. Errors reported are for one standard deviation. The constants used are:

$K\lambda_{\varepsilon} = 0.585 \times 10^{-10} y^{-1}$

$K\lambda_{\beta} = 4.72 \times 10^{-10} y^{-1}$

$^{40}K/K = 0.0119$ atom percent.

In the whole rock rubidium-strontium analyses[3], Rb and Sr concentrations were determined by replicate analysis of pressed powder pellets using X-ray fluorescence. U.S. Geological Survey rock standards were used for calibration; mass absorption coefficients were obtained from Mo Kα Compton scattering measurments. Rb/Sr ratios have a precision of 2% (1σ) and concentrations a precision of 5% (1σ). Strontium isotope composition was measured on unspike samples prepared using standard ion exchange techniques. The mass spectrometer (60° sector, 30 cm radius, solid source) is of U.S. National Bureau of Standard design, modified by H. Faul. Data aquisition is digitized and automated using a NOVA computer. Experimental data have been normalized to a $^{86}Sr/^{88}Sr$ ratio of 0.1194 and adjusted so that the NBS standard $SrCO_3$ (SRM987)

1: Potassium analyses were done by K.L. Scott of the University of British Columbia.
2: Argon mass spectrometer analyses were done by J. Harakel of the University of British Columbia.
3: Rubidium- strontium whole rock analyses were done by K.L. Scott of the University of British Columbia.

gives a $^{87}Sr/^{86}Sr$ ratio of 0.71022±2 and the Eimer and Amend Sr ratio of 0.70800±2. The precision of single $^{87}Sr/^{86}Sr$ ratio is 0.00013 (1σ). Rb-Sr dates are based on a Rb decay constant of $1.42\times10^{-11}y^{-1}$. The regressions are calculated according to the technique of York (1967).

APPENDIX G

PROCEDURES APPLIED FOR PRODUCING LEVEL PLANS WITH DIFFERENT CHRYSOTILE-FIBRE CONCENTRATION ZONES

The Clinton Creek open pit asbestos mine was mined in slices of usually 30 feet thick. On each slice information of chrysotile-fibre content in percentage are available in drill holes logs and records of blast hiles. As the blast holes were drilled within five to ten feet distance, it is fairly reliable to draw isolines on certain percentage of chrysotile-fibre in the serpentinite. In this manner isolines of one percent, three percent and seven percent were drawn on Figure 3-3, 4-9 and 4-10.